ERI/NRC 18-202
Revision 5

ASSESSMENT OF HYDROGEN COMBUSTION DURING SEVERE ACCIDENTS IN A NUSCALE PLANT MODULE

Work Performed under the Auspices of the
United States Nuclear Regulatory Commission
Office of Nuclear Regulatory Research
Washington, D.C. 20555

ENERGYRESEARCHINC
P. O. Box 2034
Rockville, Maryland 20847

October 2019

Intentionally left blank

ERI/NRC 18-202
Revision 5

ASSESSMENT OF HYDROGEN COMBUSTION DURING SEVERE ACCIDENTS IN A NuScale PLANT MODULE

October 2019

A. Krall, Z. Yuan and M. Khatib-Rahbar
Energy Research, Inc.
P.O. Box 2034
Rockville, Maryland 20847-2034

Work performed under the auspices of
United States Nuclear Regulatory Commission
Washington, D.C.
Under Contract Number NRC-HQ-25-14-E-0002 (Task Order No. 4)

Intentionally left blank

ABSTRACT

This report documents a review of the NuScale approach to the assessment of the NuScale Power Module (NPM) containment to conform to the Title 10, Code of Federal Regulations (CFR), Part 50.44, and the results of various confirmatory analyses. In addition, results of simulation studies that assess the potential for hydrogen combustion (deflagration, and deflagration to detonation transition) under the biological shield region following an accident involving a pipe break outside containment are also presented.

Intentionally left blank

EXECUTIVE SUMMARY

This report documents a review of the NuScale approach to the assessment of the NuScale Power Module (NPM) containment design to conform to the Title 10, Code of Federal Regulations (CFR), Part 50.44, and the results of various confirmatory analyses.

NuScale considers that during credible accidents the containment atmosphere is typically inert by oxygen depletion, in the early time frame, due to large amounts of oxidation-generated hydrogen. However, over the long-term, flammable conditions do arise when sufficient oxygen has been restored by radiolysis. Based on an estimate of the containment atmosphere composition at 72 hours, a bounding value for the detonation pressure of [[ ]]$^{2\,(a),\,(c)}$ bar-abs ([[ ]]$^{2(a),\,(c)}$ psia) arising in any accident has been estimated by NuScale. Simulations of severe accident progression have little or no role in arriving at this bounding detonation pressure estimate, because the simple plant design allows the containment loads to be assigned a priori. The amount of core oxidation associated with the bounding detonation pressure estimate is [[ ]]$^{2\,(a),\,(c)}$ % (where 100% would correspond to steam-oxidation of all the zirconium in the cladding on the active part of the fuel). Higher fractions would yield an atmosphere inerted by oxygen depletion for longer than 72 hours. From a regulatory point of view, the permissibility of NuScale's assumption of less than 100% is an important issue but it is not assessed by the present report.

In this report, a MELCOR simulation is used to conclude that two assumed values considered by NuScale for the estimation of the detonation pressure are non-conservative. They are:

- Containment atmosphere temperature of [[ ]]$^{2\,(a),\,(c)}$ °C, and
- Total containment atmosphere gas volume (i.e., [[ ]]$^{2\,(a),\,(c)}$).

The present simulation results indicate that the containment atmosphere temperature may not be lower than 96.5 °C, and the total containment atmosphere volume should be reduced by about 28.2 m^3 to account for accumulation of condensate inside containment. A re-application of the NuScale method with no change except the re-specification of these two assumed values with the MELCOR-informed estimates, results in a bounding detonation pressure of [[ ]]$^{2\,(a),\,(c)}$ bar-abs ([[ ]]$^{2\,(a),\,(c)}$ psia) based on the quantification process utilized by the Applicant (i.e., factors that approximately convert deflagration pressure to detonation pressure).

In spite of this finding, the NuScale detonation pressure estimate of [[ ]]$^{2\,(a),\,(c)}$ bar-abs is conservative because a third input (i.e., the pre-accident containment pressure) in the NuScale quantification process appears to have been specified conservatively. The method that leads to the estimate [[ ]]$^{2\,(a),\,(c)}$ bar-abs assumes that the pre-power-up containment pressure is 9.5 psia. Various NuScale documents indicate that in actual operations the containment pressure prior to reactor criticality is 2 psia or less. Therefore, considering the lower containment pressure during normal operation (pre-accident), the associated reduction in the initial inventory of oxygen would roughly cut the estimated detonation pressure in half, relative to the value of [[ ]]$^{2(a),\,(c)}$ bar-abs that NuScale uses in its containment structural analysis.

The design pressure of the NuScale containment vessel is [[ ]]$^{2\,(a),\,(c)}$ bar-abs ([[ ]]$^{2\,(a),\,(c)}$ psia[1]), but according to NuScale's structural analysis, the containment vessel can withstand a detonation pressure of [[ ]]$^{2\,(a),\,(c)}$ bar-abs. This is because of the extreme brevity of the detonation, estimated by NuScale as [[ ]]$^{2\,(a),\,(c)}$ milliseconds using the TNT-equivalent approach. The structural analyses performed by NuScale conclude that the containment structure will not attain the yield strain. Note, the scope of the present study does not include an assessment of the NuScale containment structural analysis.

The Applicant has based its main conclusions on the assumption that the combustion event that may challenge the containment integrity should take place, at the latest, at 72 hours (3 days) since the time of start of the accident. This report extends the confirmatory calculations, carried out at 72 hours, also to times as long as 60 days. (The Applicant also has considered combustion events at long times, in document ER-P020-4904 available in the electronic reading

[1]See January 2019 Response to RAI 9482 (ADAMS accession number ML19028A413).

room.) As the postulated fraction of the cladding that becomes oxidized varies from ~10% to ~110%, the times at which the containment becomes flammable (and, in general, detonable) ranges from ~[[ ]]$^{2\,(a),(c)}$ to ~[[ ]]$^{2\,(a),(c)}$ days. This time might indicate when operators could take actions to restore inert conditions in the containment. Inside of 60 days, the worst-case pressure result obtained here is when 110% of the cladding oxidizes. In that case, the Adiabatic Isochoric Complete Combustion (AICC) pressure at 60 days is 58.8 bar, or 853 psia. On the other hand, in this case the containment would not be flammable until about 56 days. The worst-case timing result obtained here is when only 10% of the cladding oxidizes. In that case, the containment is flammable almost immediately, with the calculated AICC pressure at 0.3 days (~8 hours) of 7 bar. In the present study it is found that the containment is almost always detonable provided only that it is flammable, and the detonation pressure is estimated using the Applicant's method (i.e., apply a multiplier of [[ ]]$^{2\,(a),(c)}$, as arrived at by the Applicant, to the AICC pressure as calculated here). The Applicant's combustion analysis is based on the AICC pressure of [[ ]]$^{2\,(a),(c)}$ psia ([[ ]]$^{2\,(a),(c)}$ bar), approximately calculated for the mixture that the Applicant predicts for the containment at 3 days (see Section 2.3, and Reference [3]). Therefore, more severe combustion events than the one considered by the Applicant are possible at times longer than the 3 days that the Applicant used, and it is not clear that the containment can structurally withstand the higher detonation loads.

The latest design of the biological shield features vents that are always open. This report includes an estimate of combustion pressures that may arise in the case of pipe breaks that lead to the gas regions under the bio-shield, as vented according to the latest design. The assessment of hydrogen build-up and combustion for severe accidents involving a break outside of the containment vessel in the region under the biological shield shows conditions that are conducive to deflagration but not detonation, especially in the case of stacked shields. However, on the assumption of stacked shields, conditions permissive of the deflagration-to-detonation transition (DDT) arise for about 3 minutes during the time of the peak rate of cladding oxidation, provided deflagration is suppressed. An estimate of the associated detonation pressure is 32 bar-abs, provided a detonation is assumed to occur at relatively low hydrogen concentration (i.e., ~13%) estimated herein, which is not considered to be highly credible based on experimental evidence, lack of a strong ignition source, uncertainties in the MELCOR-predicted concentration gradients that result in pockets of relatively high hydrogen concentrations, and if the more likely deflagration of hydrogen at lower concentration does not occur. Therefore, a detonation event under the biological shield is considered to be of negligible probability. Even assuming such a detonation, the potential to induced core damage in an adjacent module (i.e., due to impact by any missiles generated by hydrogen detonation inside the biological shield of the affected module) is small.

TABLE OF CONTENTS

Intentionally left blank

LIST OF TABLES

Intentionally left blank

LIST OF FIGURES

LIST OF ACRONYMS

AICC	Adiabatic Isochoric Complete Combustion
BAF	Bottom of the Active Fuel
CFR	Code of Federal Register
CNV	Containment Vessel
CV	Control Volume
CVCS	Chemical and Volume Control System
DDT	Deflagration to Detonation Transition
DHRS	Decay Heat Removal System
ECCS	Emergency Core Cooling System
ERI	Energy Research, Inc.
ERPRA-BURN	Computer code (not an acronym)
ERR	Electronic Reading Room
FSAR	Final Safety Analysis Report
LOCA	Loss of Cooling Accident
MW	Megawatt
NPM	NuScale Power Module
NRC	Nuclear Regulatory Commission
PSIA	Pounds per Square Inch - Absolute
RPV	Reactor Pressure Vessel
RRV	Reactor Recirculation Valve
RVV	Reactor Vent Valve
TAF	Top of the Active Fuel
TNT	Trinitrotoluene

Intentionally left blank

NOMENCLATURE

The NuScale containment consists of a steel vessel that surrounds the reactor pressure vessel. Sometimes this surrounding vessel is referred to as the containment vessel, and sometimes simply as the containment. Sometimes used are expressions such as “dry containment volume.” This means the free volume of the containment when it is dry; such expressions are used when the reduction of the containment gas volume due to the presence of water is being considered. Such expressions should not be confused with terminology such as “dry containment” that is commonly used when discussing operating Pressurized Water Reactors (PWRs) with large-dry containment designs.

Intentionally left blank

ACKNOWLEDGEMENTS

The authors are thankful to Ms. A-M Grady and Dr. A. Hathaway of the United States Nuclear Regulatory Commission, for their support in facilitating access to various design and other information for the unique NuScale design.

This work was performed under the auspices of the United States Nuclear Regulatory Commission, Office of Nuclear Regulatory Research, Under Contract Number NRC-HQ-25-14-E-0002, Task Order 4.

Intentionally left blank

1. INTRODUCTION

1.1 Background

NuScale is a small modular reactor designed for a net combined thermal power output of 1920 MW(t) for 12 reactor system modules. The NuScale Nuclear Steam Supply System (NSSS) is a self-contained assembly consisting of a reactor core, a riser section, a pressurizer, and two helical steam generator tube bundles housed within a single reactor pressure vessel (RPV). During normal operation, the core serves as a source of heat while the steam generators act as elevated heat sinks. The temperature and consequent density differences of the hot and cold coolant between the core and the steam generators creates the buoyancy force that drives the coolant flow (natural circulation), thereby eliminating the need for reactor coolant pumps. The reactor core is connected to a riser that acts as a "hot leg" transporting hot water to the top of the riser (upper plenum). The water in the upper plenum turns downwards and is cooled as it passes on the outside (i.e., shell side) of the steam generator tubes. The cooler (and denser) water returns to the reactor core via the downcomer region. In order to enable control of the primary system pressure, the top portion of the RPV serves as a pressurizer which communicates with the upper plenum via the holes in the baffle plates.

The NuScale containment vessel is a compact and evacuated (i.e., subatmospheric, at 13.3 kPa-abs [2 psia] as modeled by the MELCOR model discussed here) steel vessel under the conditions prior to reactor criticality. The containment vessel surrounds the RPV and is immersed in a large pool of water which serves as a passive heat sink for the reactor and containment under transient and accident conditions.

The NuScale design includes a number of unique accident mitigation features consisting of three Reactor Vent Valves (RVVs) on the reactor vessel head to vent steam, two Reactor Recirculation Valves (RRVs) to provide coolant recirculation, and a Decay Heat Removal System (DHRS) designed to rapidly reduce containment pressure and temperature during any Loss Of Coolant Accident (LOCA) and transient events.

1.2 Scope and Objectives

This report documents a review of the NuScale approach to the assessment of the NuScale Power Module (NPM) containment design to conform with the Title 10, Code of Federal Regulations (CFR), Part 50.44, and the results of various confirmatory analyses, including an assessment of the potential for hydrogen combustion under the bio-shield, to assess the assumptions, and conclusions reached by the Applicant.

Intentionally left blank

2. THE NUSCALE APPROACH TO ASSESSMENT OF CONFORMANCE WITH 10 CFR 50.44

The approach used by NuScale to demonstrate conformance with 10 CFR 50.44 relies little or not at all on any severe accident progression simulation studies (e.g., MELCOR calculations). Rather, it is based on a direct calculation of bounding combustion pressure using known boundary conditions (e.g., hydrogen quantity based on 100%-clad-equivalent oxidation, radiolysis, etc.); established physics (i.e., ideal gas law, and combustion reaction energy under Adiabatic Isochoric Complete Combustion [AICC] conditions); and approximate methods for estimating detonation pressures.

2.1 Review of NuScale's Bounding Calculations

A close reading of various documents, especially Section 6.2.5 of the FSAR [1], Technical Report TR-0716-50424-P [2], and the ERR document EC_B020_2877_R1, "ECCS Combustible Gas Analysis" [3] indicates that NuScale uses a series of combustion pressure calculations that do not utilize simulations of various scenarios by severe accident progression analysis codes such as MELCOR or MAAP.

An examination of Section 6.2.5 of the FSAR [1], and Reference [2] (which that section of Reference [1] references), did not identify the use by NuScale of the specific results of any of the accident scenarios that are documented in Chapter 19 of Reference [1] or elsewhere. On the other hand, if taken together with Reference [3], Reference [2] provides a stand-alone direct calculation of a key result, namely a bounding peak detonation pressure for combustion events occurring at 72 hours after reactor shutdown for design basis and severe accident scenarios, given by Table 3-3 of Reference [2] (and also by Table 5-1 of Reference [3]) as [[ ]]$^{2\,(a),(c)}$ psia ([[ ]]$^{2\,(a),(c)}$ bar-abs).

Although as has been stressed, the key result ([[ ]]$^{2\,(a),(c)}$ psia) does not depend on a simulation, it is noted that Section 6.2.5.1 of the FSAR [1] states:

> *The type of severe accidents considered were those that assume an intact containment boundary and result in varying degrees of core damage. One example of this type of severe accident is a LOCA inside containment with an ECCS failure that prevents the recirculation of coolant from the CNV back into the RPV.*

Scenario LCC-05T fits the description given in the quote. This quote provided some of the motivation for the MELCOR simulation of one of the LCC-05T scenario variants that is included in the present study, but it does not contradict the above-stated view, founded mainly in the review of Reference [3] and the quotation of its principal result documented in Reference [2], that the primary basis for NuScale's assertion to compliance with combustion-related requirements are certain analytic calculations that are carried out with specified assumptions.

2.2 NuScale's Calculation of Bounding Detonation Pressure

The NuScale calculations use prescribed amounts of oxidation-produced hydrogen and the known radiolysis sources, along with the ideal gas law, to compute the masses of the various gases in the containment. Time plays little role: the radiolysis-generated masses of hydrogen and oxygen are time-dependent according to the generation rates prescribed by the Standard Review Plan (NUREG-0800) [4], but the maximum that these sources can cumulatively attain is set by regulatory considerations as the net production at 72 hours following reactor scram. NuScale takes the view that cladding oxidation fractions higher than those that create oxygen-depleted containment atmospheres (due to dilution by hydrogen) need not be considered. On this view the relevant oxidation fraction is calculable in advance and so need not be obtained as a function of time by an accident progression code. The corresponding fraction is [[ ]]$^{2\,(a),(c)}$ (for example, see line 2 of Table 3.2 in this report, or p. 43 of Reference [3] which associates this fraction with 72 hours), to compare with fraction 1.00 called for by 10 CFR 50.44. Under stated assumptions that set the containment gas volume and temperature, using the ideal gas law the pre-burn containment pressure and composition is computed from the known and/or prescribed gas masses. All quantities are then in hand to carry out a calculation of the deflagration pressure under the usual AICC assumption. Based on referenced sources, various multipliers for the AICC pressure are introduced that yield an approximation to the detonation pressure, with account taken of various effects such as

the Deflagration to Detonation Transition (DDT) and reflection of the detonation waves. The whole of the NuScale method is thus summarized by this paragraph (but further details are given below); the key result is that [[ ]]$^{2\,(a),(c)}$ bar-abs ([[ ]]$^{2\,(a),(c)}$ psia) is stated to bound the detonation pressure that could arise in any accident for a NPM.

For calculating the molar rate $S_H(t)$ of radiolytic generation of hydrogen, NuScale follows the guidance of NUREG 0800 [4] by using the following formula:

$$S_H(t) = kP\{G_c f_c H_\gamma(t) + G_s[2f_s H_\gamma(t) + f_I H_I(t)]\} \quad (1)$$

where $S_H(t)$ is in gram-moles per second and P is the full power of the reactor in MW (163.2 MW in the case of NuScale, the value given by Reference [3] on p. 10/43 is used). The radiolytic generation of oxygen is $S_H(t)/2$. Other symbols in Eq. (1) are interpreted and evaluated as follows:

$$k = \frac{1\ x\ 10^{22}}{100\ B\ N}$$

B =1
N = 6.02x10^{23} (Avogadro's number);
G_c = 0.5 molecules per 100 eV (radiolytic hydrogen yield in the core region)
f_c = 0.1 (fraction of fission product gamma rays that are absorbed by coolant in the core region)
$H_\gamma(t)$ = $\Sigma_i\ a_i\ exp[-\alpha_i\ t]$
G_s = 0.5 molecules per 100 eV (radiolytic hydrogen yield in the solution)
f_s = 0.01 (fraction of total solid fission product energy that is absorbed by coolant outside the core region)
f_I = 0.1 (fraction of fission product gamma rays that are absorbed by coolant outside the core region)
$H_I(t)$ = $\Sigma_i\ b_i\ exp[-\beta_i\ t]$.

NUREG 0800 defines the factor B to allow for other definitions of mole (e.g., B = 454 if $S_H(t)$ is desired in pound-moles per second). Here, t is the time since reactor shutdown in seconds, and Σ_i denotes a sum over the index i. The coefficients and exponential rates appearing in the sums are given by Table 2.1.[2]

Table 2.1 Coefficients and exponential rates for formulas that give the time dependence of radiolysis

		***i*=1**	***i*=2**	***i*=3**	***i*=4**	***i*=5**
$H_\gamma(t)$	a_i	5.1912	0.8743	0.6557	0.4098	0.0150
	α_i	9.8E-5	6.5E-6	5.7E-7	7.4E-8	8.0E-10
$H_I(t)$	b_i	0.8197	0.3279	0.0574	–	
	β_i	6.1E-5	1.1E-5	1.0E-6		

Since it provides an opportunity to make a transferrable permanent record of notes taken from the ERR viewing of Reference [3], it is worth reproducing the sample calculation given in Reference [3] (see pp. 23, 26, 32). It applies one day after the start of oxidation and radiolysis.

- The gas volume and temperature of the containment are treated as known ([[ ]]$^{2\,(a),(c)}$ cubic inches[3]; 50 °F pre-criticality; [[ ]]$^{2\,(a),(c)}$ °F during the transient). Given the known initial pressure (9.5 psia before

[2] Relative to the definitions given by Standard Review Plan (SRP) (NUREG-0800), these definitions of H_γ and H_I have removed a factor of 1 x 10^{22} and included it with the global factor k.

[3] ERR document EC-B020-4365, "Containment Gas Composition Calculation," defends [[

]]$^{2\,(a),(c)}$ This argument is discussed and assessed in Section 3 of this report.

reactor power-up) and gas composition (air), the initial molar amounts of nitrogen (n_02-init = [[ ]]$^{2\,(a),\,(c)}$ moles) and oxygen (n_N2-init = [[ ]]$^{2\,(a),\,(c)}$ moles) are obtained from the ideal gas law. The nitrogen amount never changes.

- Integrate the radiolysis rates to 1 day. Radiolysis has added [[ ]]$^{2\,(a),\,(c)}$ moles of oxygen and [[ ]]$^{2\,(a),\,(c)}$ moles of hydrogen, which results in the cumulative amount of [[ ]]$^{2\,(a),\,(c)}$ moles of oxygen.
- Account for cladding oxidation. The 10 CFR 50.44 amount of hydrogen (corresponding to steam oxidation of 100% of the cladding on the active part of the fuel) is 46671 moles = 93.3 kg (see p. 28/43 of Reference [3]). On day 1 the oxidized fraction is assigned [[ ]]$^{2\,(a),\,(c)}$. (The basis of the assignment of oxidation fraction as a function of time is not provided in Reference [3]. Fraction 1 is reached on day [[ ]]$^{2\,(a),\,(c)}$, while the fractions assigned to 24 and 72 hours appear to have been tuned to yield, at both those times, containment oxygen mole fraction 0.05 according to the different radiolytic hydrogen and oxygen masses that have accrued to those times.) Therefore, there are [[ ]]$^{2\,(a),\,(c)}$ moles of hydrogen from cladding oxidation. Add [[ ]]$^{2\,(a),\,(c)}$ moles from radiolysis for the total hydrogen on day 1.
- Calculate pre-combustion pressure given the temperature, volume, and molar quantities, using the ideal gas law for the partial pressures of nitrogen, oxygen, and hydrogen. Always the steam partial pressure is the saturation pressure at [[ ]]$^{2\,(a),\,(c)}$ °F. The day 1 total pre-combustion pressure is found to be [[ ]]$^{2\,(a),\,(c)}$ psia.
- Calculate the AICC pressure. Gas temperature, pressure, and mole fractions are the only required inputs. The calculation can be done in various ways (e.g., a one control volume "toy" MELCOR model could be set up) but there is no ambiguity about the correct answer. The approximate method used by NuScale is not transparent[4]. In this case, the approximate method yields [[ ]]$^{2\,(a),\,(c)}$ psia.
- To the AICC pressure, apply a factor [[ ]]$^{2\,(a),\,(c)}$ to approximate the Chapman-Jouguet pressure.
- To the Chapman-Jouguet pressure, apply a factor [[ ]]$^{2\,(a),\,(c)}$ to approximate the reflected pressure.
- To the reflected pressure, apply a factor [[ ]]$^{2\,(a),\,(c)}$ to approximate the DDT pressure.
- Final result for day 1: detonation pressure [[ ]]$^{2\,(a),\,(c)}$ psia.

The aforementioned calculation has been reproduced as part of the present study up through the pre-burn conditions, and thus confirmed the final result (detonation pressure of [[ ]]$^{2\,(a),\,(c)}$ psia at 24 hours), assuming the approximate AICC pressure and the factor [[ ]]$^{2\,(a),\,(c)}$ that NuScale has used. For details see Table 3.2.

---

[4] For the mixture characterized by [[ ]]$^{2\,(a),\,(c)}$ °F and [[ ]]$^{2\,(a),\,(c)}$ psia with O_2:H_2:H_2O:N_2 in mole fractions [[ ]]$^{2\,(a),\,(c)}$ as given by Reference [3] for the sample calculation at day 1, the correct AICC pressure is [[ ]]$^{2\,(a),\,(c)}$ psia. The AICC pressure calculated by NuScale is [[ ]]$^{2\,(a),\,(c)}$ psi. As described in Reference [3], the method used by the Applicant involves considering a supposedly equivalent O_2/H_2 mixture with the oxygen mole fraction, n_{O2}, of the actual mixture ([[ ]]$^{2\,(a),\,(c)}$ in this case) and with an effective hydrogen concentration $n_{H2} = 1 - n_{O2}$ ([[ ]]$^{2\,(a),\,(c)}$ in this case). The effective hydrogen concentration, n_{H2}, is then used as the interpolation variable in a look-up table that NuScale defines by digitizing a figure given by a referenced source (appearing in this present report as Reference [6]); the value from the table, [[ ]]$^{2\,(a),\,(c)}$ in this case, is supposed to be the ratio of the AICC pressure to the pre-combustion pressure. Actually, the correct AICC pressure for the O_2:H_2 = 0.05/0.95 mixture at the given pre-combustion temperature and pressure is [[ ]]$^{2\,(a),\,(c)}$ psia, which also is less than [[ ]]$^{2\,(a),\,(c)}$ psi. Therefore, in at least these two instances (i.e., the actual mixture and the supposedly equivalent O_2/H_2 mixture), the method by NuScale over-estimates the AICC pressures and it is acceptable and can be viewed as conservative. Elsewhere NuScale reports some AICC calculations using MELCOR whose results appear to be accurate; see ERR document ER-P020-4904, "Hydrogen Deflagration, Adiabatic Isochoric Complete Combustion." However, the role of these calculations in the overall analyses by the Applicant is not clear.

On day 3 (72 hours), the detonation pressure arrived at by this method is [[ ]]$^{2\,(a),(c)}$ psia; see Table 5-1 of [3] which gives such pressures as a function of time to 60 days. Here again, this key result has been similarly confirmed (i.e., this result is reproduced given that all of NuScale's stated assumptions are used). This pressure value ([[ ]]$^{2\,(a),(c)}$ psi) is listed verbatim in Reference [2] and appears to be the main combustion-related input to the structural analysis of Reference [2].

It should be reiterated that for this estimate of a bounding detonation pressure, the fraction of cladding oxidation has been taken not as 1.00, but as [[ ]]$^{2\,(a),(c)}$. A fraction higher than [[ ]]$^{2\,(a),(c)}$ would yield a non-flammable mixture due to oxygen mole fraction still yet not having reached 0.05 due to radiolysis as late as 72 hours. Therefore, as a flammability limit specific to NPM containment, the [[ ]]$^{2\,(a),(c)}$ fraction may be considered acceptable even though 10 CFR 50.44 requires hydrogen amount corresponding to 100% equivalent cladding oxidation. The assumption of 72 hours is key to this limit.

While it is beyond the scope of this report to review NuScale's containment structural analysis, a few remarks are in order. It is important to the present review of NuScale's combustion analysis that [[ ]]$^{2\,(a),(c)}$ psia is indeed the final combustion-related result, for if the structural analysis were based on any other combustion-related peak pressure, then such results would need to be assessed. A reading of the containment structural analysis found in the latter half of Reference [2] allows the use of this pressure input ([[ ]]$^{2\,(a),(c)}$ psia) to be traced as far as its application to the TNT-equivalent method. (The TNT-equivalent method is briefly discussed below.) Further tracing in Reference [2] of quantities derived from [[ ]]$^{2\,(a),(c)}$ psia is intricate, making it hard to establish for certain that no other combustion-related pressure is being applied. To all appearances, [[ ]]$^{2\,(a),(c)}$ psia is the only combustion-related input, and all the subsequent containment vessel structural analysis appears to depend on it; however, this cannot be confirmed with certainty.

The main result of the analyses presented by the Applicant is the maximum (upper bound) detonation pressure of [[ ]]$^{2\,(a),(c)}$ bar-abs ([[ ]]$^{2\,(a),(c)}$ psia). The containment vessel design pressure used for Design Basis Accident (DBA) analyses is 1050 psia[5], while the ultimate pressure capacity is [[ ]]$^{2\,(a),(c)}$ psia[6]. Even though the containment vessel could not bear such a high static pressure (i.e., [[ ]]$^{2\,(a),(c)}$ psia), during the pressure pulse of estimated duration [[ ]]$^{2\,(a),(c)}$ milliseconds, the strain remains below the yield strain. The pulse duration is found by the TNT-equivalent method. According to this method, a hydrogen detonation that attains a pressure of [[ ]]$^{2\,(a),(c)}$ psia may be considered equivalent to a TNT detonation that attains [[ ]]$^{2\,(a),(c)}$ psia. The pulse duration of the equivalent TNT detonation can be estimated by a referenced method; [[ ]]$^{2\,(a),(c)}$ milliseconds is obtained. Beyond this point, the structural analysis reported in Reference [2] is not assessed/considered herein. The conclusion of the NuScale containment structural analysis appears to be that a dynamic pressure of magnitude [[ ]]$^{2\,(a),(c)}$ psia applied to the containment vessel for [[ ]]$^{2\,(a),(c)}$ millisecond induces a strain that is less than the yield strain.

In response to recent the NRC Requests for Additional Information (RAI), NuScale stated its intention to update Chapter 19 of the FSAR [11] with another datum found, it is presumed, by the same method as has been described above. The new datum applies at 45 days since the start of the transient; this time is used for computation of the radiolysis-generated inventories of hydrogen and oxygen. Hydrogen attributed to core oxidation is added in such amount as makes the containment oxygen mole fraction equal to 0.05. The calculations performed as part of the present study give 5040 moles of radiolysis-generated hydrogen, and 113 kg of oxidation-generated hydrogen. (That hydrogen mass is 121% of the cladding equivalent amount, 93.3 kg, that NuScale uses for 10 CFR 50.44 considerations). When updated, based on the NuScale mark-up (see response to RAI-9022, dated October 2017), Chapter 19 of the FSAR is expected to report AICC pressure of 920 psia, although from the pre-combustion atmospheric conditions computed by ERI, 676 psia is calculated for AICC pressure. The mark-up to Chapter 19 of the FSAR notes that 920 psia is less than the design pressure. Furthermore, the mark-up to Chapter 19 does not discuss enhancing this 45-day AICC pressure by a factor so as to estimate the corresponding detonation pressure. The present

[5] See January 2019 Response to RAI 9482 (ADAMS accession number ML19028A413).

[6] FSAR Rev 0, Section 3.8.2.4.5 states "The pressurizer access cover is determined to be the most limiting location and a flange gap of 0.03 inches is reached at the outer O-ring of the pressurizer access flange at an approximate pressure of [[ ]]$^{2\,(a),(c)}$ psi.".

report includes confirmatory calculations of combustion events at long times; see Section 3.4. There it is discussed that a MELCOR simulation predicts that, given 110% oxidation of the cladding, oxygen mole fraction equal to 0.05 is reached at 42 days, closely agreeing with the Applicant's prediction.

2.3 Factors Used to Estimate Detonation Pressure

The multiplier [[ ]]$^{2\,(a),(c)}$ (i.e., [[ ]]$^{2\,(a),(c)}$) discussed in the previous section as applied by NuScale to the AICC pressure to obtain an approximation to the detonation pressure appears to be consistent with the NuScale-cited studies. A limited discussion of this multiplier is included in the present section. Alternative methods for estimating detonation pressure are discussed in Section 4.3 (where the context is combustion occurring outside the containment vessel, under the bio-shield).

The factor [[ ]]$^{2\,(a),(c)}$ is used to estimate the Chapman-Jouguet pressure from the deflagration pressure. Reference [3] cites the work of Shepherd in Reference [5] for the factor [[ ]]$^{2\,(a),(c)}$, while Reference [6] is cited as part of the approximate method used by Reference [3] to obtain the deflagration pressure (i.e., AICC pressure) from the pre-burn pressure.

The factor [[ ]]$^{2\,(a),(c)}$ is used to estimate the reflected pressure from the Chapman-Jouguet pressure. Reference [3] cites Reference [7] for a formula giving this factor as a function of the specific heat ratio (γ factor) of the burned gas in the Chapman-Jouguet state. The γ factor itself is taken as [[ ]]$^{2\,(a),(c)}$ independent of pressure, for which value Reference [3] cites Reference [8].

The factor [[ ]]$^{2\,(a),(c)}$ is used to estimate the amplification by the deflagration-to-detonation transition. Reference [5] is cited for the value [[ ]]$^{2\,(a),(c)}$.

Whereas the AICC pressure is a thermodynamic quantity that can be calculated for any mixture, it is another matter whether a given mixture is detonable. The Applicant does not establish detonability, but conservatively assumes it. In Reference [3], the multiplier [[ ]]$^{2\,(a),(c)}$ has been applied to [[ ]]$^{2\,(a),(c)}$ psia to give the main result, [[ ]]$^{2\,(a),(c)}$ psia for the bounding combustion pressure including detonation effects. Here, [[ ]]$^{2\,(a),(c)}$ psia is the Applicant's approximately calculated AICC pressure for the mixture that the Applicant predicts for the containment at 72 hours. The composition of this mixture is not stated in Reference [3], but the composition at 24 hours is given there and those values are reproduced in footnote 4 of the present report. Also, line 2 of Table 3.2 gives the 72-hour composition, as calculated by ERI following NuScale's methods in exact accord with their description in Reference [3]. The oxygen concentration found by ERI is [[ ]]$^{2\,(a),(c)}$. (The 24-hour value, given explicitly in Reference [3], is [[ ]]$^{2\,(a),(c)}$.) A commonly used lower limit of oxygen concentration for flammability is 0.05. Therefore, the 72-hour mixture, at the extreme endpoint of the range of flammability, is likely to be actually not detonable. If so, the Applicant's estimated detonation pressure is viewed as an extrapolation of the detonation pressures of mixtures that are actually detonable. This extrapolation is considered as conservative.

Intentionally left blank

3. CONFIRMATORY ANALYSIS OF AICC PRESSURE

3.1 Scenario LCC-05T-03 (Variant with ECCS Activation After Core Damage)

In this section, a MELCOR calculation is used to critique the NuScale method for computing the pre-combustion containment conditions. It is these pre-combustion conditions that then, through further analysis, lead to NuScale's adopted value [[ ]]$^{2\,(a),(c)}$ psia ([[ ]]$^{2\,(a),(c)}$ bar-abs) for the bounding detonation pressure. The MELCOR calculation is intended to verify the NuScale's assignment of the pre-combustion conditions.

In review of NuScale's computation of the pre-combustion containment conditions, NuScale assumed that:

- The computation should be referred to 72 hours since reactor trip;
- The cumulative amounts of radiolytic hydrogen and oxygen generated to that time according to Eq. (1) are contained in the containment atmosphere whose volume is V;
- For V, the total containment volume is used (the volume occupied by water is neglected);
- The temperature of the containment atmosphere is [[ ]]$^{2\,(a),(c)}$ °F; and
- The containment volume, V, also includes:
  - The initial amounts of oxygen and nitrogen,
  - Steam at the [[ ]]$^{2\,(a),(c)}$ corresponding to [[ ]]$^{2\,(a),(c)}$ °F,
  - The hydrogen that has been generated by cladding oxidation, whose amount is fixed such that it results in an oxygen mole fraction of 0.05, given the other gas masses that are determined by the previous bullets.

The time dependence of Equation (1), plus the imposed time dependence for the cumulative cladding oxidation, imply that prior to 72 hours the containment atmosphere is inflammable due to oxygen concentration less than 0.05. Flammability arises at 72 hours due to the cumulative oxygen mass generated by radiolysis; the particular oxygen concentration of 0.05 at that time reflects the imposed cumulative amount of hydrogen generated by cladding oxidation.

Matching some of the above bullets, the MELCOR simulation computes the containment conditions at 72 hours in a scenario wherein the hydrogen generated by cladding oxidation has been curtailed prior to 72 hours such that the final (72 hour) mole fraction for the containment oxygen is 0.05. The containment water level and the containment atmosphere temperature are also calculated, allowing to assess the effects of NuScale's assumptions (i.e., the dictated temperature and the neglect of the volume of water in the containment). Differences between the pre-combustion containment conditions as predicted by MELCOR versus as predicted by NuScale's method and assumptions are assessed through their effect on the AICC pressure, which is computed from the pre-combustion conditions using the ERPRA-BURN computer code.

The scenario adopted for the MELCOR calculation is a variant of scenario LCC-05T-03 described by NuScale in Chapter 19 of the FSAR [11]. It is a variant because of the late (post-core-damage) activation of ECCS, added to the scenario by ERI as a plausible way of curtailing core oxidation. 72 hours is accepted as the time at which to consider combustion because a long time favors oxygen availability due to radiolysis, and may be consistent with regulatory requirements. (But see Section 3.4 for an extension to times as long as 60 days.) Curtailment of cladding oxidation is required because, without it, the preponderance of hydrogen results in oxygen-depleted conditions continuing longer than 72 hours, despite the radiolytic generation of oxygen.

Scenario LCC-05T-03 considers a Chemical Volume Control System (CVCS) line break inside containment. The elevation is near the top of the containment vessel. The flow area is 20% of the area of a circle of 1-inch diameter. (Although the CVCS line is a pipe of approximate ID 2", the MELCOR model follows an NRC November 2017 email directive to use 0.785 in^2 for the base break flow area – see Section 4.1 for more specific designation of this email.

For the further reduction to 20% of the corresponding area, Chapter 19 of the FSAR [11] has been followed. The reduced break flow area increases the time that the fuel rods may undergo oxidation, and could arise, for example, in a fish-mouth break of the pipe.) In the scenario version discussed in Chapter 19 of the FSAR, there is no ECCS activation (i.e., no RVV or RRV valves ever open). The present simulation chose to consider scenario LCC-05T-03 because, among several scenarios that are discussed in Chapter 19 of the FSAR, it yields the highest containment oxygen concentration. (See Figure 19.2-10 from the FSAR for the comparison of LCC-05T-03 with several other scenarios). As simulated by NuScale with no ECCS activation, the maximum oxygen mole fraction is about [[ ]]$^{2\,(a),(c)}$. This high peak oxygen concentration (relative to other scenarios) is due to the relatively small break, which results in less steam dilution of the initial containment oxygen. In the NuScale simulation of LCC-05T-03, the oxygen concentration falls rapidly from the peak value shortly after the onset of core oxidation, due to dilution by hydrogen. In particular, the oxygen concentration is always below 0.05, so the gas mixture is never flammable. In the present variant of LCC-05T-03, one RVV valve and one RRV valve are opened at a time selected to give the desired final result ([[ ]]$^{2\,(a),(c)}$ containment oxygen mole fraction at 72 hours) due to the resulting cessation of oxidation. Until that time, the oxidation proceeds according to the metal-steam reaction model in MELCOR.

The specifics of the present MELCOR include:

- The total containment volume is [[ ]]$^{2\,(a),(c)}$ m^3 (in comparison, the NuScale value used in Reference [3] as reported in Section 2 of this report is [[ ]]$^{2\,(a),(c)}$ m^3)[7]
- Initial atmosphere composition (mole fraction) consists of 0.79 nitrogen, 0.21 oxygen, no water or water vapor. The initial pressure and temperature are [[ ]]$^{2\,(a),(c)}$ bar-abs ([[ ]]$^{2\,(a),(c)}$ psia) and 37.8 °C (100.0 °F). (In comparison the NuScale values used in Reference [3] are 0.655 bar-abs [9.5 psia] and 10 °C [50.0 °F].)
- Total reactor vessel primary-side volume is [[ ]]$^{2\,(a),(c)}$ m^3, of which the initial steam volume is [[ ]]$^{2\,(a),(c)}$ m^3
- Radiolytic sources of hydrogen and oxygen governed by Eq. (1) enter the conical transition region of the riser (modeled by control volumes [CV] 171 and 172, see the Appendix)
- The CVCS line break flow path connects the top of the riser[8] (modeled by CV191, see the Appendix) to the containment at that same elevation.

For tests of the NuScale method via comparison with present MELCOR results, the MELCOR value for the dry containment volume of [[ ]]$^{2\,(a),(c)}$ m^3 is used with the NuScale method. The initial containment pressure 0.655 bar-abs (9.5 psia) used in Reference [3] to derive the final result (bounding detonation pressure [[ ]]$^{2\,(a),(c)}$ bar-abs) appears to be conservative because it overestimates the initially available oxygen. Not used here are the initial masses in the containment for various gases used with NuScale's method, instead they are taken from the present MELCOR calculation and they reflect the initial MELCOR containment pressure of [[ ]]$^{2\,(a),(c)}$ bar-abs ([[ ]]$^{2\,(a),(c)}$ psia). The initial containment pressure of [[ ]]$^{2\,(a),(c)}$ psia is cited in several ERR documents (while it is noted that the value specified in NuScale's NRELAP model, [[ ]]$^{2\,(a),(c)}$ psia, is even smaller).

The initial containment pressure and temperature are assumed by ERI to describe a pre-power-up condition when the reactor is sub-critical: both sets of initial containment data (i.e., those used in the present MELCOR model and those reported in Reference [3]) are interpreted this way. In the present MELCOR calculation, these initial data apply, not at time zero, but at t = -1000 s (i.e., at the start of the pre-transient part of the calculation that models normal steady-

[7] As of November 2018, it is known that for design basis accident analyses, the Applicant is using [[ ]]$^{2\,(a),(c)}$ m^3 = [[ ]]$^{2\,(a),(c)}$ ft^3 for the containment volume. [[ ]]$^{2\,(a),(c)}$ m^3 is adopted for Revision 9 of the present MELCOR model, and also is used here for the present simulation of the LCC-05T-03 scenario by an otherwise earlier version of the model that included the radiolytic sources. The radiolytic sources were not carried forward into Revisions 8 or 9, but Revision 10 (see Section 3.4) has restored them.

[8] It has been pointed out that the CVCS line penetrates the RPV near the bottom of the riser, so the correct name for the modelled higher-elevation break may be RCS discharge line break.

state operating conditions). By the end of the pre-transient calculation, the containment pressure and temperature are steady at higher values (i.e., [[ ]]$^{2\,(a),\,(c)}$ psia, [[ ]]$^{2\,(a),\,(c)}$ °C) that reflect RPV vessel heat loss, but the containment gas masses, which are inputs to NuScale's method, do not change during the pre-transient calculation. The last two of the above bullets may bear on present MELCOR prediction of the hydrogen and oxygen held up in the reactor vessel at long times, which is further discussed below.

For orientation, Figures 3.1 through 3.5 show the progression of the accident up to 72 hours. Hydrogen combustion events are intentionally suppressed in the containment until 72 hours. Reactor scram and closure of the feedwater and steam line isolation valves are assumed to occur at time zero, co-incident with the opening of the CVCS line break. The core water level falls to the top of the active fuel at 30.94 hours, and hydrogen generation by steam-oxidation of the zirconium and steel structures in the core begins at about 43 hours. At about 44.4 hours, the core water level falls so low as to unblock the lower core region, and this uncovery initiates a period of steam cooling during which oxidation is much reduced. This period ends, and at 49.38 hours the cumulative generation of hydrogen by oxidation attains [[ ]]$^{2\,(a),\,(c)}$ kg. For orientation, this amount is 19% of the value, 93.3 kg, that NuScale uses for consideration of compliance with CFR Part 50.44 (i.e., the hydrogen mass generated by steam-oxidation of 100% of the cladding associated with the active fuel). Via some preliminary trials, [[ ]]$^{2\,(a),\,(c)}$ kg has been found to be the amount of oxidation-generated hydrogen that yields approximately 0.05 for the containment oxygen molar concentration at 72 hours. Therefore, ECCS is activated at 49.38 hours, with ECCS consisting in this case of one opened RVV and one opened RRV. Moreover, a MELCOR modeling switch is exercised to turn off any further oxidation[9]. The calculation is run without further intervention to 72 hours, during which time a quasi-steady state condition is achieved.

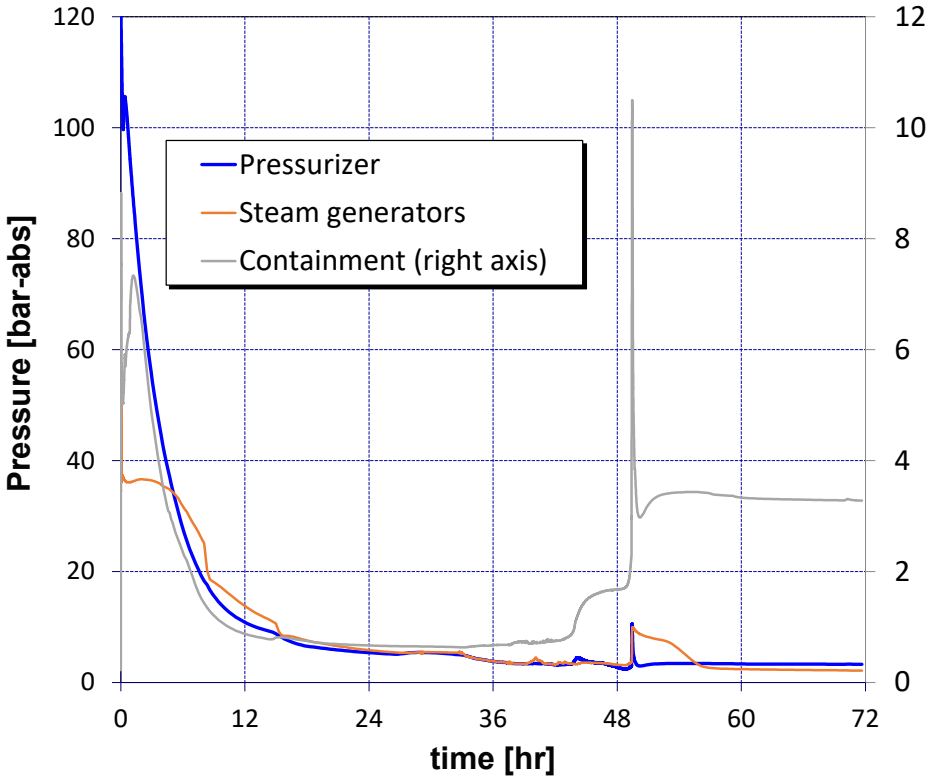

Figure 3.1 Primary, secondary coolant systems and containment pressures

[9] This unphysical treatment, i.e., forcing the curtailment of the oxidation to be simultaneous with the start of ECCS action, is convenient and of insignificant final impact. ECCS action soon re-covers the core with water and would bring about the curtailment naturally. A side calculation with ECCS actuation but without artificial curtailment established that natural curtailment occurs within about 10 minutes. User-dictated curtailment makes it easier to arrive at the desired 72-hour oxygen concentration without many trial and error calculations and leads to the same 72-hour end-state.

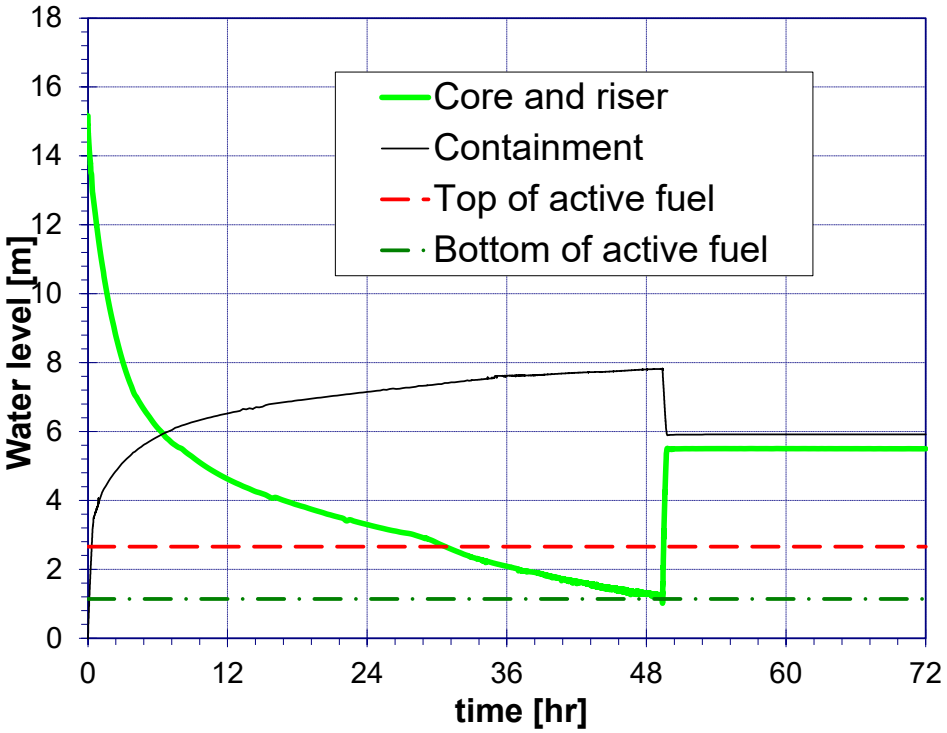

Figure 3.2 RPV and containment water levels

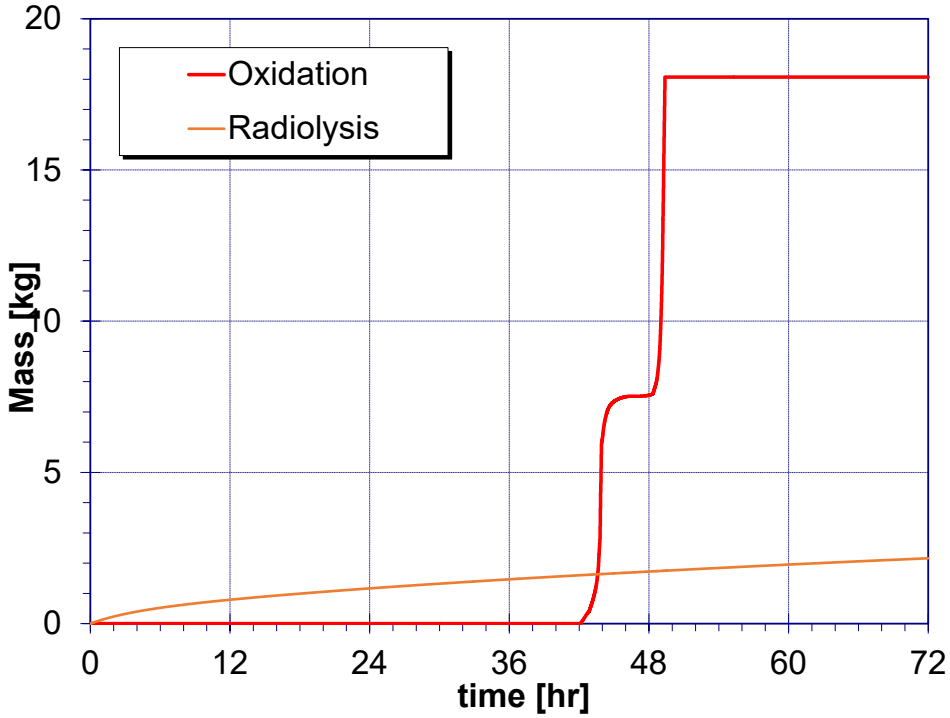

Figure 3.3 Cumulative hydrogen generated by cladding oxidation and radiolysis

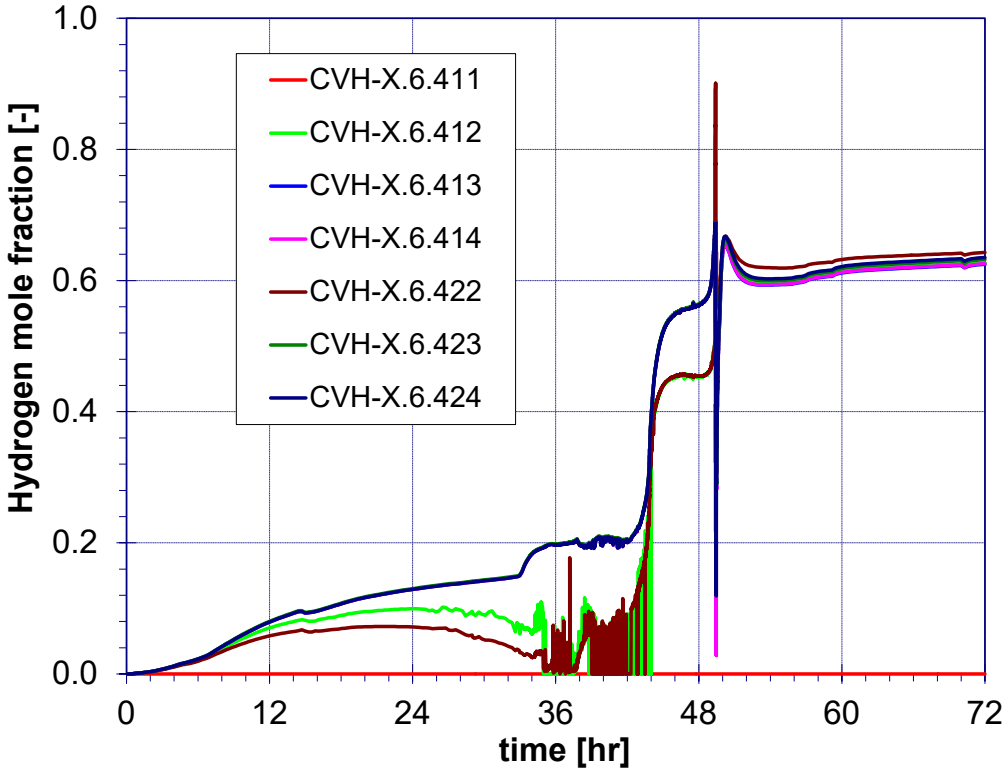

Figure 3.4 Spatial dependence of containment hydrogen concentration

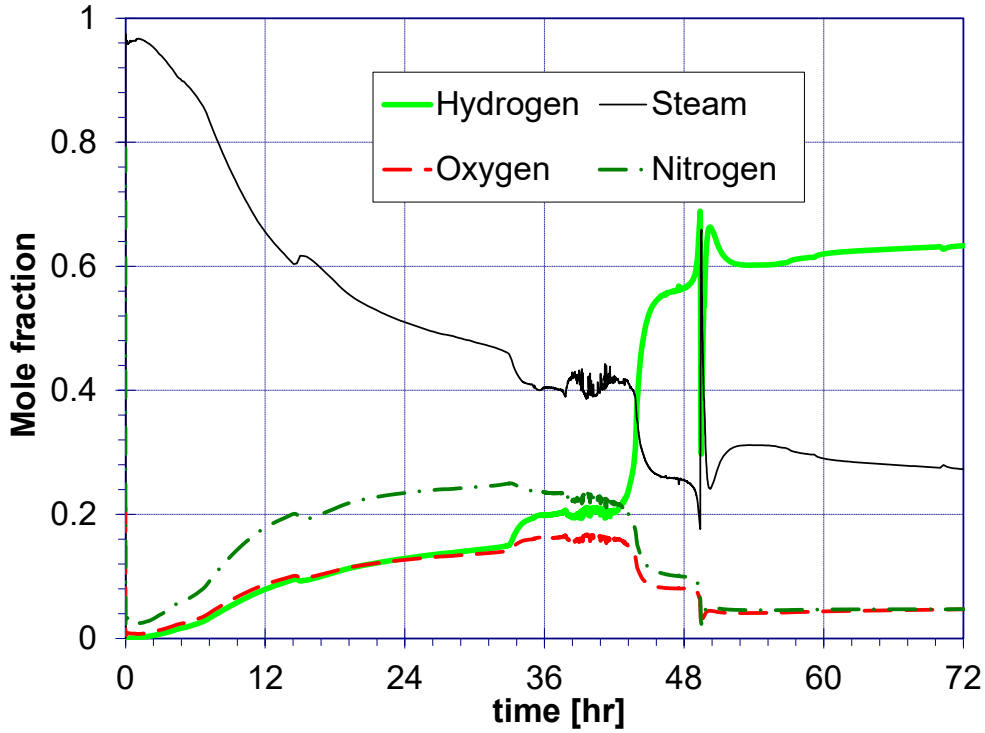

Figure 3.5 Control-volume-averaged containment atmosphere composition

The MELCOR-predicted quantities of chief interest are the final (72 hours) pre-burn containment atmospheric conditions (i.e., pressure, temperature, composition, and gas volume). Also of interest is the temperature of the containment water. These quantities are given by the first line of Table 3.1, along with the AICC pressure and temperature (which are determined by the pre-burn pressure, temperature, and composition, which are the inputs to ERPRA-BURN). The AICC calculation results are 11.12 bar-abs and 1316K. It is noteworthy that the containment pressure peak produced by opening the ECCS valves at 49.38 hours (see Figure 3.1) is similar to the ERPRA-BURN computed AICC pressure associated with the MELCOR-predicted atmospheric conditions arising at 72 hours. No MELCOR-predicted combustion events are reflected in Figure 3.1 (hydrogen combustion is suppressed until after 72 hours).

The desired 72-hour oxygen mole fraction, 0.05, was not precisely obtained; instead, 0.0470 was obtained for the CV-averaged fraction. A closer value could be obtained by choosing a slightly earlier time for the activation of ECCS and thus the cessation of core oxidation at somewhat less than [[ ]]$^{2\,(a),(c)}$ kg of cumulative hydrogen production. In fact, the obtained oxygen mole fraction does not support combustion, which is usually considered to require at least 0.05. This shortfall necessitates an adjustment of the default inputs to ERPRA-BURN, which normally carries out the AICC calculation only if the oxygen concentration exceeds 0.050. (The adjustment is to set the lower limit to 0.0460.) Although 0.05 was aimed at to reproduce the assumption of the Applicant's analyses, this inadequacy does not affect the intended purpose of the calculation, which is to verify NuScale's approximate method for predicting the pre-burn containment conditions, relative to the present MELCOR results, in an appropriate scenario. In effect, the approximate method is judged by how nearly it predicts 0.0470 for the oxygen mole fraction, and the fact that the present MELCOR value is not precisely the desired target is not a serious drawback. The criterion for judging the acceptability of the approximate method is the effect of any error on AICC pressure, and AICC calculations can be carried out for any gas mixture, whether actually flammable or not.

The remaining lines of Table 3.1 test the accuracy of the NuScale method for computing the pre-combustion conditions. The second line uses the NuScale method just as NuScale has done. In this line, the containment atmosphere volume is marked with colored font because, according to the NuScale method, the volume of the dry containment, [[ ]]$^{2\,(a),(c)}$ m^3 (MELCOR model value, not the Reference [3] value which is [[ ]]$^{2\,(a),(c)}$ m^3), has been dictated as the gas volume. Also indicated by blue font as an assumed input is the dictated containment atmosphere temperature, which is [[ ]]$^{2\,(a),(c)}$ °C ([[ ]]$^{2\,(a),(c)}$ °F) according to the NuScale method. The third, fourth, and fifth lines relax the assumptions by replacing some dictated values by the MELCOR-predicted values. Not listed in lines 2 through 5 as inputs to NuScale's method are the dictated 72-hour amounts of hydrogen and oxygen due to radiolysis and cladding oxidation, and the pre-power-up containment pressure and temperature. In all of lines 2 through 5, these quantities are: [[ ]]$^{2\,(a),(c)}$ kg of hydrogen from oxidation; [[ ]]$^{2\,(a),(c)}$ gram-moles of oxygen and [[ ]]$^{2\,(a),(c)}$ gram-moles from radiolysis; [[ ]]$^{2\,(a),(c)}$ bar-abs ([[ ]]$^{2\,(a),(c)}$ psia) and [[ ]]$^{2\,(a),(c)}$ °C ([[ ]]$^{2\,(a),(c)}$ °F). Note that the last two quantities agree with the MELCOR model and not with the values used in Reference [3] (i.e., 9.5 psia and 50 °F). Also, according to the method used by NuScale, the containment steam partial pressure is the saturation pressure at the specified containment gas temperature. The rest of the approach by NuScale is the simple application of the ideal gas law to these inputs. The resulting total (pre-burn) pressure and molar compositions are the outputs of the analysis. For each line, Table 3.1 also gives the corresponding AICC pressure and temperature as computed by ERPRA-BURN. Line 2 shows that, for this scenario, the two marked assumptions by the Applicant, considered together, are non-conservative for the AICC pressure, relative to the present MELCOR prediction.

To test individually for conservatism the assumptions about containment gas volume and temperature, the third and fourth lines of Table 3.1 are provided. These lines each use one assumed value, marked with blue font, and one MELCOR-predicted value, not marked. Line 3 shows that dictating the containment temperature as [[ ]]$^{2\,(a),(c)}$ °C ([[ ]]$^{2\,(a),(c)}$ °F), which is lower than the MELCOR-predicted value (96.5 °C), results in a lower AICC pressure relative to MELCOR, i.e., is non-conservative. Line 4 shows that dictating the containment gas volume as [[ ]]$^{2\,(a),(c)}$ m^3, which is the dry containment volume and thus neglects the free volume reduction due to water build-up (28.2 m^3 according to MELCOR), also lowers the AICC pressure and thus is non-conservative. Of the two quantities assigned by assumption, the neglect of the water volume has the bigger effect on AICC pressure. For the pre-burn pressure, the effect of assumed temperature is bigger.

Lines 2 and 3 are the ones that assume the low containment atmosphere temperature, [[ ]][2 (a), (c)] °C. This assumption yields the highest AICC temperatures tabulated in Table 3.1. This is because of the resulting lower pre-burn steam content. Such steam acts as a heat sink that moderates the AICC temperature.

For completeness, line 5 of Table 3.1 uses the NuScale method but takes the present MELCOR-predicted values for both the containment gas volume and the gas temperature as inputs. The remaining assumptions included in line 5 are only that the problem's entire pre-specified inventories of non-condensable gases reside in the containment; that the steam there is saturated at the present MELCOR-predicted containment atmosphere temperature; and that the ideal gas law applies to the non-condensable gases. These assumptions are common to all applications of the NuScale method; therefore, for the most un-ambiguous evaluation of the separate effects of the assumed containment gas temperature and gas volume, lines 3 and 4 are best compared to line 5. As comparison of line 5 with line 1 shows, these common assumptions turn out to be fairly good for predicting the MELCOR results, although as is discussed below MELCOR predicts that there are small amounts of hydrogen and oxygen held up in the vessel, contrary to the first of these assumptions. The lower MELCOR-predicted pre-combustion pressure (line 1) may reflect that the water is predicted by MELCOR to be significantly cooler than the atmosphere, while a part of the NuScale method is that the steam partial pressure is the saturation pressure calculated at the atmosphere temperature. The AICC pressure associated with line 5 is somewhat higher than that of line 1, which is attributed to non-condensable gases held up in the vessel (MELCOR, line 1) versus the assumption of no such hold-up (NuScale method, line 5). Line 1 does not use the NuScale method at all: there the pre-burn containment gas pressure, temperature, and composition are taken directly from MELCOR for use in the ERPRA-BURN calculation.

The present MELCOR simulation makes a prediction for hydrogen and oxygen held up in the vessel at long times. Whereas at 72 hours there is 19.3 kg of hydrogen and 22.9 kg of oxygen in the containment, MELCOR predicts the hold-ups in the RPV as 0.95 kg of hydrogen and 0.36 kg of oxygen. (At 72 hours, the nitrogen mass in the vessel is ~1×10^{-7} kg.) These noncondensible gases are almost entirely located above the water line in the lower, radially-outward parts of the reactor vessel, i.e., the downcomer and the lower parts of the primary side of the steam generators. Almost none is located in the upper parts of the primary side of the steam generators, or elsewhere. The radiolytic sources add hydrogen and oxygen to the conical part of the riser, which is above the core and near the RPV centerline. Other locations relevant to the hold-up are the RRV inlet (submerged in the downcomer water), the break (from the top of the riser) and the RVV inlet (from the pressurizer). While some hold-up may occur actually (it is reasonable that bubbles may be trapped beneath various structures), the precise value predicted by MELCOR should not be given much credence. In particular, the location of the hold-up (lower parts of the primary side of the steam generators) appears spurious: no obvious reasons explain why the noncondensible gases cannot mix into the upper regions of the steam generators, and then leave the vessel through the RVV. Provided that the true containment gas volume is used, the neglect of the hold-up of hydrogen and oxygen in the reactor vessel by the NuScale method is conservative for AICC pressure purposes (compare lines 1 and 5 of Table 3.1).

Table 3.1 MELCOR results at 72 hours for ERI's variant of Scenario LCC-05T-03 (with dry containment volume [[ ]]$^{2\,(a),(c)}$ m^3) *

#	Pre-burn containment conditions								Post-burn containment conditions (by ERPRA-BURN)	
	Gas pressure (bar-abs)	Gas temperature (°C)	Gas volume (m^3)	Water temperature (°C)	Gas composition (mole fraction)				AICC pressure (bar-abs)	AICC temperature (K)
					N_2	O_2	H_2O	H_2		
Line 1 reports MELCOR predictions for the pre-burn pressure, temperature, and composition.										
1+	3.276	96.46	[[ ]]$^{2\,(a),(c)}$	82.3	0.0470	0.0470	0.2728	0.6332	11.12	1316
In lines 2 through 5, the NuScale method is used to predict pre-burn pressure and composition, with assumed values marked with blue font.										
2	2.173	[[ ]]$^{2\,(a),(c)}$	[[ ]]$^{2\,(a),(c)}$	–	0.0546	0.0557	0.1181	0.7715	9.16	1512
3	2.554	[[ ]]$^{2\,(a),(c)}$	[[ ]]$^{2\,(a),(c)}$	–	0.0557	0.0568	0.1005	0.7870	10.96	1541
4	2.983	96.5	[[ ]]$^{2\,(a),(c)}$	–	0.0434	0.0443	0.2989	0.6133	9.72	1260
5	3.399	96.5	[[ ]]$^{2\,(a),(c)}$	–	0.0457	0.0466	0.2623	0.6454	11.51	1313

* Initial nitrogen and oxygen inventories reflect pre-power-up pressure [[ ]]$^{2\,(a),(c)}$ psia and temperature [[ ]]$^{2\,(a),(c)}$ °C. Cumulative hydrogen produced by oxidation: [[ ]]$^{2\,(a),(c)}$ kg.

+ MELCOR predictions for pre-burn conditions. Gas temperature and pressure are evaluated in CV423; liquid water temperature in CV422. Mole fractions are computed from the gas masses in the whole containment.

Table 3.2 AICC calculations for mixtures of specified pre-burn composition, based on the NuScale method (with dry containment volume [[ ]]$^{2\,(a),(c)}$ m^3)

#	O_2 from radiolysis (gram-moles)	H_2 from oxidation (kg)	Pre-burn temperature (°C)	Containment water volume (m^3)	Pre-burn pressure (bar-abs)	Pre-burn composition (mole fraction)				Post-burn AICC Pressure (bar-abs)	Post-burn AICC temperature (K)
						N_2	O_2	H_2O	H_2		
1+	288.2 [t = 24 hr]	[[ ]]$^{2\,(a),(c)}$ [fraction [[ ]]$^{2\,(a),(c)}$]	[[ ]]$^{2\,(a),(c)}$	[[ ]]$^{2\,(a),(c)}$	[[ ]]$^{2\,(a),(c)}$	[[ ]]$^{2\,(a),(c)}$	[[ ]]$^{2\,(a),(c)}$	[[ ]]$^{2\,(a),(c)}$	[[ ]]$^{2\,(a),(c)}$	16.8	1420
2+	540.0 [t = 72 hr]	[[ ]]$^{2\,(a),(c)}$ [fraction [[ ]]$^{2\,(a),(c)}$]	[[ ]]$^{2\,(a),(c)}$	[[ ]]$^{2\,(a),(c)}$	[[ ]]$^{2\,(a),(c)}$	[[ ]]$^{2\,(a),(c)}$	[[ ]]$^{2\,(a),(c)}$	[[ ]]$^{2\,(a),(c)}$	[[ ]]$^{2\,(a),(c)}$	20.2	1429
3§	540.0 [t = 72 hr]	[[ ]]$^{2\,(a),(c)}$ [fraction [[ ]]$^{2\,(a),(c)}$]	96.5	28.2	7.1	0.1134	0.0463	0.1252	0.7152	24.8	1350

* Initial nitrogen and oxygen inventories reflect pre-power-up pressure 9.5 psia and temperature 10 °C.
+ Lines 1 and 2 reproduce NuScale calculations [3] of pre-burn conditions at 24 and 72 hours.
§ Line 3 re-calculates line 2 with MELCOR-informed values replacing NuScale's non-conservative assumed values (in blue font in line 2).

As has been discussed, the simulation suppresses deflagrations in the containment until 72 hours; the AICC pressure has been calculated at that time. Then the simulation is extended for a final ~5 minutes enabling hydrogen deflagration events to occur. The MELCOR-predicted deflagration pressure may be of interest, although its regulatory significance, if any, is unclear. (Recall, detonations, much more than deflagrations, can pose a challenge to containment integrity; established methods for approximately estimating detonation pressure begin with calculating the AICC pressure; detonations are little affected by heat sinks and expansions (into the RPV) that may mitigate actual deflagration pressure relative to AICC pressure.) In the calculation, burns, suppressed until 72 hours, are enabled at that time. With that enabling is a re-specification of the minimum oxygen concentration, set in MELCOR by default to 0.050, to 0.045, so that all the predicted containment atmosphere, with local oxygen concentrations as low as [[ ]]$^{2\,(a),(c)}$, can burn. The burn lasts about 0.6 seconds and consumes 2.9 kg of hydrogen. Before and after the burn, the amounts of hydrogen in the containment are 19.3 and 15.7 kg. The inventory reduction, 3.6 kg, is greater than the consumed amount, 2.9 kg, because of unburned hydrogen that is pushed into the RPV. The containment oxygen mass is reduced from 22.9 kg pre-burn to zero post-burn. The peak containment pressure is 10.7 bar-abs, less than the AICC pressure (11.1 bar-abs) due to the heat sink provided by the vessel and containment heat structures, and to gas expansion into the vessel. Many past calculations have established that, absent such heat sinks and possibilities of expansion into the RPV, MELCOR-predicted deflagration pressures agree with ERPRA-BURN-predicted AICC pressures.

The main conclusions of this sub-section are that:

- NuScale's method becomes increasingly non-conservative as the assumed values for the containment gas temperature and containment water volume are reduced;
- Unless the scenario (LCC-05T-03, variant with ECCS activation after core damage) considered herein is deemed implausible, the containment atmosphere temperature and water volume values should not be assumed any lower than 96.5 °C and 28.2 m^3, respectively; and
- NuScale has assumed [[ ]]$^{2\,(a),(c)}$ °C and [[ ]]$^{2\,(a),(c)}$ m^3.

It should be noted that the MELCOR results for the containment atmosphere temperature and water volume (96.5 °C and 28.2 m^3, respectively), apply with a containment of total volume [[ ]]$^{2\,(a),(c)}$ m^3 (NuScale uses [[ ]]$^{2\,(a),(c)}$ m^3 when applying the NuScale method), and an RPV of total volume [[ ]]$^{2\,(a),(c)}$ m^3, of which the initial steam volume is [[ ]]$^{2\,(a),(c)}$ m^3. The MELCOR results also reflect [[ ]]$^{2\,(a),(c)}$ psia for the pre-power-up containment pressure.

3.2 Other Variants of Scenario LCC-05T-03

Results from the simulation of two variants of the accident scenario analyzed in Section 3.1 are briefly discussed here. Both variant simulations yield lower 72-hour AICC pressures than does the base case, consistent with the use of the base-case version as a bounding scenario for evaluation of the NuScale method. One of the variant scenarios, however, yields a higher AICC temperature than does the base case.

The dependence on containment gas volume studied in Section 3.1 suggests that a higher AICC pressure may result in a scenario that considers containment combustion while there is a greater amount of water in the containment (i.e., greater than the 28.2 m^3 found for the scenario considered in Section 3.1). Since ECCS activation returns much of the water inside the containment to the reactor vessel, scenarios that consider combustion prior to ECCS activation may be contemplated. Generally, cladding oxidation has to be suppressed to avoid inerting of the containment atmosphere, except perhaps at the earliest times, by oxygen dilution due to high hydrogen concentrations. However, curtailment of cladding oxidation without ECCS activation is implausible. Therefore, an LCC-05T-03 variant is considered in which ECCS is not activated, but combustion in the containment is considered before the containment atmosphere becomes oxygen-depleted.

The calculation is identical to the base case (described in Section 3.1) up until 49.38 hours, when ECCS is activated (and the core oxidation model is disabled) in the base case. In the variant, the calculation continues from 49.38 hours

with no ECCS and with ongoing oxidation, until 72 hours, with burning suppressed. The time of maximum AICC pressure for a containment deflagration, subject to the requirement that the CV-averaged containment oxygen mole fraction is at least 0.05, is found to be 49.56 hours. In fact the oxygen mole fraction falls through 0.05 precisely at this time. Cumulative hydrogen generation to this time is 25.4 kg. At this time, the volume of water in the containment is 42.8 m^3, thus the desire for a smaller containment atmosphere is achieved. The AICC pressure for a containment combustion event at this time is 10.40 bar-abs. This is less than in the base case (although for the base case calculation the requirement of at least 0.05 oxygen mole fraction was relaxed: that calculation was made at 0.0460 mole fraction oxygen for the purpose of evaluating the NuScale method for evaluating pre-burn atmospheric conditions). This is because the pressure gained in the variant case by the smaller gas volume is compensated by the loss of the greater amount of radiolytic-produced reactants included in the base case by virtue of the 72 hour time for the postulated combustion event in the base case.

The second variant is more similar to the scenario considered in Section 3.1, differing only in the timing of ECCS activation and thus in the final hydrogen generated by oxidation. In particular, like the base case, the postulated combustion event occurs at 72 hours, during the quasi-steady state provided for by ECCS action. The difference is an earlier timing for ECCS activation (and oxidation suppression), such that an approximately stoichiometric mixture of hydrogen and oxygen exists in the containment at the end of the calculation (72 hours). In some cases such mixtures could be more detonable, and/or could produce a higher flame temperature, than the situation considered in Section 3.1.

The calculation is identical to the one described for the base case, except that ECCS activation and oxidation suppression, which occur at 49.38 hours in the base case, now occur at 43.19 hours. Only 0.8 kg of hydrogen has been produced by oxidation. At 72 hours, the CV-averaged hydrogen and oxygen mole fractions are 0.214 and 0.108, respectively, i.e., are approximately stoichiometric. The hydrogen mass in containment is 2.9 kg, and approximately all of it would participate if the atmosphere were ignited since the mixture is approximately stoichiometric. Actually, the CV-averaged steam mole fraction is 0.572, making the mixture not flammable (mixtures with more than 55% steam are considered inert). An AICC calculation can still be made for this otherwise, steam-inerted containment vessel. The AICC pressure for a containment combustion event at this time is 7.29 bar-abs (much lower than the base case value); the AICC temperature is 2089K (much higher than the base case value).

3.3 Application of Findings to NuScale's Analyses

For 10 CFR 50.44 conformance, the key result of NuScale's analyses [3] is the calculation, by the method described in Section 2, of a pre-burn containment atmosphere whose AICC pressure is estimated by NuScale as [[ ]]$^{2\,(a),(c)}$ bar-abs. Through the use of the various factors discussed in Section 2, this estimated AICC pressure becomes the basis for the supposedly bounding estimate of the detonation pressure, [[ ]]$^{2\,(a),(c)}$ bar-abs ([[ ]]$^{2\,(a),(c)}$ psia), on which NuScale bases its structural analysis. This section includes a reproduction of NuScale's calculation of the pre-burn atmosphere parameters using NuScale's methods and assumptions, plus a re-calculation that reconsiders and/or corrects two of these assumptions using the findings of Section 3.1.

Table 3.2 shows applications of the NuScale method for predicting the pre-burn containment atmosphere conditions, plus the corresponding post-burn AICC pressures and temperatures as calculated by ERPRA-BURN. The first two lines reproduce calculations documented by NuScale [3]. As such, the dry containment volume is taken as [[ ]]$^{2\,(a),(c)}$ m^3, and the pre-at-power containment pressure and temperature are taken as 0.655 bar-abs (9.5 psia) and 10.0 °C (50.0 °F), respectively. These values differ from the ones used in Table 3.1 ([[ ]]$^{2\,(a),(c)}$ m^3; [[ ]]$^{2\,(a),(c)}$ psia; [[ ]]$^{2\,(a),(c)}$ °F), these being inputs to the present MELCOR model. NuScale's use of 9.5 psia (rather than [[ ]]$^{2\,(a),(c)}$ or [[ ]]$^{2\,(a),(c)}$ psia) as the initial pressure is especially notable because it implies a much larger initial inventory of oxygen.

According to NuScale, the first line of Table 3.2 applies 24 hours since the start of a transient. The conditions of this line have no final significance, because the conditions that yield the supposedly bounding detonation pressure hold at 72 hours. However, line 1 is included here because Reference [3] has a step-by-step description of the calculation at 24 hours (its essentials are reproduced in Section 2 of the present report), including all the detailed results (i.e., the

pre-burn containment atmosphere composition and pressure). All these details are not provided for the key calculation at 72 hours, so line 1 is included for the sake of ready comparison with NuScale's document. The present re-calculation using NuScale's method precisely reproduces the pre-burn pressure and composition that Reference [3] reports for 24 hours.

Line 2 of Table 3.2 applies at 72 hours and gives the key result for NuScale's conclusion of conformance with 10 CFR 50.44 requirements. According to the NuScale method, the containment atmosphere of prescribed volume [[ ]]$^{2\,(a),\,(c)}$ m^3 (i.e., the dry volume) and temperature [[ ]]$^{2\,(a),\,(c)}$ °C ([[ ]]$^{2\,(a),\,(c)}$ °F) holds the initial inventories of oxygen and nitrogen (which reflect pressure 9.5 psia, temperature 50.0 °F, and volume [[ ]]$^{2\,(a),\,(c)}$ m^3); the cumulative hydrogen and oxygen produced by radiolysis (which reflect Eq. (1) with t = 72 hours); and the cumulative hydrogen produced by of oxidation of [[ ]]$^{2\,(a),\,(c)}$% of the fuel cladding (which appears to reflect tuning to yield oxygen mole fraction of [[ ]]$^{2\,(a),\,(c)}$). The present re-calculation using the method precisely reproduces the pre-burn pressure that Reference [3] reports for 72 hours. The accurate post-burn AICC pressure (by ERPRA-BURN) is 20.2 bar-abs. NuScale uses an approximate approach to estimate the AICC pressure, reporting [[ ]]$^{2\,(a),\,(c)}$ bar-abs. With a factor [[ ]]$^{2\,(a),\,(c)}$ to account for DDT and reflection of detonation wave, [[ ]]$^{2\,(a),\,(c)}$ bar-abs becomes [[ ]]$^{2\,(a),\,(c)}$ psia, the key input to NuScale's structural analysis.

According to the insights provided by Section 3.1, the values assumed by NuScale at 72 hours for the containment gas temperature ([[ ]]$^{2\,(a),\,(c)}$ °C) and the containment gas volume reduction by water buildup ([[ ]]$^{2\,(a),\,(c)}$ m^3) are non-conservatively low in their effect on post-burn AICC pressure. Line 3 of Table 3.2 re-assigns the containment gas temperature as 96.5 °C and the containment gas volume reduced by water buildup as 28.2 m^3, these being the MELCOR results predicted for the LCC-05T-03 variant scenario documented in Section 3.1. (Note, those MELCOR results reflect a containment of dry volume of [[ ]]$^{2\,(a),\,(c)}$ m^3 and initial pressure of [[ ]]$^{2\,(a),\,(c)}$ psia.) The NuScale method is re-applied with this temperature and with containment gas volume of [[ ]]$^{2\,(a),\,(c)}$ m^3 ([[ ]]$^{2\,(a),\,(c)}$). With these adjustments, the NuScale method yields the pre-burn containment gas pressure and composition tabulated by line 3. The associated AICC pressure is 24.8 bar-abs.

The main conclusion of this sub-section is that, if NuScale's method is accepted without any changes except for the re-specification of two assumed values (containment gas temperature assumed as [[ ]]$^{2\,(a),\,(c)}$ °F, reduction of containment gas volume due to water build-up assumed as [[ ]]$^{2\,(a),\,(c)}$) by MELCOR-informed values, the AICC pressure is increased from [[ ]]$^{2\,(a),\,(c)}$ bar-abs to 24.8 bar-abs. Accepting the factor [[ ]]$^{2\,(a),\,(c)}$ that NuScale uses to represent DDT and reflected detonation wave, the bounding detonation pressure is not lower than [[ ]]$^{2\,(a),\,(c)}$ bar-abs ([[ ]]$^{2\,(a),\,(c)}$ psia). NuScale has carried out the structural analysis using [[ ]]$^{2\,(a),\,(c)}$ psia as the detonation pressure.

This sub-section has adopted NuScale's value for the initial containment pressure, 9.5 psia, which is listed in Reference [3]. If [[ ]]$^{2\,(a),\,(c)}$ psia, listed in several ERR documents, is used instead, then either of lines 1 of Table 3.1 (present MELCOR simulation of LCC-05T-03 variant) or 5 of Table 3.1 (NuScale method, with two assumptions improved by results of that simulation), provides a better estimate of the AICC pressure. These estimates range from 11.1 to 11.5 bar-abs, and would yield a substantially lower upper bound for the detonation pressure than the NuScale value [[ ]]$^{2\,(a),\,(c)}$ psia.

3.4 Extension to Long Times

In the previous sections, it has been reviewed that the Applicant assumed that the bounding combustion event could be supposed to occur 72 hours (3 days) after the start of an accident, and that flammable conditions should arise for the first time at that time due to the cumulative radiolytic generation of oxygen. The Applicant assumed that containment gases would be contained in a volume equal to the dry free volume of the containment; further, the Applicant assumed a temperature [[ ]]$^{2\,(a),\,(c)}$ °C for the containment at 72 hours. Knowing the pre-accident containment gas masses; the rates of radiolytic generation of oxygen and hydrogen; and with the amount of hydrogen generated by oxidation of metals in the core treated as a parameter, on these assumptions it is easy to compute the pressure and composition of the containment atmosphere (an additional assumption is that the steam partial pressure should be the saturation pressure at [[ ]]$^{2\,(a),\,(c)}$ °C). The introduction to Section 2 referred to this computation as the

"direct calculation" of containment conditions, noting that it involves little more than the ideal gas law. The Applicant found that oxygen mole fraction 0.05, which is minimal for flammability, occurs at 72 hours if the amount of hydrogen generated by oxidation of metals in the core corresponds to oxidation of about [[ ]]$^{2\,(a),\,(c)}$% of the cladding on the active fuel (where 100% corresponds to 93.3 kg and represents the hydrogen generated by oxidizing all the zirconium in the cladding on the active fuel, as calculated by the Applicant in Reference [3]). With the containment conditions so determined, the Applicant went on to calculate the corresponding AICC pressure, then proceeded with all the rest of the combustion analysis.

With a view to critiquing two of the Applicant's assumptions (neglect of the reduction of the containment gas volume by the volume of the water in containment, and the particular value [[ ]]$^{2\,(a),\,(c)}$ °C for containment temperature), in Section 3.1 the present study reported a MELCOR simulation of a modified version of scenario LCC-05T-03. ECCS was actuated shortly after the start of core damage, with the timing adjusted such that the containment oxygen mole fraction at 72 hours was 0.05. The simulation predicted a final containment temperature of 96.5 °C, and also a reduction of the containment gas volume by 28.2 m^3 due to the water in the containment. It was then found that repetition of the Applicant's direct calculation, modified to include the higher temperature and the reduced volume, yielded for the supposedly bounding combustion event an AICC pressure that is higher than when carried out with the Applicant's assumed temperature and gas volume. Because of the different temperature and gas volume predicted by MELCOR, a different amount of oxidation[10] was required in order that the 72-hour oxygen mole fraction should still be 0.05. The required oxidation fraction was about 19%.

Not previously critiqued is the Applicant's assumption that the bounding combustion event may be supposed to occur 3 days after the start of an accident. By waiting longer, radiolytic oxygen generation eventually makes flammable a containment atmosphere that contains a greater mass of hydrogen, as would correspond to more complete oxidation of core metals. The direct calculation can be carried out as before, but instead of fixing the oxidation fraction such that the oxygen concentration reaches 0.05 at a prescribed time (such as 3 days), one can instead assign the oxidation fraction as an input and then calculate the time. The calculated times could be relevant in assessing when operators could intervene to restore inert containment conditions (i.e., supposing that operators would not act while the containment was already inert due to insufficient oxygen). For example, it appears that the Applicant has used the direct calculation to estimate that the oxygen concentration reaches 0.05 at 45 days in the case that 52000 moles of hydrogen (i.e., 104 kg, or 111 % of 93.3 kg) is present in the containment at day 0; see Table 5.1 and Figure 5.1 of the Applicant's ERR document "ER-P020-4904." As before, however, necessary inputs to the direct calculation are the containment temperature and the volume of the water in the containment. Again, these inputs need to be reliably estimated via accident progression simulations, especially since at such long times they may be affected by much greater heat-up of the cooling pool water than has occurred before 72 hours.

Based on the above considerations, this section extends the analysis to times much longer than 3 days, such that much higher oxidation fractions can be considered. The following two sub-sections apply to two general lines of approach:

1) Similar to Section 3.1, simulations of two LCC-05T-03 variants are carried out with MELCOR. In these variants (and unlike the one considered in Section 3.1), there is no ECCS actuation. One simulation adheres to MELCOR's prediction of metallic oxidation and accordingly generates 69% of 93.3 kg of hydrogen. The other invokes a user-controlled source to augment the MELCOR-calculated hydrogen generation and so simulate an accident in which 110% of 93.3 kg of hydrogen is generated by oxidation. Both simulations use the full-plant MELCOR model to simulate the first ~6 days of the accident. Subsequently, for faster calculations to long times (60 days), the predictions of the full-plant model are fed into a containment-only

[10] Actually, much more significant for the different oxidation fractions ([[ ]]$^{2\,(a),\,(c)}$% vs. 19%) are the different initial masses of oxygen in containment. For unidentified reasons the Applicant used an initial pressure of 9.5 psia in the direct calculation; the MELCOR simulation used [[ ]]$^{2\,(a),\,(c)}$ psia based on the NRELAP5 input and other ERR documents. This [[ ]]$^{2\,(a),\,(c)}$ psia applies prior to criticality. During normal operation, the pressure rises to 3 psia due to heat loss from the vessel (without, of course, changing the initial masses).

model for simulation of the rest of the problem. This approach works for the present scenario because, after the first few days, the RPV remains in a quiescent state that can be modeled as merely a heat source to the containment.

2) The "direct calculation" is undertaken with the containment temperature and the volume of the water in the containment assigned based on the results from one of the simulations of approach "1" above.

3.4.1 Scenario LCC-05T-03 (Variants with no ECCS Activation)

In this section, MELCOR models are used to simulate two variants of the scenario that has been described in Section 3.1, the main difference being that now the RRVs and RVVs remain closed at all times. In consequence, significant oxidation and fuel damage ensue. These calculations, new for Revision 3 of this report, are carried out with a combination of Revision 10 of the full model, and a "containment-only" model.

For the present purpose and apart from remarks included here, Revision 10 of the full model[11] is not significantly different from the model version used for the calculation documented in Section 3.1. One important difference is that here it is assumed that the severe accident occurring in one NPM is cause for the whole plant to be shut down, and so the heat dumped to the whole-plant cooling pool is the decay heat of 12 NPMs[12]. On the time scales now of interest (many days), the resulting heat-up of the cooling pool is significant. In fact the pool reaches 100 °C at about 6 days. As shown below, however, the containment cooling pool level fall due to boil-off is slow enough as to have little effect for several tens of days.

A MELCOR model of only the containment vessel and its associated cooling pool (the so-called containment-only model) was been used for various Design Basis Accident (DBA) analyses [19]. For such analyses, it is not necessary to model the RPV and its internals, since the RPV/containment interactions (e.g., break flows, ECCS flows) are treated as prescribed boundary conditions. On the other hand, the full-model simulations of these LCC-05T-03 variants predict that, at times after about 5 days, there are no longer occurring any significant events associated with the RPV (e.g., essentially all available water has evaporated, relocated fuel remains in the lower plenum and cooled from outside, etc.). Thus again it becomes possible to reduce the modeling of the RPV to simple prescribed boundary conditions. In the containment-only model, all that remains of the RPV is its wall heat structures (retained for account of heat sink and stored heat release), and a decay heat source added directly to the containment. This model can complete the long simulations within acceptably short computational times. All hydrogen generated by oxidation of the core metallic constituents is during the part of the problem that is simulated by the full model. This hydrogen is then specified in the initial data that set up the containment-only model at its initial time (where that initial time, ~6 days, is the end time of the full model simulation).

Two accidents have been simulated such that two different amounts of oxidation-produced hydrogen are obtained via various user specifications. In the most fully documented case, no special specifications are made and the MELCOR "COR" package is left free to simulate the oxidation of core metallic constituents according to its built-in models. In that case, the final cumulative hydrogen generated by oxidation is 64.2 kg, or 69% of 93.3 kg (see Reference [3] for the derivation of 93.3 kg as the mass that corresponds to 100% oxidation). In the other case, starting from the time of the effective cessation of oxidation as modeled by the MELCOR COR package, a user-defined source of hydrogen is

[11] Revision 10 is basically Revision 9 (as used for the calculations described in Section 4 of this report) with reinstatement of the radiolytic sources that had been missing in Revisions 8 and 9. Reference [20] provides calculation notes for Revision 10.

[12] Technically, this has been accomplished by modifying CV599 in Revision 10. See Figure A.4 and a nearby footnote that implies that, in Revision 9, CV599 models the balance of plant cooling pool (i.e., 11 bays and the whole of the channel). But in Revision 10, CV599 is reduced to model only one twelfth of the channel. Then the decay heat of only one NPM is considered.

activated to steadily release an additional 38.2 kg of hydrogen[13] into the core during the next 0.5 hour. In this manner, that case simulates an accident that releases 102.4 kg of oxidation-produced hydrogen (110% of 93.3 kg). In both cases, the full model is used to simulate the first 5.8 days of the scenario, then the containment-only model simulates the rest.

The in-vessel processes that the full model simulates are discussed only briefly. In the case where the oxidation of core metals is calculated only by the default models included in the MELCOR COR package, the final cumulative hydrogen generated by oxidation is 64.2 kg, or 69% of 93.3 kg. Most of the core relocates to the lower plenum, and further oxidation does not occur. Decay heat is removed by conduction into the lower head and from there into the containment water whose level is high enough to cover the lower head. Thus vessel breach is prevented and at times after ~5 days the scenario slowly progresses in a quasi-steady state. The case where the hydrogen production is augmented with the user-defined source progresses very similarly. In fact it is identical to the first case until the MELCOR COR package has generated 64.2 kg of hydrogen. Subsequently, the additional hydrogen is released by user specification into the RPV over the next 0.5 hours. In both cases, the containment-related predictions at 5.8 days are used to set up a corresponding version of the containment-only model (i.e., versions that consider 69% oxidation fraction versus 110% oxidation fraction). Also used for that purpose are the 5.8-day values of the structural temperatures of all walls (i.e., the RPV wall, the containment vessel wall, and cooling pool walls).

The containment- and cooling pool-related predictions made by the full model are used to provide initial conditions for the containment-only model. Of the RPV, all that remains in the containment-only model are its wall heat structures, and the decay heat. In the containment-only model, the RPV walls are initialized to the temperatures that the full model predicts at 5.8 days. The decay heat is modeled as a heat source to the containment. The time-dependent decay heat is referred, of course, to the running problem time, which starts at 5.8 days. Note that in this no-ECCS scenario, no fluids (i.e., water, steam or hydrogen) are considered to pass between the RPV and the containment. (In typical DBA analyses, such exchanges would occur and would be modeled by mass/energy sources/sinks. These sources/sinks are zeroed out in the present application.) The containment-only model used here represents the containment with only one control volume; the full model uses multiple control volumes (see Figure A.2). Therefore, the full-model-predicted well-mixed composition and temperature data at 5.8 days are the initial data for the containment-only inputs. The containment-only model uses a multi-level nodalization for the containment vessel wall and the cooling pool, but the number of levels and the level spacing are somewhat different from the corresponding nodalization for the full model (shown by Figure A.4). These differences entail some proportioning and interpolating so that the axial dependence of initial (5.8 days) wall and water pool temperatures can be carried forward from the full- to containment-only models.

Figures 3.1.1 through 3.1.4 apply to the case that models final cumulative hydrogen mass produced by oxidation as 64.2 kg (i.e., 69% of 93.3 kg). The parts of the curves before 5.8 days are as predicted by the full model. The later parts are predicted by the containment-only model. Figure 3.1.1 shows the containment pressure. Figure 3.1.2a shows the containment gas temperatures; Figure 3.1.2b shows the containment water temperatures; and Figure 3.1.2c shows the cooling pool water temperature. Figure 3.1.3 shows the depths of the containment and cooling pool water pools. Figure 3.1.4 shows the (well-mixed) composition of the containment atmosphere.

Containment temperatures show a slow falling behavior at long times. This trend occurs because, as of about 5.7 days when the cooling pool water attains 100 °C, the cooling pool water is boiling, providing good heat sink to the containment interior. The peculiar features occurring in the containment gas temperature (Fig. 3.1.2a) at 26 and 49 days are MELCOR artifacts related to the successive uncovery on the cooling pool side of modeled sections of the containment vessel wall as the water level falls in the cooling pool due to boil-off. (The so-called MELCOR critical pool fraction for apportioning gas- versus liquid-convective heat transfer into the cooling pool plays a role.) Up to 5.8

[13] The additional mass was defined with reference to the ERI/NRC MELCOR model, not the Applicant's value 93.3 kg. That is, 102.4 kg is the amount of hydrogen generated by oxidizing 100% of the zirconium cladding on the active fuel, where the zirconium mass is taken from the MELCOR model input deck. The Applicant's citation in ERR document ER-P020-4904, noted above, of 104 kg of hydrogen in the containment at day 0 also played a role in this choice.

days, the figures that show containment temperatures give data from three representative Control Volumes (CVs) of the full model (see Figure A.2: CV414 never contains water; CV411 almost never contains gas; CV423 almost always contains both water and gas).

In some of these figures, jumps at 5.8 days (the time for switch-over between full- and containment-only models) are due to a MELCOR limitation that does not permit the user to specify initial thicknesses of the condensate water films on various heat structures, which exist based on the full-model results at the time of the switchover to the "containment-only" model[14]. Therefore, in the containment-only model, the parts of the containment vessel wall above the water level are necessarily set up as dry at 5.8 days. On the other hand, due to condensation that had been going on earlier, the full model predicts water films on the wall that are of order 0.05 mm thick at 5.8 days. The sudden acquisition of films at 5.8 days entails sharp drops of pressure (Fig. 3.1.1) and steam concentration (Fig. 3.1.4b) at the start of the containment-only calculation.

As Figure 3.1.4a shows, the oxygen concentration attains 0.05 at 23 days. Figure 3.1.5 is similar to Figure 3.1.4a but it applies to the case where, by means of a user-defined source, the 64.2 kg of hydrogen generated by the COR package is augmented such that the final oxidation-generated hydrogen is 102.4 kg (110% of 93.3 kg). The oxygen concentration reaches 0.05 at 42 days.

[14] In the case of containment temperatures, the discontinuities are of course due to the presence of multiple CVs in the full model (versus a single-volume in the "containment-only" model: as the legends indicate, the figures show plots of individual containment CV temperatures during the times up to 5.8 days.

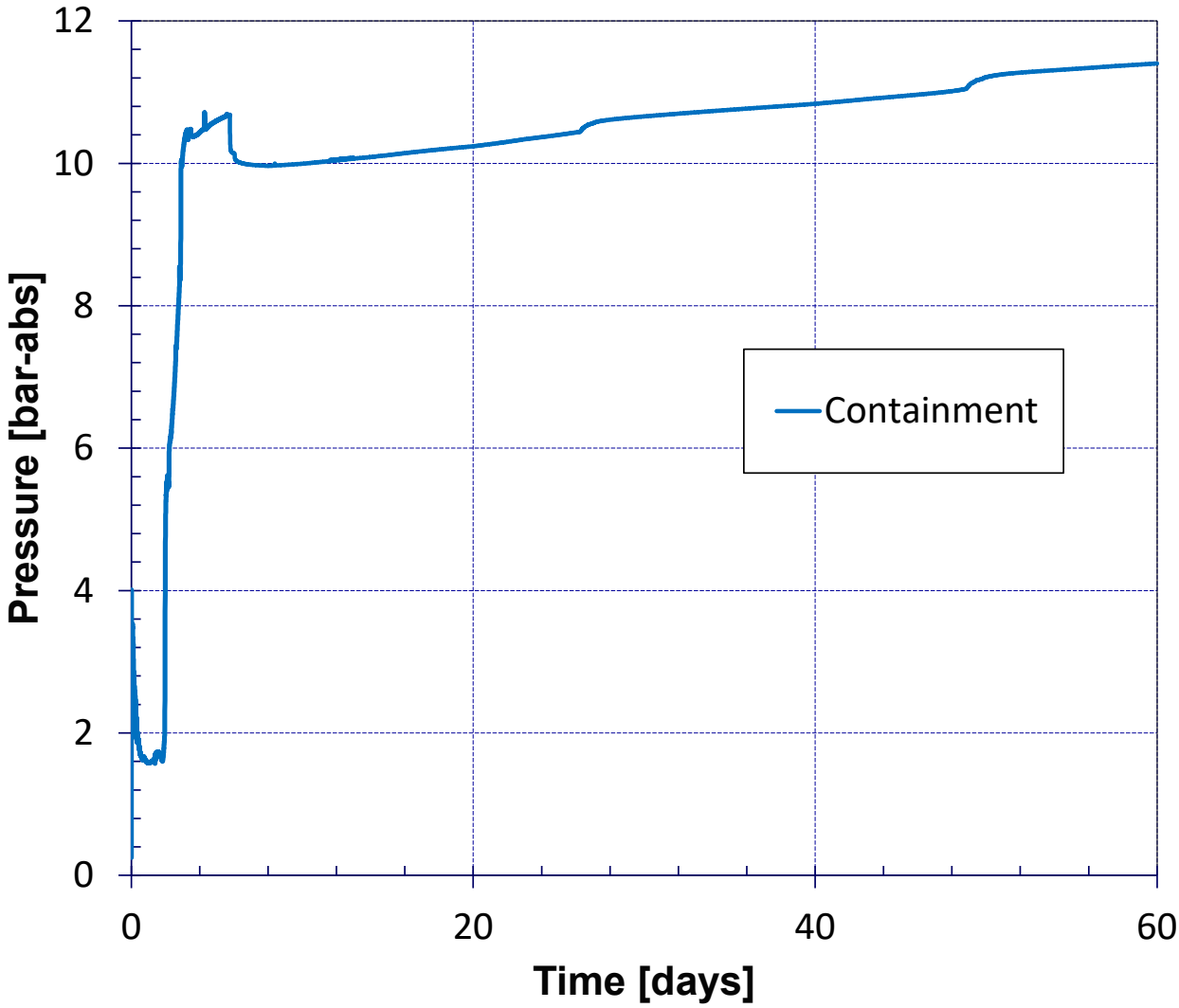

Figure 3.1.1 Containment pressure, scenario LCC-05T-03 with 69% oxidation

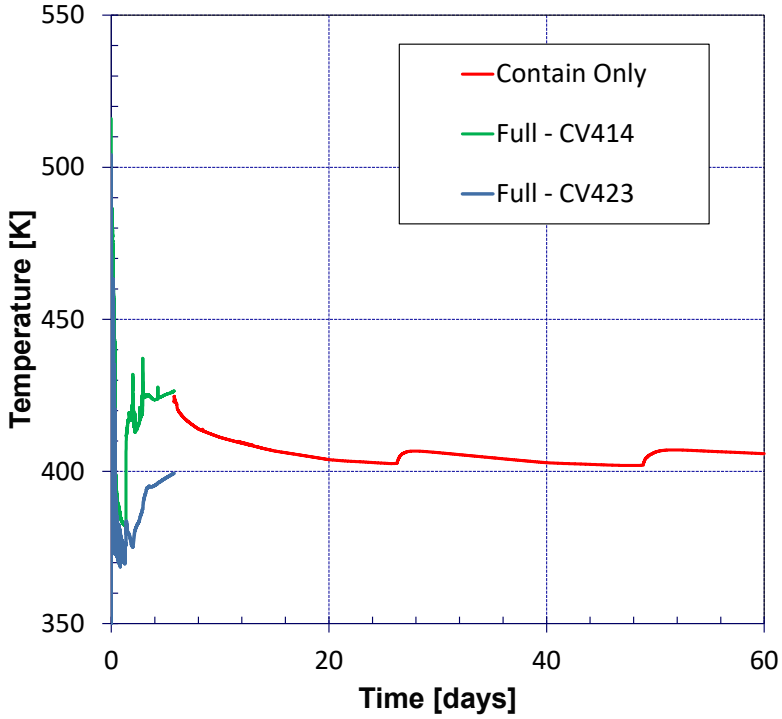

Figure 3.1.2a Containment gas temperature, scenario LCC-05T-03 with 69% oxidation

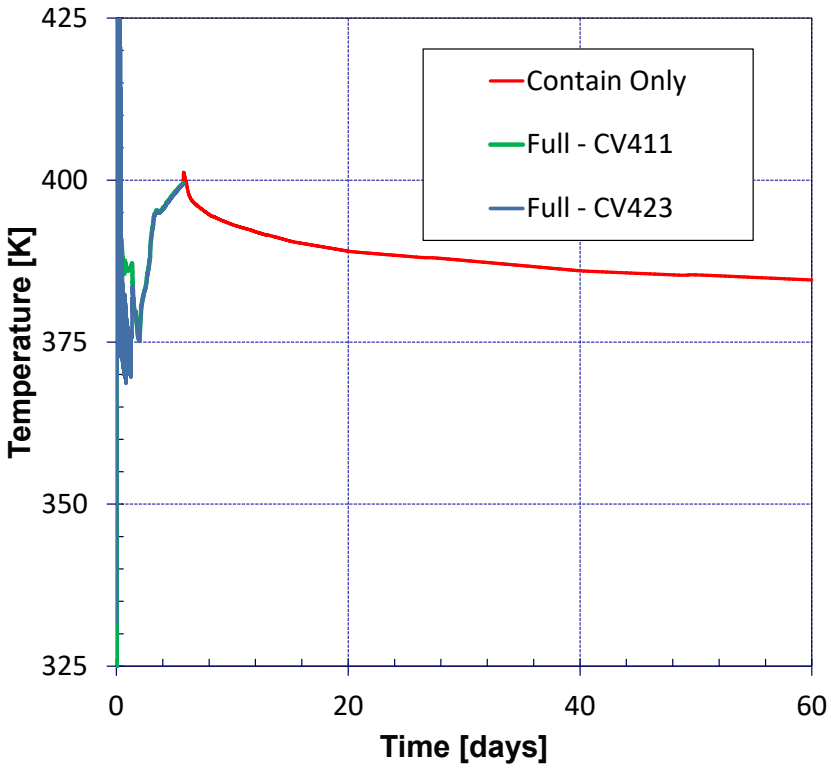

Figure 3.1.2b Containment water temperature, scenario LCC-05T-03 with 69% oxidation

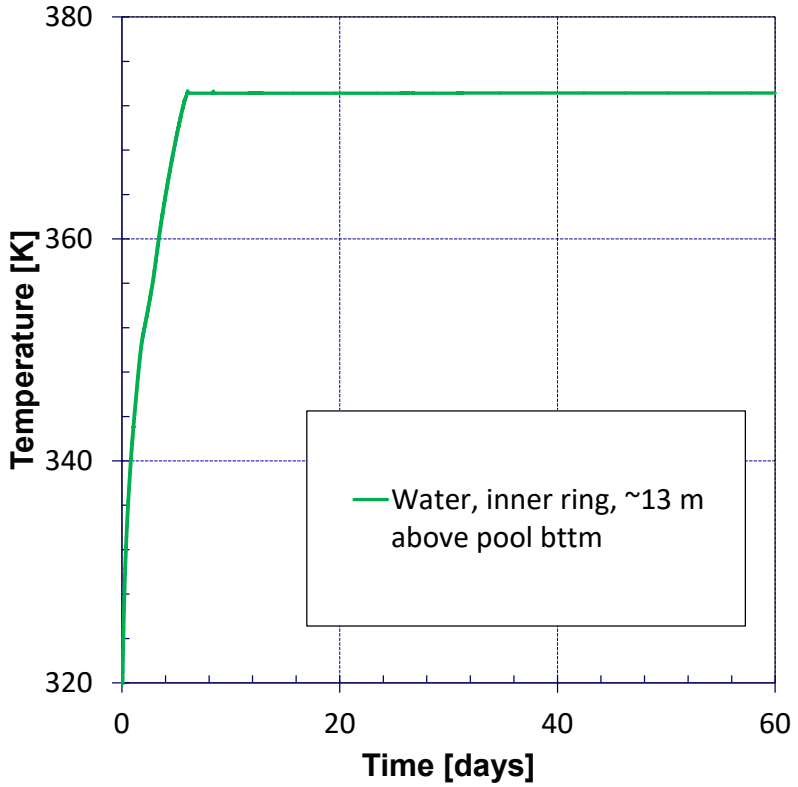

Figure 3.1.2c Cooling pool water temperature, scenario LCC-05T-03 with 69% oxidation

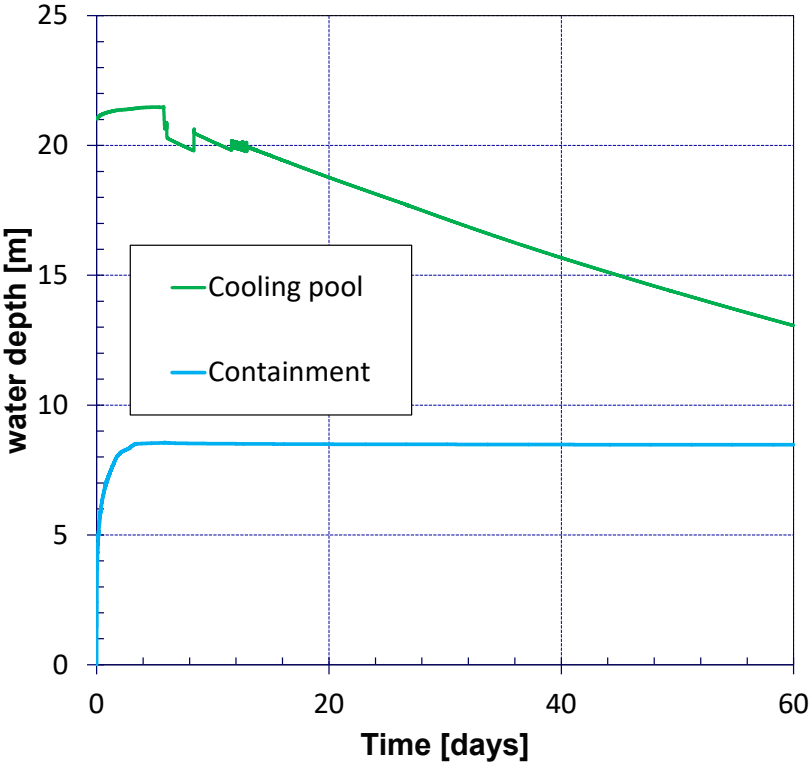

Figure 3.1.3 Water depths, scenario LCC-05T-03 with 69% oxidation

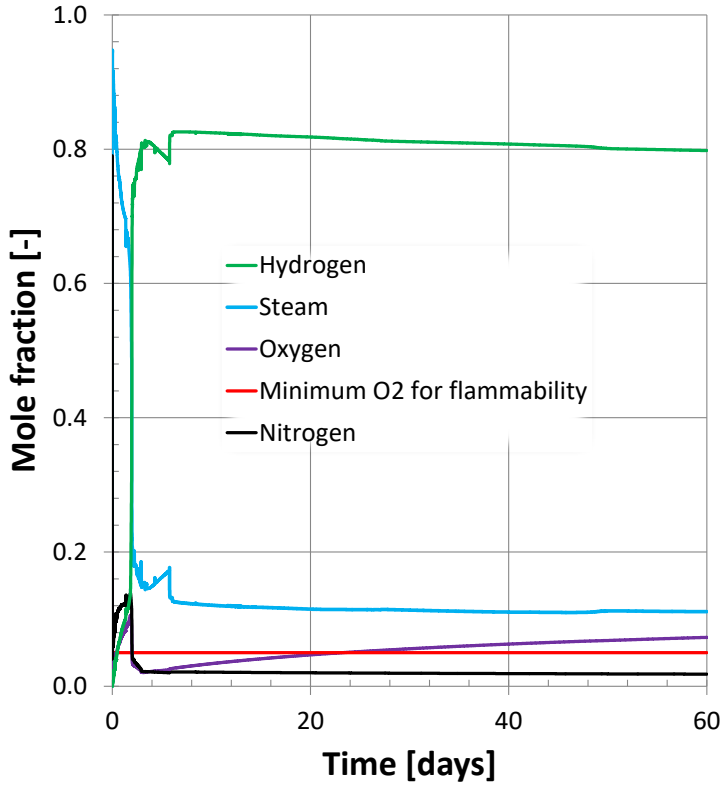

Figure 3.1.4a Containment atmosphere composition, scenario LCC-05T-03 with 69% oxidation

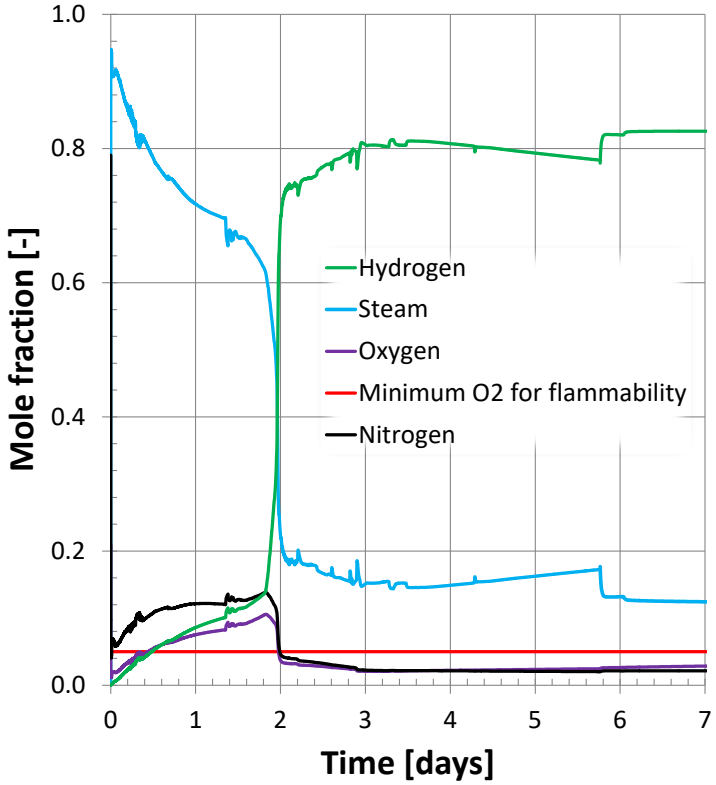

Figure 3.1.4b Containment atmosphere composition, scenario LCC-05T-03 with 69% oxidation - detail

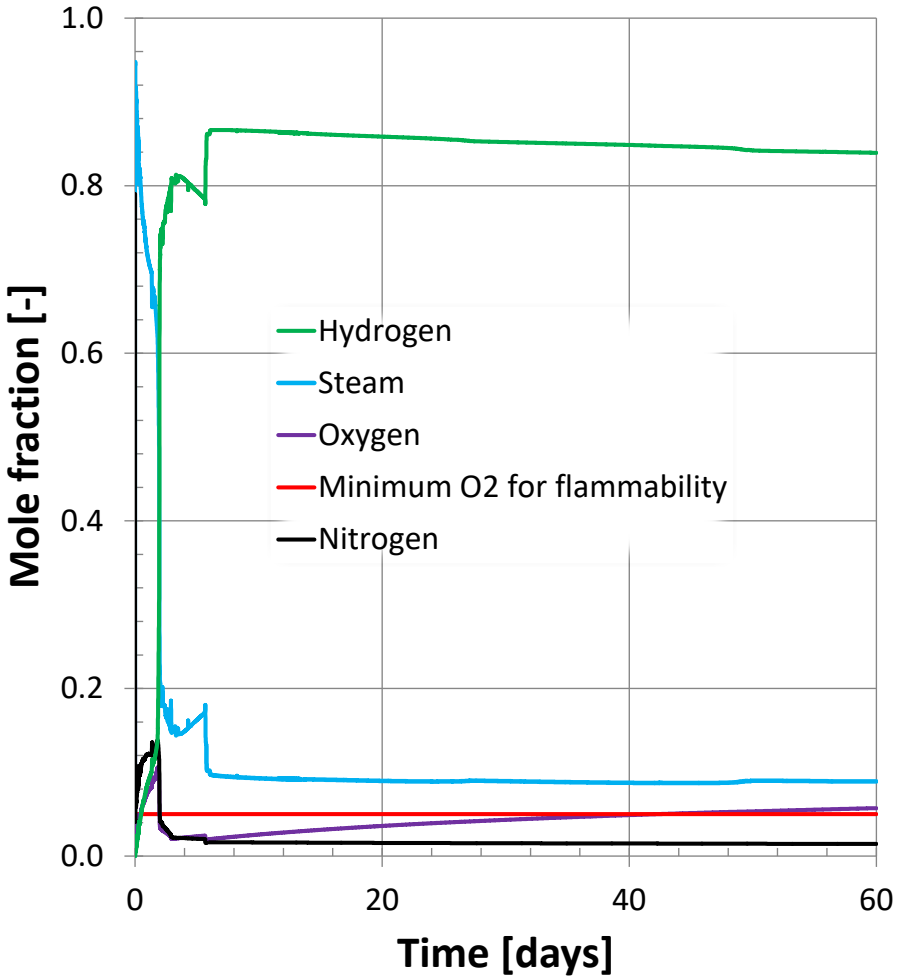

Figure 3.1.5 Containment atmosphere composition, scenario LCC-05T-03 with 110% oxidation

3.4.2 Direct Calculation of Containment Atmosphere Conditions

The direct calculation approximately provides the containment atmosphere conditions with minimal need of supporting accident progression simulation. The MELCOR simulation of one of the no-ECCS variants of scenario LCC-05T-03, described in Section 3.4.1, provides the following data:

Table 3.3 Data from the MELCOR calculation at 19.905 days (inputs to the direct calculation)

Parameter	Value
Volume of water in the containment, m^3	47.71
Steam partial pressure, bar	1.1643
Containment gas temperature, K	403.9
Fraction of oxidation-produced hydrogen that is held up in the RPV (at 5.8 days)	0.094
Containment water temperature, K	389.1
Final in-vessel produced hydrogen, kg	64.2 (69% of 93.3 kg). No extra H_2 added by special source

With one exception, the tabulated conditions apply at time 19.905 days. A priori, any time late enough that all phenomena have become quasi-steady would be equally appropriate. This late time was selected so as to include some of the long-time cooling trend mentioned above in connection with Figure 3.1.2a. No other account of this cooling trend is taken in the simplistic direct calculation. The quantities in blue font are not required for the direct calculation but are recorded for interest. As applied by the Applicant (at least in the main combustion analysis computation), the direct calculation assumes that the steam partial pressure can be fixed as the saturation pressure at the containment temperature. Here, the steam partial pressure is instead taken directly from the MELCOR simulation. Equivalent to that pressure, 1.1643 bar, is the saturation temperature at that pressure: 377.1K. This temperature is interestingly compared with both the gas temperature (403.9K) and the water temperature (389.1K). Thus the steam is indeed not too far from saturation (~12K), but with respect to the temperature of the containment water, not the containment gas.

One entry in Table 3.3 is the fraction of oxidation-produced hydrogen that is held up in the RPV. This quantity is predicted, of course, by the full MELCOR model, and it applies at 5.8 days, as predicted for the MELCOR run in which the final oxidation-produced hydrogen mass is 64.2 kg (fraction 69%). The corresponding containment-only MELCOR model has accordingly been set up with an initial (i.e., t=5.8 days) containment hydrogen inventory of 58.1 kg. It is thus an assumption of the MELCOR containment-only model that there is no release of the held-up hydrogen at times later than 5.8 days. Probably this is a fair assumption in the case of this LCC-05T-03 variant scenario (since the break flow area is so small; see Section 3.1.) It is decided to take account of this hold-up in the direct calculation (while in a LOCA with a more typically sized break flow area a good assumption probably would be to neglect to hold-up). Any hold-up of radiolytic-generated hydrogen or oxygen is ignored in the direct calculation.

The direct calculation has no need for information about the containment water, except for its volume which acts to reduce the available gas space. The MELCOR calculation of Section 3.4.1 predicts the volume of the water in containment as 47.71 m^3 (at 19.905 days), which is much more than 28.2 m^3 (at 3 days) predicted by the MELCOR calculation of Section 3.1. This difference reflects successful ECCS operation in the MELCOR calculation of Section 3.1, wherein the core is kept covered. The calculations of Section 3.4.1 assume that the ECCS valves remain shut, so eventually the RPV becomes nearly dry with all the water residing in containment instead.

The MELCOR input deck provides the initial masses of the containment atmosphere: 22.94 kg of nitrogen and 6.97 kg of oxygen. These masses initially reside in the containment of dry free volume [[ ]]$^{2\,(a),\,(c)}$ m^3. The direct calculation is therefore carried out with containment gas volume [[ ]]$^{2\,(a),\,(c)}$ m^3 which is treated as a constant. The mass of hydrogen in the containment that is attributable to core metals oxidation is treated as a varying parameter, expressed as a fraction of 0.906 × 93.3 kg, where the factor 0.906 accounts for the 9.4% hold-up in the RPV. In the direct calculation, this mass is treated as present as of t=0. Additional time-dependent contributions to the hydrogen and oxygen inventories are made by radiolysis (see Eq. (1) in Section 2.2 for the rates). These considerations fix all the non-condensable gas masses, which are then used with the ideal gas law to compute pressures.

The heat-up of the cooling pool water is important on time scales of several days. For an account of this heat-up, Figure 3.2.1 shows how a time dependence has been added to some of the data, tabulated by Table 3.3, that MELCOR predicts at 19.905 days. The cooling pool water temperature, itself not needed for the direct calculation, is shown by the blue curve. (It can be compared with the MELCOR-predicted curve shown by Figure 3.1.2c.) MELCOR is not used in any way to calculate this curve. It is calculated from the initial temperature (316.6K = 110 °F) of the cooling pool water; the full-plant cooling pool water mass ([[ ]]$^{2\,(a),\,(c)}$ metric tonnes); and the decay heat of 12 NPMs. The temperature reaches 373.15K (normal boiling point) at about 5.7 days; after that the temperature remains unchanged. The present direct calculation assumes that the containment gas temperature exceeds the cooling pool temperature, as calculated here, by a constant difference, where this difference is calculated from the MELCOR datum at 19.905 days. Since as of 19.905 days the cooling pool temperature has long since become constant, it follows that the direct calculation uses the fixed MELCOR-computed temperature, 403.9K, for the containment gas temperature at all times after 5.7 days. At earlier times, the direct calculation supposes cooler containment gas temperatures, shown

by the red curve and calculated as just described. (This curve can be compared with the MELCOR-predicted curves shown by Figure 3.1.2a.) The same time dependence has been imposed on the green curve, which shows the saturation temperature calculated at the steam partial pressure. (At 19.905 days, MELCOR gave 389.1K corresponding to 1.1643 bar.) Via the known relation between saturation pressure and temperature, this curve lets the steam partial pressure be assigned values less than 1.1643 bar at times before 5.7 days. (After 5.7 days it remains constant at the MELCOR value, 1.1643 bar.) Thus just two time-dependent processes are accounted for in the direct calculation: the radiolytic generation of oxygen and hydrogen, and the heat-up of the cooling pool. However, the heat-up of the cooling pool introduces a time dependence only during times before 5.7 days.

Partial pressures of gases other than steam are computed from the ideal gas law, while the steam partial pressure is assigned as has been described. For the case that the oxidation fraction is set to 69% (corresponding to 64.2 kg of in-vessel-produced hydrogen, of which 58.1 kg is credited to reach the containment), Figure 3.2.2 shows the total pressure and some of the partial pressures. (The total pressure can be compared with the MELCOR-predicted curve shown by Figure 3.1.1.) The gas component mole fractions are identified with the ratio of the corresponding partial pressure to the total pressure. Figure 3.2.3a shows the mole fractions for the 69% oxidation case. Oxygen mole fraction 0.05 is attained at about 24 days. This figure can be compared to Figure 3.2.4a, which is the MELCOR prediction (MELCOR predicted 23 days to reach 5% oxygen). Figure 3.2.3b shows the mole fractions for the 110% oxidation case (corresponding to 102.4 kg of in-vessel-produced hydrogen, of which 0.906 × 102.4 kg = 92.7 kg is credited to reach the containment[15]). Note that this and all direct calculations take only the MELCOR-predicted inputs that Table 3.3 shows; these come from the 69% fraction MELCOR calculation. Oxygen mole fraction 0.05 is attained at about 56 days. This figure can be compared to Figure 3.2.5, which is the MELCOR prediction (MELCOR predicted 42 days to reach 5% oxygen).

In the case of 69% oxidation fraction, the agreement between the direct calculation and the MELCOR simulation is good, keeping in mind that the direct calculations do not take account of any time-dependent processes except for radiolysis and the heat-up of the cooling pool water. Therefore, there are qualitative differences at early times (e.g., in MELCOR, high initial steam concentration due to the break, zero hydrogen concentration until oxidation starts: see Figure 3.1.4b). The good agreement at later times reflects the use of results from the MELCOR simulation of the 69% case for set-up of the direct calculation, as well as the essential correctness of the method (e.g., the ideal gas law applies; late-time changes of containment temperature are small). In the 110% fraction case, the direct calculation's over-prediction, relative to MELCOR, of the time for the oxygen to attain 0.05 molar concentration is mostly due to the larger RPV hold-up of hydrogen that MELCOR predicts in that case. The larger hold-up could be accounted for, but it appears beyond the scope of the direct calculation to use a different set of MELCOR-predicted set-up data for each direct calculation.

Figure 3.2.4a shows the AICC pressure and AICC temperature for the 69% cladding oxidation case. The flat red curve shows the times when the mixture is detonable[16]. In the present case (69% oxidation), the mixture is detonable at all the times that it is flammable, i.e., from 24 days until the end of the calculation at 60 days. Figure 3.2.4b shows the AICC pressure and the estimated detonation pressure, as fractions of the design pressure. The estimated detonation pressure is just the AICC pressure times [[ ]][2 (a), (c)]. The AICC and detonation pressures are shown only at the

[15] For the case of 110% oxidation fraction, MELCOR predicted a much larger hold-up fraction, 0.211, to compare with 0.094 in the 69% fraction case. It is decided, however not to take account of calculation-specific MELCOR data in the set-up of the direct calculations.

[16] For this purpose, detonable is simplistically defined as at least 15% hydrogen, at least 5% oxygen, and at most 35% steam. AICC pressure and temperature may be calculated as continuous functions of time, i.e., from the inputs represented by Figures 3.2.1, 3.2.2, and 3.2.3a which show the evolving atmosphere in the absence of combustion. (That is, AICC calculations can be made from point to point without including the effect of the prior combustion events on the initial data.) In an actual combustion event, the pressure and temperature would spike to high values, then fall back, leaving the atmosphere inert at least for a while until combustible mixtures can be formed. Figure 3.2.4a shows the AICC pressure at three discrete times, and the AICC temperature as a continuous curve.

time of the onset of flammability (and, in this case, detonability). This is only the earliest time when the combustion becomes possible: it could happen later, in which case the pressures would be higher. The AICC pressure is about [[ ]]$^{2\ (a),\ (c)}$ the design pressure; the estimated detonation pressure is about [[ ]]$^{2\ (a),\ (c)}$ times the design pressure, most likely resulting in containment failure. Figure 3.2.4c shows the masses of hydrogen and oxygen.

Figures 3.2.5 and 3.2.6 are analogs to Figure 3.4.4b for the cases, respectively, of 10% and 110% oxidation. Note that the direct calculations for all considered oxidation fractions assume the same inputs for containment temperature, steam pressure, water volume, and RPV hydrogen hold-up as have been used for the 69% fraction case (and which have been supplied by the MELCOR calculation in which the fraction was 69%; see Table 3.3). In the 10% case (Figure 3.2.5), oxygen concentration 0.05 is attained at about 0.3 days (~8 hours), which also is when the mixture becomes detonable. (The inset graph helps to resolve the very early time of this event.) This figure does not show the period of detonability, but in fact the mixture is detonable at all times after 0.3 days except during a period lasting about one day centered at about 6.5 days, when detonable conditions are not achieved because of excessive steam (greater than 35%). (The mixture is still flammable during this time. This is the only example found in these calculations of a mixture that is flammable but not detonable.) After about 7 days the steam concentration falls below 35% and the mixture is again detonable until the end of the calculation. Notably high AICC temperatures (not shown, but up to ~4000K) arise in this case because of the relative lack of excess hydrogen that, unburned, contributes heat sink. At 3 days, when the oxygen concentration is about 0.08, the AICC pressure is about 11 bar. This is very similar to the AICC pressure that was found at 3 days in the MELCOR simulation discussed in Section 3.1. That simulation included ECCS operation, with results that the oxidation fraction was 19%; the 3-day oxygen concentration was 0.05; and larger volume existed for the containment gas.

Figure 3.4.6 shows the results for 110% (102.4 kg of in-vessel-produced hydrogen, with 92.7 kg credited to reach containment). Flammability and detonability are simultaneously attained when the oxygen concentration attains 0.05, which happens at 56 days. The AICC pressure at 60 days is 58.8 bar, or 853 psia. The detonation pressure, as estimated by the usual methods, would much exceed the design pressure, 1050 psia. (But recall that the Applicant argues that detonation pressure in excess of the design pressure does not imply vessel failure: Applicant claims that the strain cannot attain the yield strain during the short life of a detonation load.) The Applicant's combustion analysis is based on the AICC pressure of [[ ]]$^{2\ (a),\ (c)}$ psia as approximately calculated for the mixture that the Applicant predicts for the containment at 3 days (see Section 2.3, and Reference [3]).

Figure 3.2.7 shows the time required for the oxygen concentration to attain 0.05 as a function of the oxidation fraction. (Recall, this fraction is defined such that the hydrogen mass produced by oxidation is this fraction times 93.3 kg; the calculation has been carried out assuming that 9.4% of the oxidation-generated hydrogen remains held up in the RPV.) As has been discussed, these times may represent the earliest times when operators might take action to restore inert conditions in containment, as a function of the severity of the accident, as quantified by the oxidation fraction. The earliest times (less than 1 day) may correspond to successful but somewhat late ECCS actuation, such that some metal oxidation and fuel damage has occurred, but not so much as to oxygen-deplete the containment for more than a few days. The times for fractions around 50% to 70% (~20 days) might be the best estimates for typical unmitigated severe accidents, since MELCOR typically predicts such fractions in such cases. The 100% value (93.3 kg of in-vessel hydrogen, ~47 days to flammability) could arise in consideration of 10 CFR 50.44 requirements.

In general, it seems that the Applicant's analysis, which is believed to be based on direct calculations similar to those used here, predicts shorter times than those estimated by the present implementation of the direct calculation (Figure 3.2.7). One MELCOR calculation carried out here also gives a shorter time. Thus, the above-quoted results from ERR document ER-P020-4904 include that 104 kg of in-vessel produced hydrogen (or oxidation fraction 1.11 as estimated here) keeps the containment inert for 45 days, quite consistent with MELCOR's prediction of 42 days for fraction 1.10. The estimate by the direct calculation of this report is 56 days for fraction 1.10. As has been discussed, the 42 vs. 56 day discrepancy is largely accounted for by MELCOR's use of its own fraction-dependent prediction of the RPV hydrogen hold-up fraction, which in the 110 % case reduces the hydrogen in the containment in MELCOR, relative to the direct calculation. The direct method uses the same hold-up fraction for all oxidation fractions. As has

been discussed (especially, see the first footnote in Section 3.4), relative to the present study, the Applicant tends to over-predict the time to attain flammability, with such discrepancies at least qualitatively attributable to the Applicant's use of a too high (9.5 vs. 2.0 psia) pre-power-up containment pressure.

Table 3.4 tabulates the ratios of the AICC pressure and the estimated detonation pressure to the design pressure as a function of the fraction of the core that becomes oxidized. Also tabulated are the masses of hydrogen and oxygen in the containment, and the estimated detonation pulse period (i.e., duration of the detonation pressure). For each fraction, the time of the postulated combustion event is the earliest time when the containment atmosphere is flammable (in all cases the atmosphere becomes detonatable at that same time). If later times were considered, the pressures would be higher. The Applicant's analyses suggest that the containment will withstand those detonations for which the detonation pressure ratio is less than [[ ]]$^{2\,(a),\,(c)}$, although as has been mentioned, strictly speaking, this conclusion requires a new analysis at each detonation pressure. For ratios greater than [[ ]]$^{2\,(a),\,(c)}$, the ability of the containment to withstand the detonation load cannot be determined from available information. The ratio is about 6 in the case that the oxidation fraction is 0.30. In that case, the atmosphere first becomes flammable and detonable at 6.6 days. This time may be interpreted as just a little earlier than the earliest time at which operators would ever need to act to avert the possibility of detonations that could potentially fail the containment. (On this interpretation, detonability that does arise earlier – even as early as 0.3 days – would be considered tolerable as incapable of challenging the containment integrity.) Figure 3.2.8 reiterates the data of Table 3.4 graphically, showing the detonation pressure as a function of the earliest time when the detonation could occur. For the tabulated estimates of pulse periods, that utilizes the general method documented in Reference [2] by the Applicant, nonetheless, a few specific parameters (e.g., characteristic length, heat of combustion for TNT, etc.) not documented in Reference [2] had to be assumed. The estimates show that the detonation pulse duration varies between 0.37 to 0.64 ms; which compare to a value of about [[ ]]$^{2\,(a),\,(c)}$ ms estimated by the Applicant for their limiting case (Applicant's limiting case is extensively discussed in Section 2). Therefore, a large variability in the calculated detonation pulse is estimated, implying that the containment integrity is not expected to be challenged by detonations provided the detonation pressure is less than about [[ ]]$^{2\,(a),\,(c)}$ times the containment design pressure[17].

Table 3.4 AICC and estimated detonation pressures; hydrogen and oxygen masses and detonation pulses

Oxidation of metal in the core (%)	Time (days) (1)	Mass of Hydrogen in CNV (kg)	Mass of Oxygen in CNV (kg)	$P_{AICC}/P_{CNV\ design}$ (-) (2)	$P_{Detonation}/P_{CNV\ design}$ (-)	Detonation pulse period (ms) (3)
10	0.3	9.2	13.2	0.10	2.22	0.64
30	6.6	28.7	33.6	0.26	6.10	0.45
69	24.8	65.6	65.2	0.53	12.2	0.37
110	60.1	104.5	99.1	0.81	18.7	0.47

(1) First time when the flammable conditions (H_2>10%, O_2>5% and Steam<55%) or detonation conditions (H_2>15%, O_2>5% and Steam<35%) are reached (Note that in the calculations reported in this report, both flammable and detonation conditions are almost always reached at the same time)

(2) NuScale CNV design pressure is 72.4 bar-abs (1050 psia)

(3) Estimated herein based on the general method described in Reference [2], but with assumed values for some parameters not documented in Reference [2].

[17] Note that the present study has not verified the Applicant's dynamic strain analysis. Also, not very likely but conceivable is the possibility that some detonable condition could entail a relatively low detonation pressure – less than [[ ]]$^{2\,(a),\,(c)}$ times the design pressure – yet have a long-enough a pulse period as to challenge the containment. In this context, note that the longest pulse period tabulated by Table 3.4 arises in the case of smallest detonation pressure.

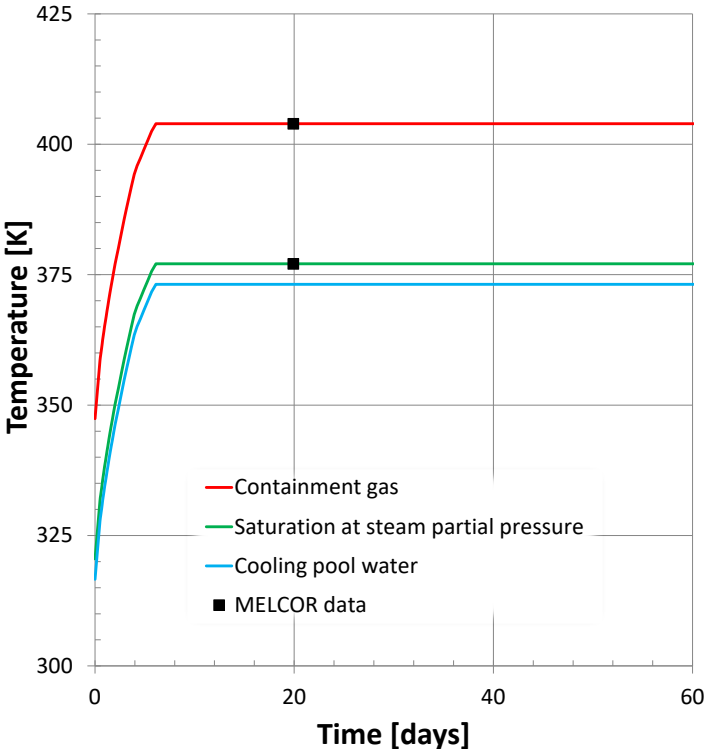

Figure 3.2.1 Temperatures affected by cooling pool heat-up

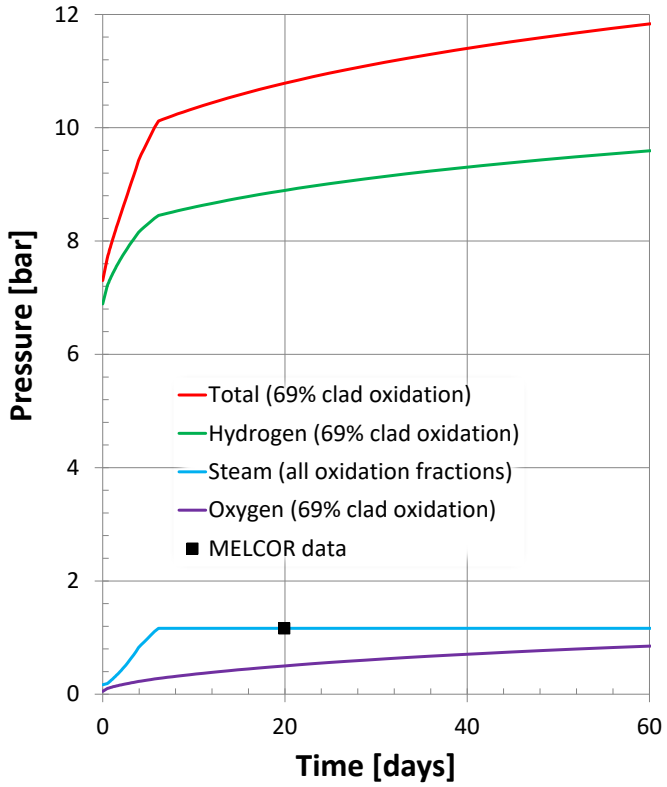

Figure 3.2.2 Containment partial pressures in the case of 69% oxidation

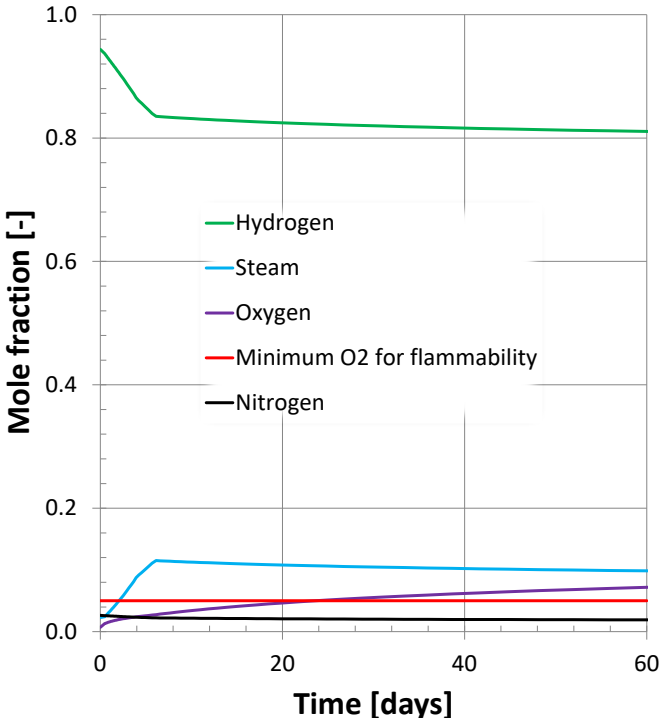

Figure 3.2.3a Containment atmosphere composition in the case of 69% oxidation

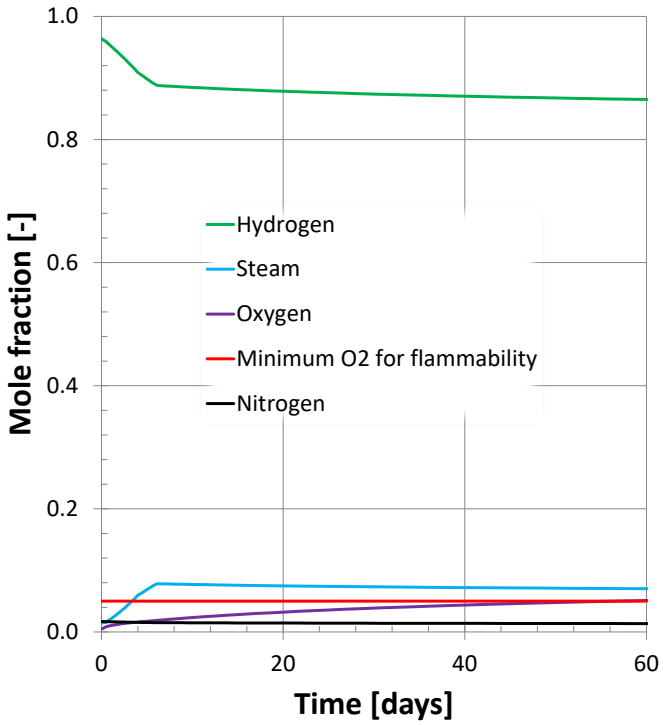

Figure 3.2.3b Containment atmosphere composition in the case of 110% oxidation

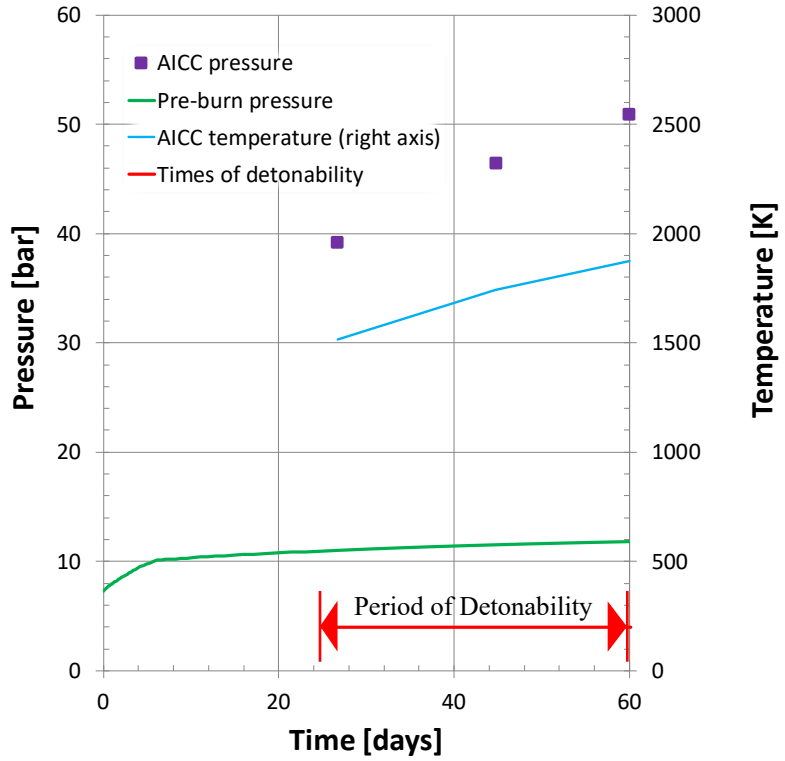

Figure 3.2.4a AICC pressure, AICC temperature, and period of detonability in the case of 69% oxidation

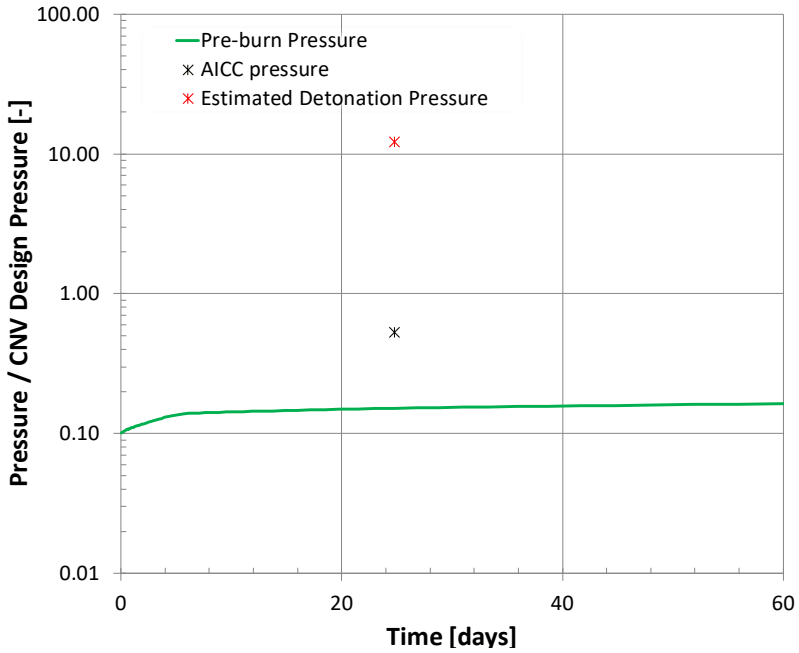

Figure 3.2.4b Pre-combustion pressure, AICC pressure, and estimated detonation pressure in the case of 69% oxidation, as fractions of the design pressure

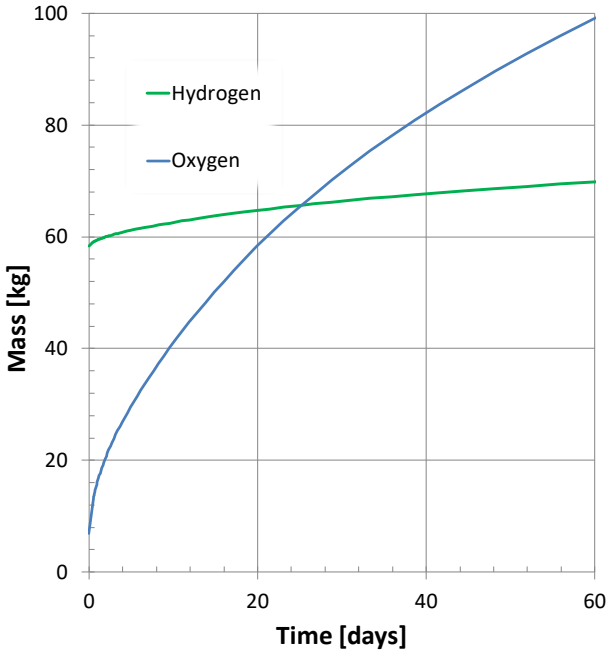

Figure 3.2.4c Masses of hydrogen and oxygen in containment in the case of 69% oxidation

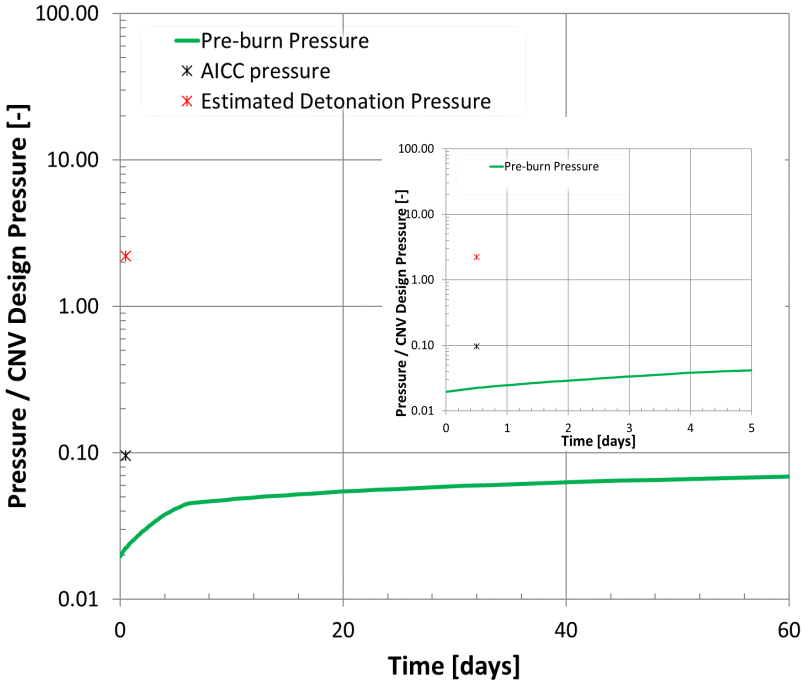

Figure 3.2.5 Pre-combustion pressure, AICC pressure, and estimated detonation pressure in the case of 110% oxidation, as fractions of the design pressure

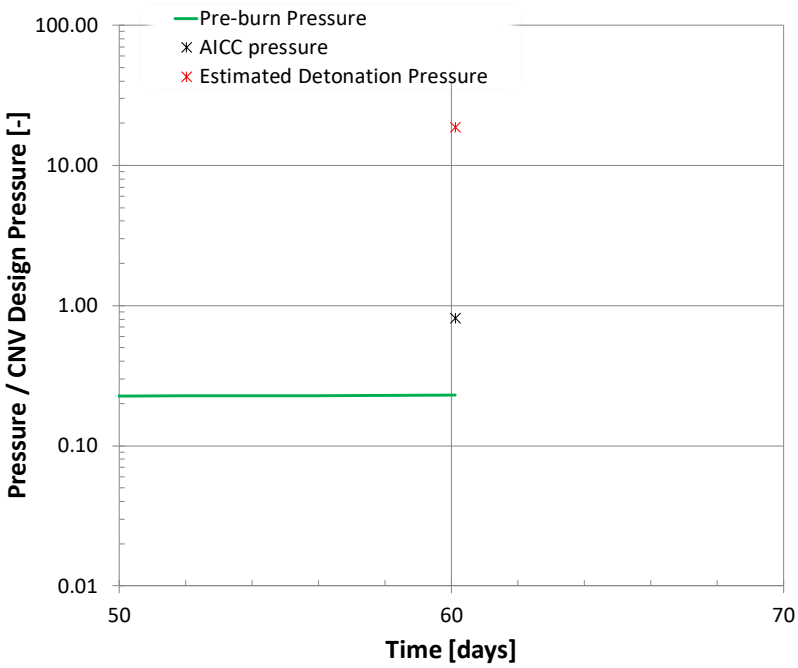

Figure 3.2.6 Pre-combustion pressure, AICC pressure, and estimated detonation pressure in the case of 110% oxidation, as fractions of the design pressure

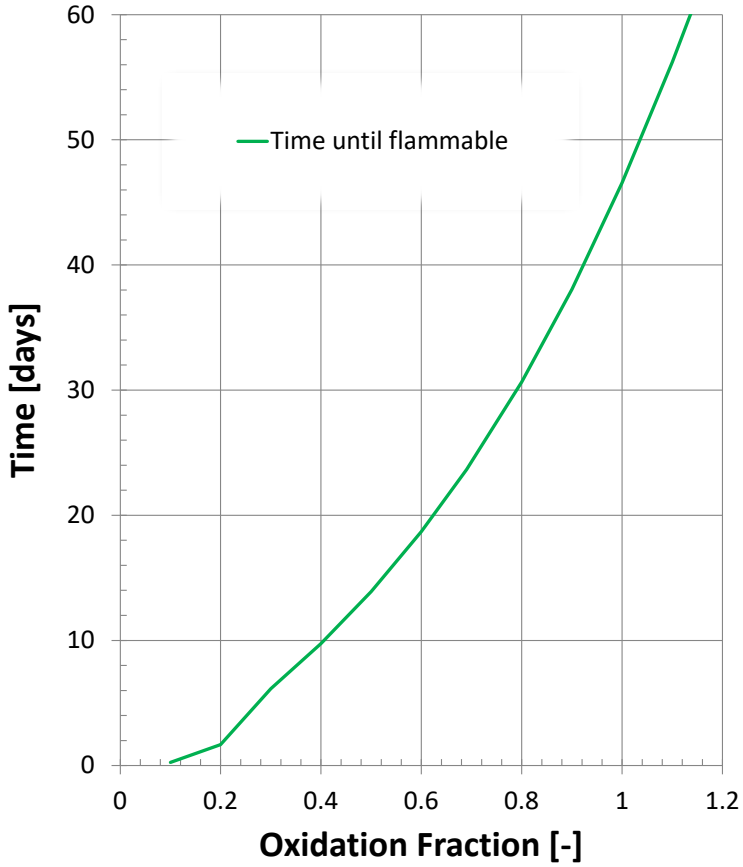

Figure 3.2.7 Time required for the oxygen concentration to attain 0.05

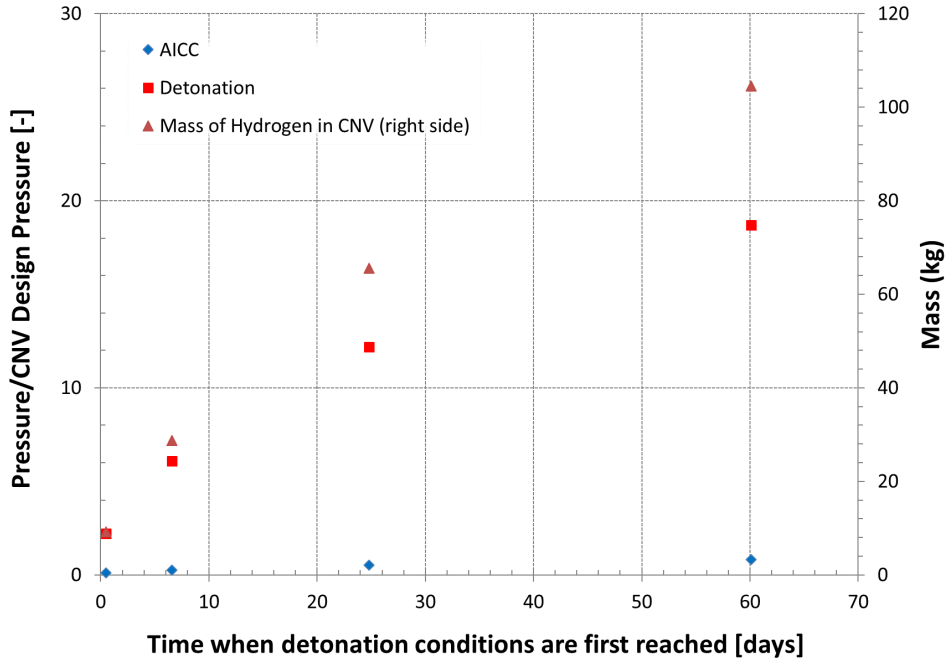

Figure 3.2.8 Combustion pressures and hydrogen mass as functions of the time of earliest combustion

Intentionally left blank

4. HYDOGEN ACCUMULATION AND COMBUSTION UNDER THE BIOLOGICAL SHIELD

The Revision 8 [10] of the ERI/NRC MELCOR model of the NuScale plant has included updates and additions to the heat structure and flow path modeling in the region of the reactor cooling pool that is directly under the bio-shield. These features enable consideration of hydrogen build-up and combustion in this region that could become possible for accidents that can result in containment bypass (e.g., breaks in the CVCS pipe).

More recently [14], NuScale has simplified the design such that the gas space under the bio-shield connects to the gas space of the balance of the plant only through fixed vents in the vertical steel part of the shield. An earlier design accounted for in Revision 8 called for swing panels, HVAC ducts with dampers and fan-forced flows, and a small passive hole at the top of the shield. These features have been eliminated in favor of the vents of fixed flow area. Accordingly, Revision 9 of the MELCOR model[18] was prepared to take account of the simpler new design [15].

Related to the above remarks, and for clarity, it is helpful to be explicit that the bio-shield vents of the new design are now represented by flow paths 5684, 5686, and 5688 (see Figure A.4 in the Appendix).

This section documents the results of simulation studies for the scenario identified in the NuScale Final Safety Analysis Report (FSAR) [11] as LCU-03T-01. The results of these simulation studies also include assessment of the impact of various assumptions and conditions through sensitivity calculations (see Table 4.1). The Applicant has reported in References [11] and [12] the results of simulations of this scenario (although Reference [12] does not use the designator LCU-03T-01). In those references the emphasis is not mostly on combustion (in fact, Chapter 19 of Reference [11] mentions that LCU-03T-01 is considered only for issues not related to combustion, because in this scenario the hydrogen bypasses the containment [19]). Therefore, the Applicant's predictions reported in References [11] and [12] are not compared to the simulation results reported herein, apart from a few in-text remarks.

The accident scenario that is considered for the present study is referred to in the FSAR as LCU-03T-01 (see FSAR [11], Chapter 19, p. 349/412). As discussed below, some parameters have been assumed, considering that Reference [14] has not eliminated every uncertainty. The uncertainty in these parameters is addressed through sensitivity calculations.

Table 4.1 Calculation matrix for the LCU-03T-01 scenario and several sensitivity cases

Case	Total vent flow area (m^2)	Deflagrations under the bio-shield	Vent form loss coefficient (K)	Remarks
1	[[ ]]$^{2\,(a),(c)}$	Suppressed in MELCOR	[[ ]]$^{2\,(a),(c)}$	"Suppressed deflagrations" case prohibits burning in the MELCOR simulation, but detonation is considered in post-run analyses. The loss coefficient represents the stacked shields.
2	[[ ]]$^{2\,(a),(c)}$	Suppressed in MELCOR	[[ ]]$^{2\,(a),(c)}$	The loss coefficient represents only one un-stacked shield. Otherwise, identical to Case 1

[18] Revision 10 now exists and has been used for the calculations discussed in Section 3.4. Revision 10 is essentially the same as Revision 9, but with the reinstatement of radiolytic sources that had been deleted in Revisions 8 and 9. Reference [20] provides calculation notes for Revision 10.

[19] It is noteworthy that this mentioned exclusion of consideration of LCU-03T-01 for combustion issues, included in Revision 0 of Reference [11], has been struck out in the available draft version of Revision 1 of Reference [11]. (Markup for the draft version of Revision 1 of Reference [11] is available in the Response to RAI-9022.)

Case	Total vent flow area (m^2)	Deflagrations under the bio-shield	Vent form loss coefficient (K)	Remarks
3	[[ ]]$^{2\,(a),(c)}$	Allowed in MELCOR	[[ ]]$^{2\,(a),(c)}$	"Allowed deflagrations" case allows combustion starting at 10% H_2. Otherwise, identical to Case 1.

4.1 Simulation Model

Reference [15] provides the complete calculation notes for Revision 9 of the present MELCOR model of the NuScale plant. For ready reference, this section explains the present use of the various flow paths that connect the region under the bio-shield to the balance of the plant according to the current (November 2018) design. See also Figure A.4 in the Appendix.

Flow path FL 322 models the broken CVCS line. Based on information provided by the NRC staff (see an email titled "ERI disposition of design information-staff response.docx", dated Nov. 14, 2017), for the CVCS line break outside the containment, the break area is 0.56 in^2 (= 3.613×10^{-4} m^2). The "from" CV is CV 174, which is a part of the riser below the steam generators and above the transition cone. The "to" CV is CV 518, which is the second-from-top, innermost control volume that represents the cooling pool (see Fig. A.4). The concrete walls of the cooling pool, the vertical part of the bio-shield, the horizontal part of the bio-shield, and the cooling pool water surface form a box-like gas-occupied region modeled by the entireties of CVs 519 and 529, CVs 518 and 528, and those parts of CVs 517 and 527 that are above the water line. As modeled, the volume of this gas space is [[ ]]$^{2\,(a),(c)}$ m^3, and the height is [[ ]]$^{2\,(a),(c)}$ m. The water line elevation is [[ ]]$^{2\,(a),(c)}$ m, i.e., [[ ]]$^{2\,(a),(c)}$ feet above the pool bottom[20]. The elevation of FL 322 is [[ ]]$^{2\,(a),(c)}$ m (i.e., well above the water line). The MELCOR flashing model has been invoked for FL 322.

A figure on p. 6/81 of [14] shows the staggered radiation panels that comprise the vertical side of the bio-shield according to the new design. The right-most part of the figure mentions, but does not show, the detail "M" whose dimensions determine the gas flow area in terms of the spacing between the staggered panels. This detail, however, can be found on p. 10/14 of document ED-F012-3661, Revision 3 (available on the ERR). With aid of scaling, the spacing is estimated as [[ ]]$^{2\,(a),(c)}$ inches. Page 7/14 of that same document gives the width of the shield as [[ ]]$^{2\,(a),(c)}$ inches. From these dimensions, the flow area is estimated as [[ ]]$^{2\,(a),(c)}$ (i.e., [[ ]]$^{2\,(a),(c)}$ m^2) per each of the four strip-like vents that the cited figure from Reference [14] shows running across the width of the shield, for an estimated total flow area of [[ ]]$^{2\,(a),(c)}$ m^2 for the bio-shield vents. The flow path through the staggered panels being tortuous, however, it appears preferable to set aside this estimate in favor of the value actually used by the Applicant. This value has been provided by the Applicant in another ERR document, namely EC-0000-6746_R0. That source gives the total bio-shield vent flow area as [[ ]]$^{2\,(a),(c)}$ m^2. Also given there are the hydraulic diameter and the hydraulic form loss coefficient. The hydraulic diameter is [[ ]]$^{2\,(a),(c)}$ m. The form loss coefficient is [[ ]]$^{2\,(a),(c)}$ if the bio-shield of the considered module has stacked on it the bio-shield of a neighboring module, as happens when the neighboring module is being re-fueled. At times when there is no such stacking, the form loss coefficient is [[ ]]$^{2\,(a),(c)}$.

In the model, the gas space in contact with the vertical part of the bio-shield is modeled by three control volumes: CVs 529 and 528 (of equal height; their net elevation range covers 77% of the height of the gas-occupied region enclosed by the bio-shield) and CV527 (whose elevation range includes the water line; its fraction of the height of the gas-occupied region is 23%). The total vent flow area is apportioned among CVs 529, 528, and 527 according to these fractions. That is, the corresponding flow paths, FLs 5688, 5686, and 5684, are respectively assigned fractions 0.385,

[20] Revision 9 of the MELCOR model adheres to the value used in Revision 8 and earlier. For design basis accident calculations, NuScale has reconsidered that a conservative 65 feet should be used.

0.385, and 0.230 of the total flow area of [[ ]]$^{2\,(a),(c)}$ m^2. These flow areas are fixed[21] in accord with the new simpler design. The hydraulic diameter and the form loss coefficient are set to [[ ]]$^{2\,(a),(c)}$ m and [[ ]]$^{2\,(a),(c)}$, respectively, as given by the Applicant for stacked shields. The "to" CV for all of these flow paths is CV 599, whose atmosphere models the gas-occupied regions of the balance of the plant. The liquid-occupied part of CV 599 lumps the cooling pools below the eleven other reactor modules, plus the channels between them. The atmosphere of CV 599 models the balance of plant gas space and connects to the environment. Several submerged flow paths freely connect the cooling pool of the modeled module to the pool of CV 599.

The most recent information indicates that no fans act to force air to circulate in and out of the bio-shield vents. On the other hand, in the actual plant HVAC systems do exist to forcibly circulate air around the balance of plant gas space, and to cool the balance of plant water. It is supposed that the actual HVAC systems tend to maintain the balance of plant gas and water temperatures in spite of the heat lost through the walls of every one of the containment vessels. The heat lost at each module into its bio-shield region then supports a buoyancy-driven natural circulation in and out of the bio-shield vents. The model neglects balance of plant HVAC systems. In the model, the gas and water under the bio-shield (CVs 511 through 529; see Figure A.4), as well as the balance of the plant (CV599) have equal initial temperature 37.75 °C (99.95°F); the balance of plant connects to an "environment" CV whose temperature, 34.85 °C (94.73°F), is kept constant in the present simulation studies. At the end of the 1000 second-long pre-transient steady state calculation, the model predicts balance of plant air entering the bio-shield region through FLs 5684 and 5686 (the two lower FLs that model the vents) at net steady rate 0.15 kg/s (about 279 cubic feet per minute), and leaving the region at the same rate through FL5688 (the highest FL that models the vents). The accuracy of this prediction is not considered, but at least qualitatively it corresponds to the actual design according to present understanding. As discussed below, during the transient, the vent flows are dominated by transient conditions, and are assumed to be relatively little affected by any contribution to the flows that could be made by the actual balance of plant HVAC systems.

4.2 Simulation Results

The LCU-03T-01 scenario consists of initiating the CVCS line break that discharges to the gas-occupied region under the bio-shield (FL 322), with the assumption of no mitigation being possible. This means that the break remains un-isolated and ECCS never actuates. Scram and isolation of the steam generators occur simultaneously with the break, at least in the ERI calculation.

The Applicant reports a simulation of this scenario[22] in Reference [12]. Most of the discussion and figures in the Applicant's document [12] pertain to the behavior of the LHC model (i.e., the new MELCOR package that simulates crust formation and other phenomena that occur at the inside bottom of the containment vessel after the reactor vessel breaches). Combustion events in the bio-shield region are mentioned in Reference [12] but no details are given.

In Cases 1 and 2 (see Table 4.1), the MELCOR simulation proceeds with deflagrations intentionally suppressed in the six control volumes that represent the gas region under the bio-shield. (Case 3 re-considers this assumption.) The MELCOR-predicted atmospheric conditions that arise under the bio-shield in the absence of combustion are used in post-processing calculations of AICC pressures and temperatures. Section 4.3 considers the possibility of detonations for Case 1.

[21] Actually, for convenience, each of the three flow paths is set up with a base flow area of 2 m^2 and a valve control function that appropriately reduces the base area to the desired actual area. In a given calculation, these valve control functions are fixed, but can be conveniently adjusted for tests of the sensitivity of the results to the vent flow area.

[22] That is, the case of CVCS line break to the bio-shield region. Reference [12] does not use the name LCU-03T-01. Table 7-14 of Reference [12] gives the timings. A few of the Applicant's timings mentioned here are taken verbatim from there, including the timings for combustion events under the bio-shield and in the containment. Table 19.2-8 of the FSAR [11] gives similar, but not exactly the same, timings. FSAR [11] figures pertaining to LCU-03T-01 appear to be limited to Figures 19.2-11 and 19.2-12, with content not relevant to the present issue.

4.2.1 Suppressing Hydrogen Deflagration under the Bio-shield

In these "suppressed deflagrations" cases, hydrogen deflagrations are suppressed in the gas space under the bio-shield only (combustion elsewhere in the plant, such as the containment, has not been suppressed). Using the gas composition results, the potential impact of consequential combustion events in the bio-shield region are then considered in Section 4.3.

In the first of the calculations ("Case 1" as defined by Table 4.1), the flow area of the bio-shield vents (i.e., net flow area of FLs 5688, 5686, and 5684) is [[ ]]$^{2\,(a),(c)}$ m^2 as given by the Applicant in document EC-0000-6746_R0. Also as given by that source, the vents form loss coefficient is [[ ]]$^{2\,(a),(c)}$, modeling stacked shields. ECCS and isolation of the CVCS line, lost at the start of the transient, are never recovered. Combustion is suppressed under the bio-shield but allowed everywhere else.

Figure 4.1 shows the calculated water level in the RPV. Figure 4.2 shows the cumulative generation of hydrogen due to oxidation of zirconium and steel in the core. For consideration of 10 CFR 50.44 requirements, NuScale's value for the amount of hydrogen that corresponds to steam oxidation of 100% of the cladding on the active part of the fuel is 93.3 kilograms.[23] As the following results show, for the present study the rate of hydrogen generation is more consequential than is the cumulative amount. The rate is at maximum at about 5 hours.

Figure 4.3 shows the well-mixed gas composition of the atmosphere under the bio-shield. This composition corresponds to a post-processing summation of the gas inventories of CVs 519, 529, 518, 528, 517, and 527. Figure 4.4, showing the temperatures of the gas under the bio-shield, indicates that, although CVs 519, 529, 518, 528, 517, and 527 are well-connected to each other by flow paths of large flow area, considerable stratification results in both the axial and radial directions. (The second digit in the CV serial numbers is 1 for the inner ring; the third digit is 9 for the highest level.) Also shown is the well-mixed temperature.

At the start of the transient, most of the initial air under the bio-shield is pushed out in about 60 seconds, a time too short to be shown on the scales of Figure 4.3, making the initial steam concentration appear to be about 0.7 molar (instead of ~0.0 as is actually the case). The (well-mixed) steam concentration reaches a maximum of 0.88 at 0.91 hours, just after the break flow rate sharply decreases due to the RPV water level falling below the entrance to the break. Until this time the break is liquid/water, some of which however flashes to steam as soon as it enters the region under the bio-shield. Air begins to re-appear in significant amounts starting from this time. Hydrogen first appears in minute amounts at 4.35 hours, when the (well-mixed) oxygen concentration is 0.17. The well-mixed atmosphere first becomes flammable at 5.09 hours[24]. The flammability definition used here is: at least 5% oxygen; at least 7% hydrogen; at most 55% steam. In post-processing, AICC calculations are carried out on the evolving well-mixed atmosphere[25], and the time at which the AICC pressure is at maximum is 5.12 hours (see Figure 4.5). This is also the time of the maximum well-mixed hydrogen concentration, 0.096 molar, and the time of maximum hydrogen mass, 1.6 kg. The AICC calculation carried out at this time results in the burning of all the hydrogen under the bio-shield, leaving leftover oxygen. The pre-burn hydrogen concentration is 0.096; the pre-burn oxygen concentration is 0.168. With pre-burn nitrogen and steam concentrations of 0.631 and 0.105 respectively, this mixture is not detonable,

[23] Revision 9 of model has the capability to let the user define sources of "extra" hydrogen injected to the core exit so that, for example, amounts closer to the 100%-clad-equivalent amount could be generated. However, this feature was not invoked for the LCU-03T-01 calculations. Revision 9 does not, however, retain the sources set up for correspondence with radiolytic hydrogen generation: that was a special feature of a pre-Revision 8 variant model used for the calculations of Section 3. The radiolytic sources have been restored to Revision 10, used for the calculations of Section 3.4.

[24] The Applicant's time for the first combustion event under the bio-shield is 2.7 hours; see Table 7-14 of Reference [12]. This and other timing differences may reflect a different CVCS line break flow area.

[25] Calculation of the AICC pressure and temperature follows the standard approach, but it is noted that as an estimate for conditions arising in actual deflagrations (slow combustion), the AICC pressure and temperatures are over-estimates since the assumption of isochoric combustion is not valid in the considered situations, which include widely open flow paths leading away from the region of combustion.

according to a simple definition[26] used in some analyses. The definition is re-considered in Section 4.3. The AICC pressure is 3.04 bar-abs; the AICC temperature is 1387K. The pre-burn well-mixed temperature is 437K (but the temperatures of the individual CVs range from 316K to 478K, as Figure 4.4 showed). To this time the cumulative in-vessel-generated hydrogen production is 25 kg. For inflammable mixtures the AICC pressure[27] (Figure 4.5) is just the pre-burn pressure; the well-mixed atmosphere under the bio-shield is not flammable later than 5.15 hours due to low hydrogen concentration.

Though of secondary interest in the present context, important events in the accident progression are vessel breach at 17.9 hours with combustion in the containment occurring immediately after vessel breach. The Applicant's timings (see Table 7-14 of Reference [12]) are 11.2 hours for vessel breach with containment deflagrations starting at 11.5 hours.

It can be concluded that, in the considered scenario, the new design for the bio-shield vents allows the well-mixed atmosphere under the bio-shield to avoid flammability apart from a brief interval (duration about 3 minutes) around the time that hydrogen is being produced in the core at the maximum rate (~5.1 hours). With respect to the well-mixed atmosphere, this calculation avoids detonability at all times and finds a peak well-mixed hydrogen concentration of less than 10%. The inflammability at times away from ~5.1 hours can be attributed to insufficient hydrogen (rather than insufficient oxygen or excessive steam), itself due to the ability of the hydrogen to quickly escape from the bio-shield region through the vents. At 5.0 hours, the vent flows are at rates ~2.0 kg/s for net inward-flowing air from the balance of the plant (carried by the lower vent flow paths, FLs 5684 and 5686) and ~2.3 kg/s for net outward-flowing air plus hydrogen and steam from the bio-shield region (carried by the highest vent flow path, FL5688). Figure 4.6 shows these flows. These flows are much larger than the inward- and outward-flows of order ~0.15 kg/s that this model predicts during the pre-transient period. During the short pre-transient period, the predicted balance of plant temperatures do not have time to change appreciably, and so behave much as do the actual balance of plant temperatures during ongoing operations, which benefit from the action of the actual HVAC systems. The predicted pre-transient flows may therefore roughly represent the buoyancy-driven bio-shield vent flows that actually arise from the operation of the plant's un-modeled balance of plant HVAC systems. Although this speculation is not investigated, the smallness of the predicted pre-transient vent flows compared with the predicted transient vent flows suggests that the results of interest would not change much if the balance of plant HVAC systems were included in the model.

Whereas the peak well-mixed hydrogen concentration is 0.096 molar, the peak local hydrogen concentration (found by maximizing over the six CVs) is 0.126. This peak concentration is predicted to occur in CV518, but CVs 519 and 529 give peak concentrations only negligibly smaller. These peaks occur at 5.12 hours. The peak hydrogen concentrations that occur in CVs 528 and 517 are respectively 0.104 and 0.054, and occur at about the same time. The peak hydrogen concentration that occurs in CVs 527 is only 0.0037, and occurs at 9.3 hours. Recall that, most of the time, balance of plant air flows into CVs 527 and 528 while CV529 is the exit point for the bio-shield gases, and the break from the RPV is into CV518. (Also see Figs. 4.6 and A.4.) Figures 4.7 and 4.8 respectively show the molar compositions of the atmospheres of CVs 518 and 527. Except for the appearance of some steam, the composition of the gas of CV527 is never much different from normal air. To the eye, the composition of the gas of CV518 is never much different from the well-mixed atmosphere (Fig. 4.3), but the hydrogen peak is higher (0.126 instead of 0.096). Section 4.3 examines the detonability, implication and potential loads results from detonation of a 12.6% hydrogen mixture.

[26] Derived mainly from Reference [9], simplified criteria of detonability used by ERI in many analyses are: hydrogen and oxygen molar concentrations greater than 0.15 and 0.05 respectively, steam concentration less than 0.35, and temperature less than 850K. See Section 4.3 for a more careful treatment of detonability.

[27] Note: Each AICC calculation assumes no prior burn.

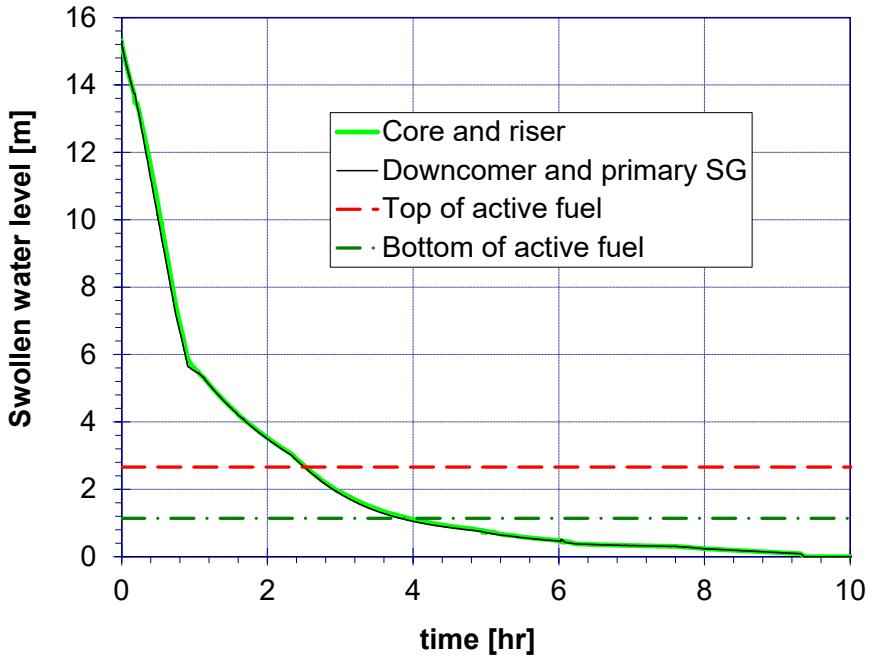

Figure 4.1 Water levels in the RPV (Case 1)

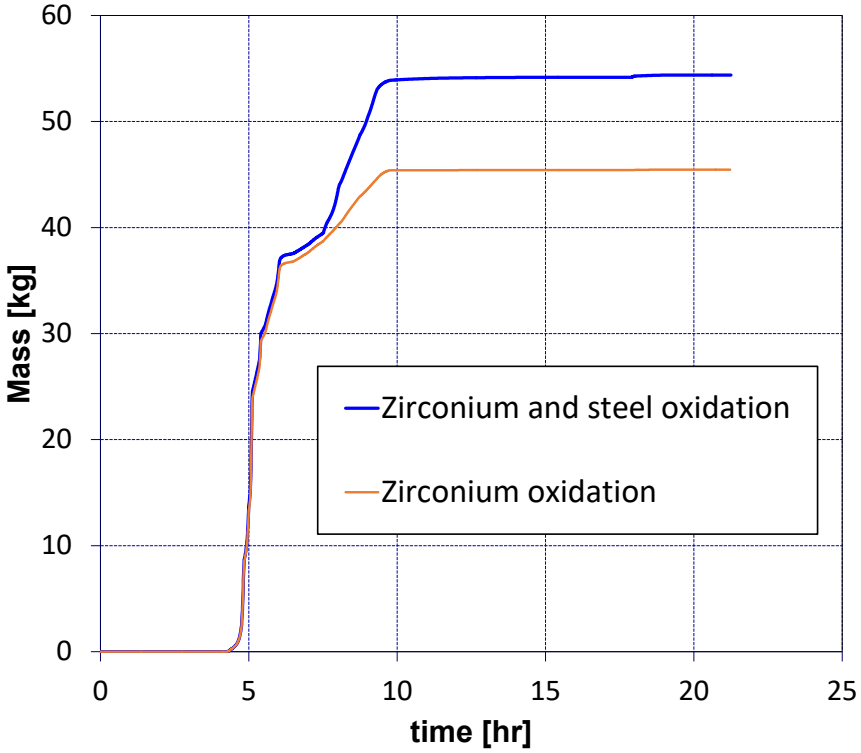

Figure 4.2 Cumulative hydrogen generation (Case 1)

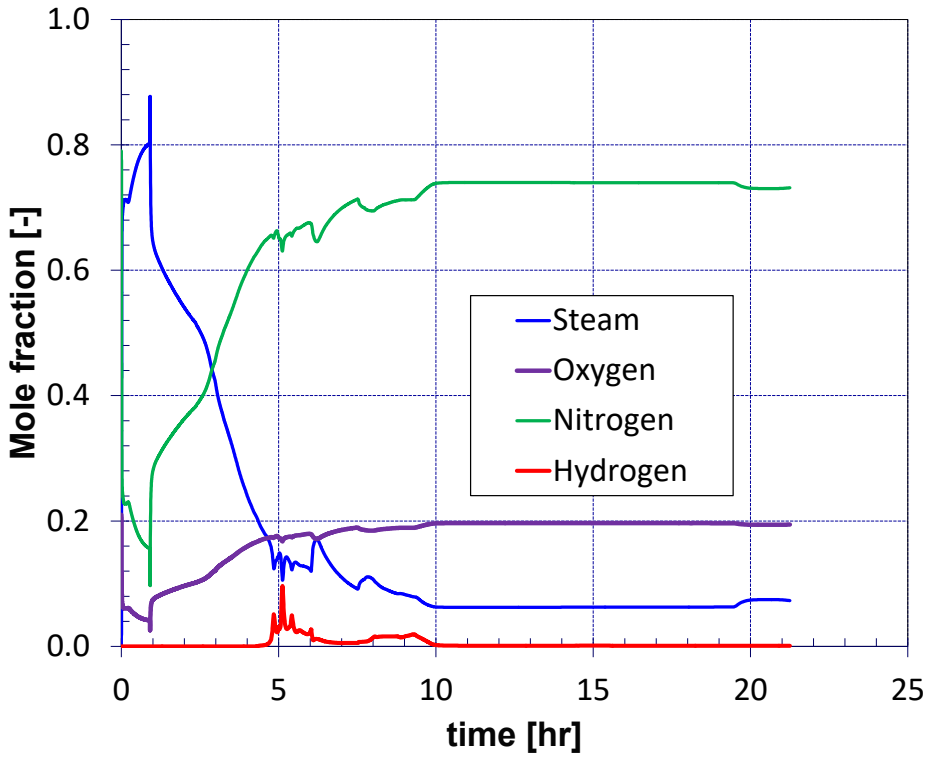

Figure 4.3 Well-mixed atmosphere composition under the bio-shield (Case 1)

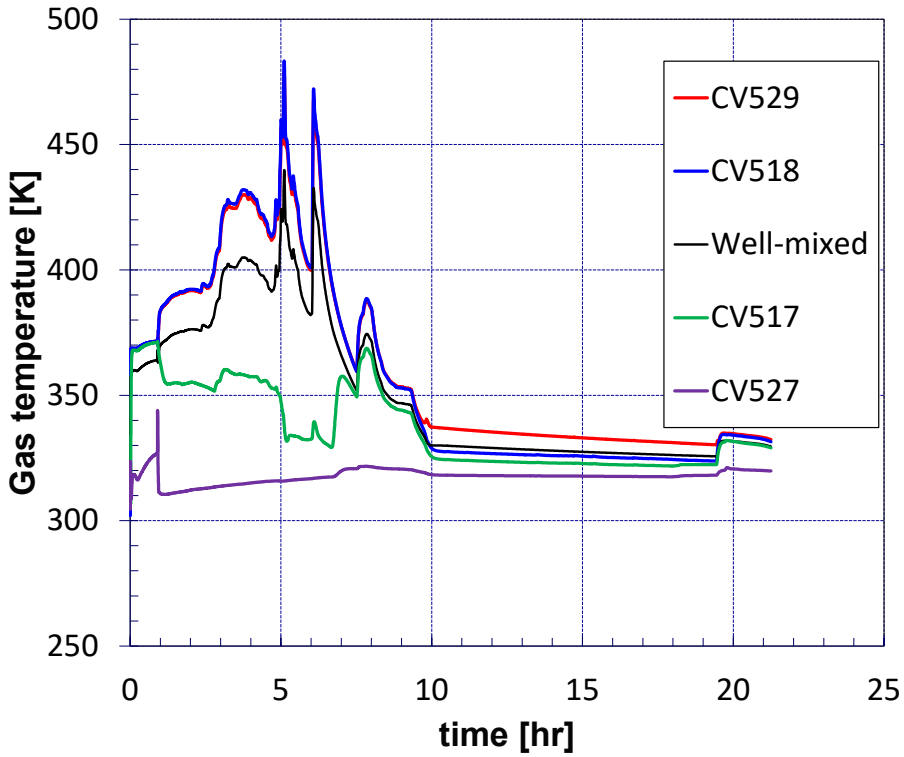

Figure 4.4 Atmosphere temperatures under the bio-shield (Case 1)

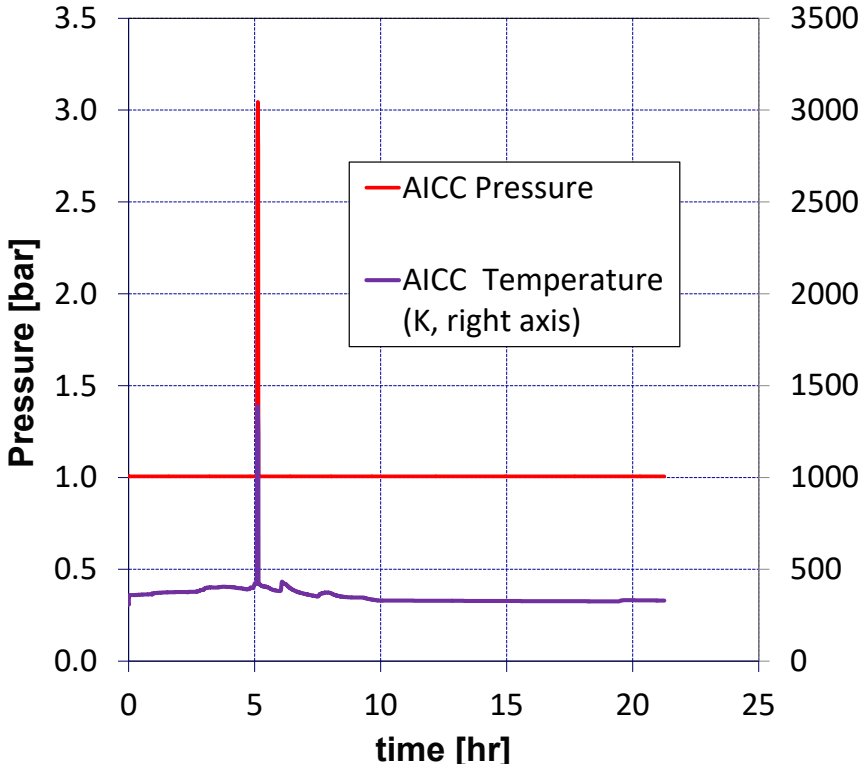

Figure 4.5 AICC pressure and temperature (Case 1)

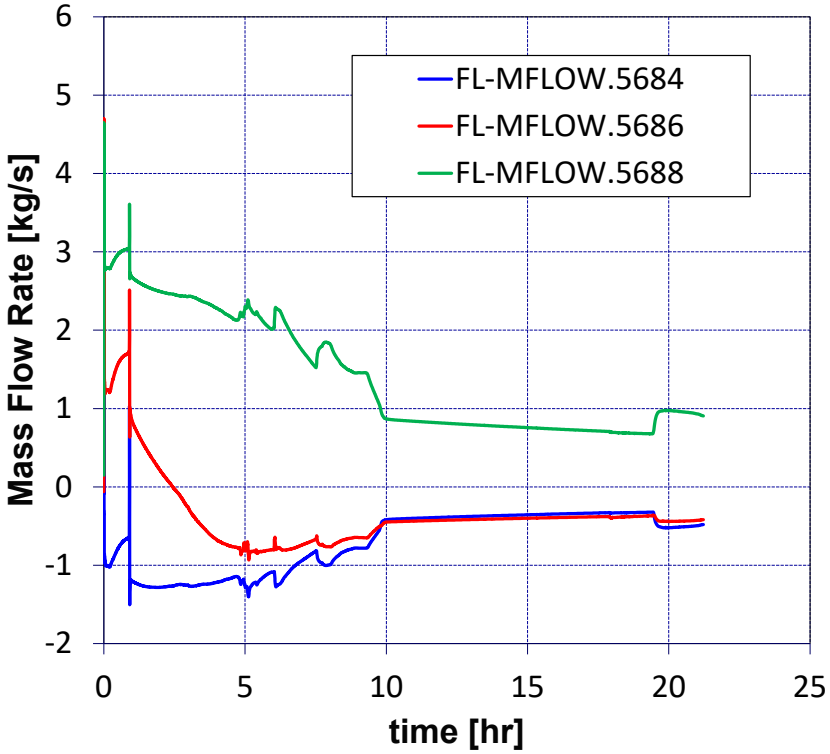

Figure 4.6 Gas flows through the three flow paths representing the bio-shield vents (Case 1)

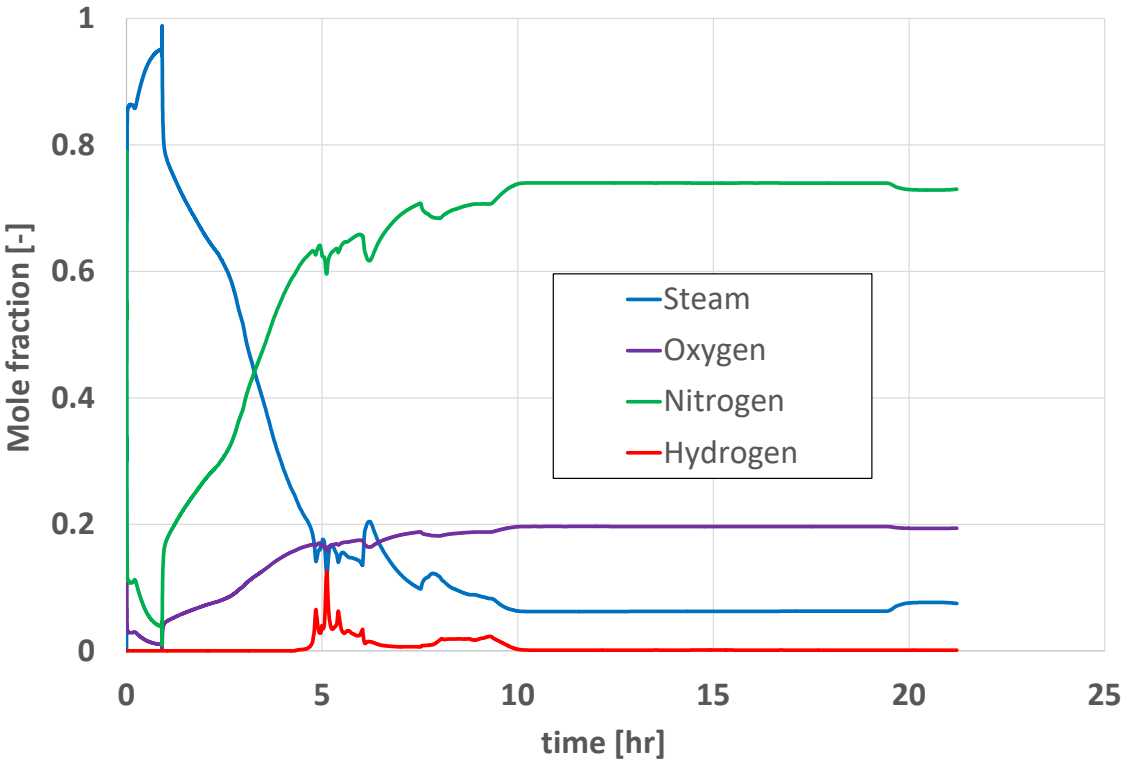

Figure 4.7 Atmosphere composition of control volume CV518 (Case 1)

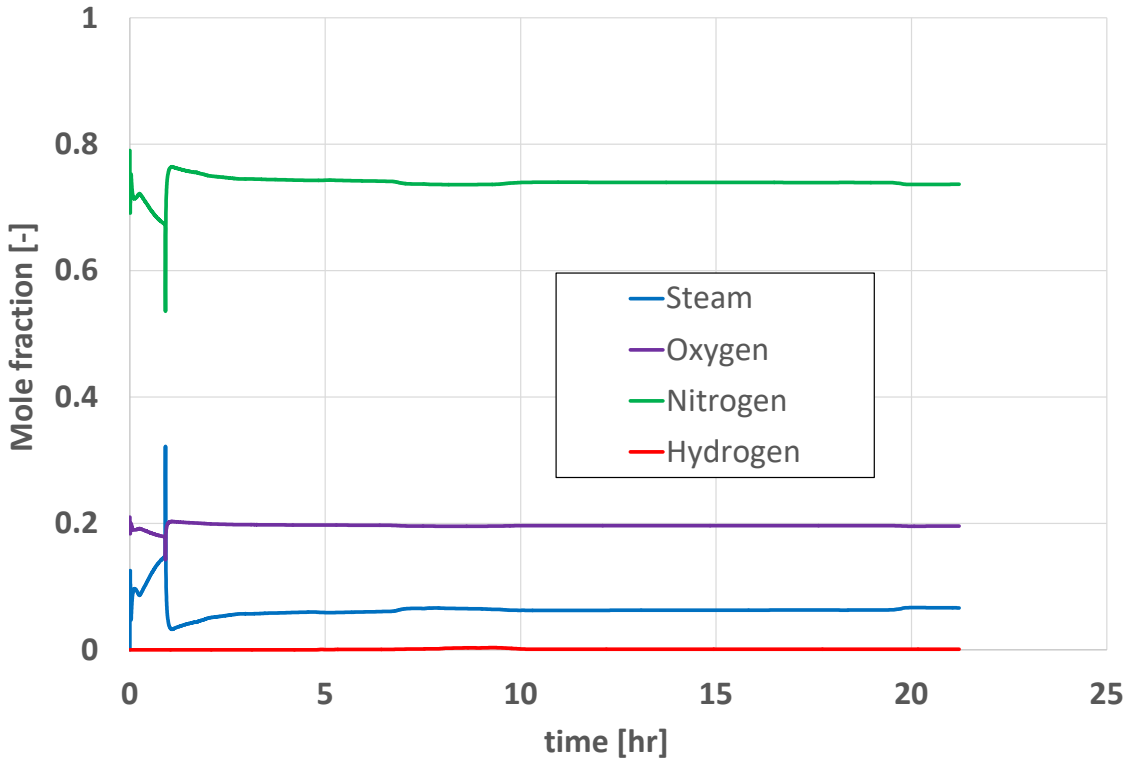

Figure 4.8 Atmosphere composition of control volume CV527 (Case 1)

Case 2 (Effect of reduced form loss coefficient for the bio-shield vents)

This case is the same as Case 1 except that the three flow paths that represent the bio-shield vents are assigned a form loss coefficient of [[ ]]$^{2\,(a),(c)}$ instead of [[ ]]$^{2\,(a),(c)}$. In ERR EC-0000-6746_R0, the Applicant has given a form loss coefficient of [[ ]]$^{2\,(a),(c)}$ as the value that describes the vents associated with a single bio-shield, versus [[ ]]$^{2\,(a),(c)}$ which describes the action of the vents in the case that one bio-shield is stacked on another (as may occur during the re-fueling of a module that neighbors the modeled module). On the assumption that the higher value is more conservative, Case 1 adopted [[ ]]$^{2\,(a),(c)}$; now the sensitivity of the results to the lower value is checked.

Because the vent flow areas are rather large, the flow velocities are small most of the time, so most of the time the effects of this change is small. Figure 4.9 shows the bio-shield vent gas flows, which are the quantities most directly affected by the considered change. Comparison with Figure 4.6 show that this direct effect is modest. However, at times of more vigorous flows the freer vent flows of Case 2 result in lower hydrogen concentrations than those of Case 1. Figure 4.10 shows the composition of the well-mixed atmosphere under the bio-shield. Differences between it and Figure 4.3 are not conspicuous to the eye, but in Case 2 the peak well-mixed hydrogen concentration is 0.065, to compare with 0.096 in Case 1. This peak occurs at 5.08 hours in Case 2, versus 5.12 hours in Case 1. For the calculation of AICC pressure, it is usual to consider the minimum hydrogen concentration for combustion to be 0.07. For the purposes of Figure 4.11, a lower minimum of 0.06 was allowed. This lower minimum is attained during a period of duration ~3 minutes at about 5.1 hours. The peak AICC pressure occurs at 5.08 hours and is 2.60 bar-abs, to compare with 3.04 bar-abs in Case 1. The peak local hydrogen concentration, occurring in CV518 in both cases, is 0.085 in Case 2 versus 0.126 in Case 1. It is concluded that, due to threshold effects, whether or not a second shield is stacked on top of the shield of the module undergoing the accident could be decisive on whether or not combustion occurs under the shield. Detonability, barely possible in Case 1 as is discussed in Section 4.3, seems positively ruled out in Case 2, due to the low peak local hydrogen concentration of only 8.5%.

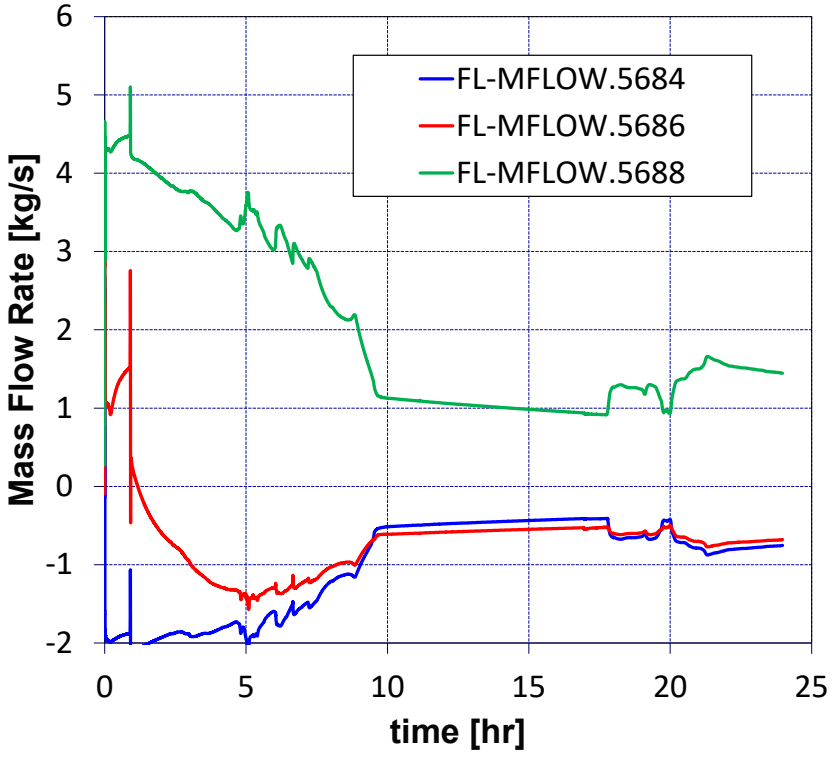

Figure 4.9 Gas flows through the three flow paths representing the bio-shield vents (Case 2)

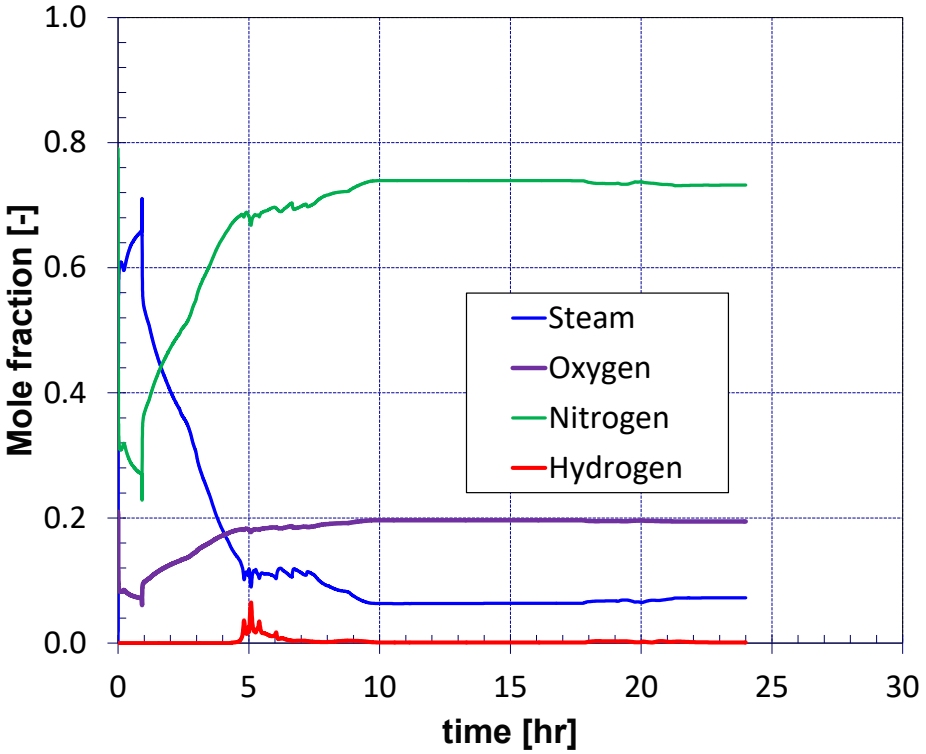

Figure 4.10 Well-mixed atmosphere composition under the bio-shield (Case 2)

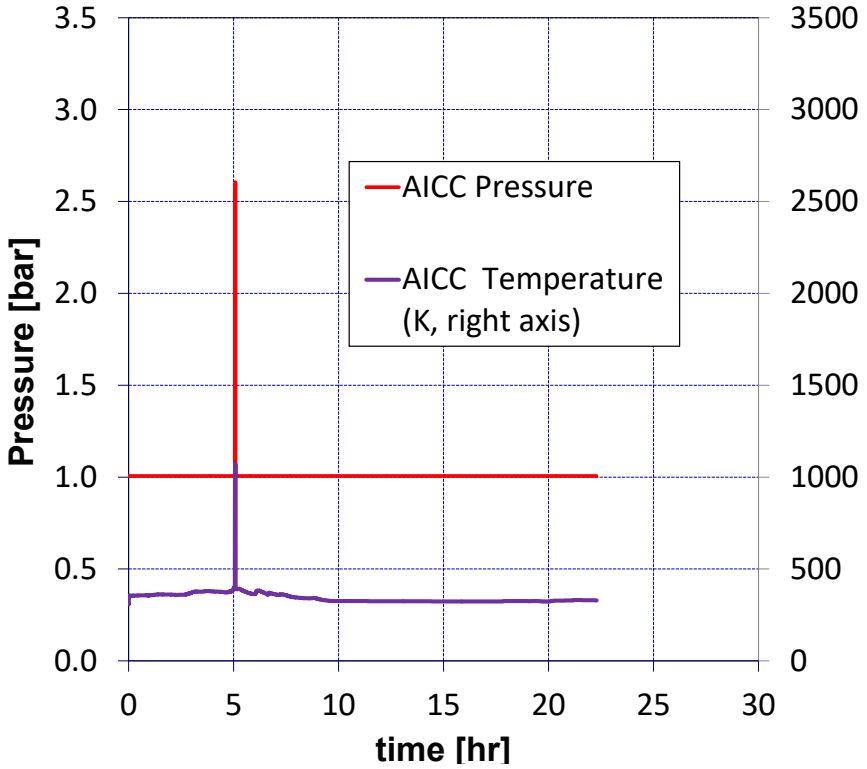

Figure 4.11 AICC pressure and temperature (Case 2)

4.2.2 Enabling Hydrogen Deflagration Events in the Bio-shield Region

This case (Case 3 as defined by Table 4.1) is the same as Case 1 except that deflagrations under the bio-shield are allowed to occur in the MELCOR simulation (according to its built-in models). MELCOR defaults are assumed, meaning that combustion is initiated in any region when the mixture becomes flammable (according to the definition given above) and, additionally, the hydrogen concentration exceeds 10%.[28] An automatic consequence of this assumption is that there are no regions (i.e., CVs) that can have both a flammable atmosphere and a hydrogen concentration above 10%; therefore, this is a mitigating assumption. All the resulting burning occurs in four of the six CVs (namely the four that do not include any water) at 5.07 hours. All burns start simultaneously to within 0.1 s and take less than 0.5 s to complete.

In Case 3, the maximum hydrogen amount in the bio-shield region is 1.2 kg which occurs at 5.07 hours just before the burns; the burns then consume 0.8 kg of that hydrogen. (To compare, in Case 1 the maximum hydrogen amount is 1.6 kg, that is reached at 5.12 hours when the AICC pressure also is maximum, and the AICC combustion at that time consumes the entire hydrogen inventory.) Maximized over the six CVs, the peak local hydrogen concentration is 0.100 (to compare with 0.126 in Case 1). The peak well-mixed hydrogen concentration is 0.075 (to compare with 0.096 in Case 1). The MELCOR-predicted pressure is shown by Figure 4.12; the peak occurs at the time of the combustion event and is 1.045 bar (to compare with the initial pressure 1.006 bar-abs, and with the peak AICC pressure 3.04 bar-abs of the well-mixed atmosphere in Case 1). The last comparison probably reflects the poorness, in the case of the bio-shield region, of the isochoric assumption in estimating the MELCOR-predicted pressure as an AICC pressure, since MELCOR accounts for the free connection of the bio-shield region to the balance of the plant through the vents of total flow area [[ ]]$^{2\,(a),\,(c)}$ m^2. This calculation was ended at 13.5 hours.

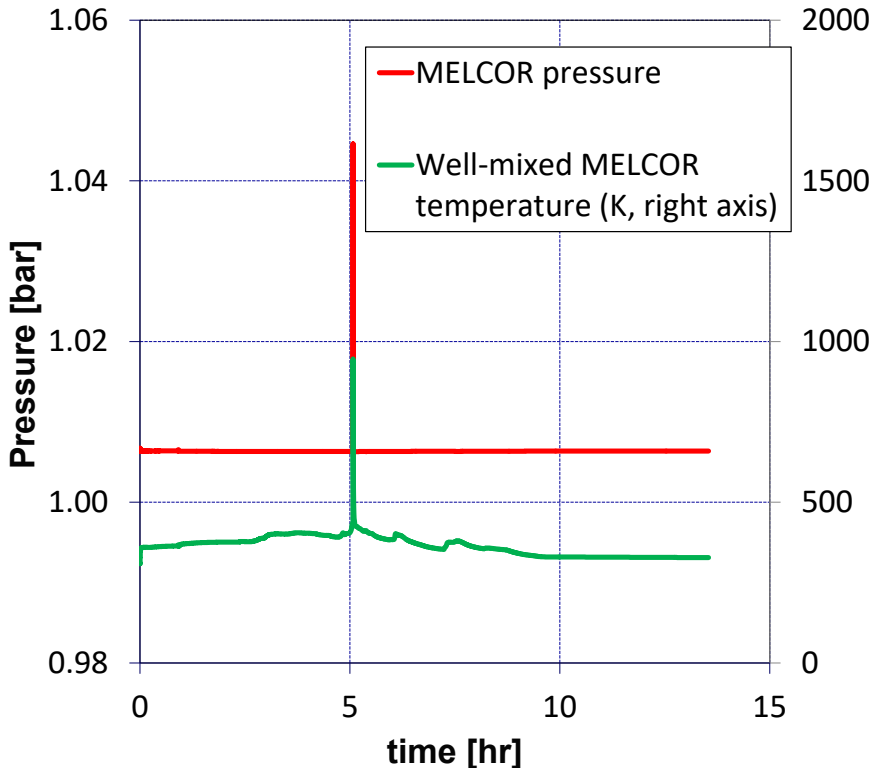

Figure 4.12 MELCOR-predicted pressure and well-mixed temperature (Case 3)

[28] Also, once a burn begins in some control volume according to these criteria, the flame can propagate to nearby control volumes and ignite their atmospheres if they are flammable.

4.3 Potential for Hydrogen Detonation

In Case 1, the bio-shield atmosphere attains a maximum local hydrogen concentration of 12.6% in CV518, approaching the lowest limit of detonability that has been observed experimentally [16]. The potential for detonation of hydrogen in the bio-shield region is investigated in the present section. All inputs are taken from the Case 1 simulation, in which deflagrations under the bio-shield according to MELCOR's built-in models were suppressed, allowing hydrogen build-up.

As discussed in Section 4.2.1, at 5.12 hours, when the local hydrogen peak is attained, the composition of CV518 is: 0.1191 (steam), 0.1586 (oxygen), 0.5964 (nitrogen), 0.1259 (hydrogen), 1.006 bar-abs (pressure), 478K (temperature). For a gas of this composition, the AICC pressure is 3.31 bar-abs (see again footnote 15). This is a modest increase over the AICC pressure of the well-mixed atmosphere, 3.04 bar-abs, reported above for Case 1.

Combustion waves are usually classified as deflagrations or detonations. Deflagrations are combustion events in which unburned gases are heated by thermal conduction to temperatures high enough for chemical reaction to proceed. Deflagrations typically travel at subsonic speeds and result in quasi-static pressurization. On the other hand, detonations are combustion processes in which heating of the unreacted gases is due to compression from the resulting shock waves. Detonation waves travel supersonically and produce dynamic or impulsive loads on the surrounding structures.

The combustion of hydrogen as it enters the region under the bio-shield is governed by a number of factors, including the mixture composition, pressure, temperature and ignition sources, among other factors.

Ignition of dry hydrogen in air when the mixture is well within the flammability limits can occur with a very small energy input (e.g., sparks). The minimal energy required for ignition of a quiescent mixture is a function of hydrogen concentration and pressure, and it is of the order of 0.02 milli-joule at atmospheric pressure and 30% hydrogen and increases to as much as 0.6 milli-joule at the minimum flammability concentration and at hydrogen concentrations approaching 60% (see Figure 2-18 of Reference [16]).

When hydrogen is injected into a compartment in the form of steam/hydrogen mixture (e.g., following a break), hydrogen can start to burn as turbulent diffusion flame, whereby combustion rate is controlled by the rate of mixing of hydrogen and oxygen, provided flammability limits are reached. Combustion can occur either due to an external ignition source or because the mixture is above the spontaneous ignition temperature (i.e., 959 – 1076 °F [515 – 580 °C]).

Prediction of deflagration-induced conditions (i.e., temperature and pressure spikes) involves energy addition due to the reaction process and energy removal from the reaction zone by heat transfer to the surrounding structures, provided conditions (e.g., flammability limit, ignition source, etc.) conducive to combustion exist.

Prediction of likelihood of detonation is subject to uncertainties. Albeit less uncertain, the determination of the conditions under which a mixture can detonate, and the resulting pressure loads, are discussed below.

Hydrogen-air mixtures near stoichiometric (i.e., two parts hydrogen and one part oxygen) are detonatable. Other mixtures (less than stoichiometric) are much more difficult to detonate. Reference [16] states that at mixture ratios of about 28% and 58% hydrogen, hydrogen-air mixtures could not be detonated.

In general, the potential for detonation can be assessed based on the mixture intrinsic flammability (i.e., detonation cell width), and the specific geometry. Measured cell width for mixtures have been reported in the literature [17-18]. Reference [18] shows a correlation of experimental data in terms of the detonation cell width λ and the characteristic mixture size L (i.e., characteristic mixture size L is proportional to volume to 1/3 power). The results of the experiments [18] show that:

$$\lambda = L/7 \tag{4.3.1}$$

This represents, from the experiments, the limit for possibility of detonation or Deflagration-to-Detonation Transition (DDT), which is believed to be accurate to within a factor of 2. Furthermore, cell size data are necessary for application of the DDT criterion. Detonation cell sizes of hydrogen-air and hydrogen-air-steam mixtures have been measured experimentally [18]. Fits to experimental data can be used to estimate the cell sizes for arbitrary composition and initial conditions within the range of tested parameters. The correlation given by Reference [9] has been used for the present study.

The results of experimental data show that the detonability of insensitive mixtures (i.e., very large λ approaching several meters) requires clouds with a very large mixture size (i.e., based on criterion of Equation 4.3.1, which defines the minimum cloud size L that supports DDT), which is physically not possible. On the other hand, the detonability of more sensitive mixtures (i.e., smaller λ) is conceivable. It is noted that detonations have been observed at hydrogen concentration as low as 13.8% [16]; however, for large geometric scales detonations may propagate in leaner mixtures.

A detonable mixture may only deflagrate and not detonate. Detonations can initiate either by a vigorous shock wave from a high explosive, a strong spark, or a laser [16]. Detonations can also start from deflagrations that accelerate to high speeds pushing shock waves ahead of the flame front until at some point shock heating is sufficient to initiate the detonation [16]. These include high speed jets from semi-confined regions or flames passing through obstacles. Therefore, DDT allows an easier path to develop conditions for a detonation.

In the case of the gas space under the bio-shield, the characteristic mixture size is about 8 m, this being the diameter of a sphere of volume ~300 m^3. Assuming the following conditions for the maximum local hydrogen concentration as shown in Figure 4.7 (Case 1 results for control volume CV518 at the time of highest H_2 concentration):

H_2O	0.11
O_2	0.16
N_2	0.60
H_2	0.13
$P_{pre\text{-}burn}$	1.006 bar-abs
$T_{pre\text{-}burn}$	478K

Using the composition of gases, the pressure, and the temperature, the corresponding detonation cell width λ is about 0.5 m as calculated from the correlation given in Reference [9]. It is seen that the characteristic mixture size L≈8 m is about [[ ]][2] [(a), (c)] times larger than the smallest mixture size that would support detonation (i.e., 7 λ ~ 3.5 m using Equation 4.3.1). The excess allows that L > 7 λ could still hold even if a more careful calculation reduced L by as much as a factor of ~2 (i.e., since not all the ~300 m^3 used to define L attains 12.6% hydrogen – see Figure 4.8 and the discussion of stratification in Section 4.2.1). Therefore, there is some potential for hydrogen detonation under the bio-shield for Case 1, and as implied in Section 4.2.1, the duration of the period of susceptibility to detonation is at most about 3 minutes.

Chapman and Jouguet (CJ) found that the conservation equations of mass, energy and momentum with appropriate thermodynamic equations of state did not lead to a unique solution of detonation velocity, and hence pressure and temperature. Consequently, they assumed the detonation traveled at a speed such that the flow behind the detonation was sonic relative to the detonation. Using the CJ model for about 14% hydrogen (Figure 2-22 of Reference [16] and extrapolating the curve to 13%), the detonation velocity is about 1650 m/s. Therefore, considering the distance from the location of maximum hydrogen concentration (CV518 mid-elevation) to the structures (top of the containment vessel as a lower structure, underside of horizontal part of the bio-shield as an upper structure) is about 2 m and 5 m respectively, any detonation waves will travel to those lower and upper structures in about 1.2 and 3 milliseconds, respectively. In addition, at 13% hydrogen concentration (and using Figure 2-25 of Reference [16] by extrapolation), the ratio of detonation pressure (P_{CJ}) to pre-burn pressure ($P_{pre\text{-}burn}$) of the detonation wave is about 9. Similarly, the estimated detonation temperature (Figure 2-26 of Reference [16]) is about 1900 K.

The reacted gases behind the detonation wave are moving in the direction of the detonation. When the detonation wave collides with the rigid structure, the reacted gases come to rest due to the reflected shock wave from the structure (in the opposite direction to the gases). The reflected shock wave further compresses the reacted gas resulting in an increase in detonation pressure. The estimated pressure ratio associated with the reflected shock wave using the present condition, again using Figure 2-25 of Reference [16] (by extrapolation), is about 23 and similarly, the estimated detonation temperature is about 2250 K.

In general, there can be a series of rarefaction/expansion (i.e., pressure increase and reduction) waves behind the detonation, thus reducing the gas velocity to zero midway between the detonation wave and the rear structure. In case of spherically expanding waves, the effect of rarefaction is even more pronounced, while for cylindrically expanding detonation, the rarefaction waves are midway between the planar and spherical geometries [16].

The total pressure loading on the structure can be estimated using the CJ assumption that the maximum pressure is the sum of the pressure due to detonation and reflected wave, that is:

$$P_{max} = [(P_{CJ}+P_{reflection})/P_{pre\text{-}burn}] \times P_{pre\text{-}burn} = (9+23) \times 1.006 = 32 \text{ bar-abs } (\sim 473 \text{ psia}).$$

It is possible that DDT can produce pressures in excess of the CJ or reflected CJ pressure. This has been observed in situations where the flame pre-compresses the mixture prior to onset of detonation [5], a phenomenon also referred to as "pressure piling." A condition more conducive to large pressurization due to DDT has been attributed to CJ detonation that reflects from the end of reaction apparatus (i.e., tubes). It is not clear if such conditions can be expected in relatively open geometries such as the bio-shield; therefore, the additional contribution to maximum detonation pressure due to DDT is not considered here. Reference [5] reports factors in the range of 4.5 to as high as 150 times the CJ or reflected CJ pressure, stating that "special set of circumstances is required to produce these pressures." These observations as reported in Reference [5] are for stoichiometric mixture, in closed systems, which are very different as compared to the bio-shield region and the conditions therein as calculated here.

The initial conditions for the aforementioned analyses are conservative since build-up of hydrogen beyond deflagration limit without combustion, to levels as high as about 13% is highly unlikely (see Section 4.2.1). In addition, the MELCOR-predicted concentration gradients that result in a small pocket of relatively high hydrogen concentration in the bio-shield is subject to large uncertainties. Furthermore, even if hydrogen concentration reaches 13%, it is not expected that detonations can be initiated through rapid flame acceleration, given the absence of any significant obstacles in the region of interest. Finally, absence of strong ignition sources would most likely eliminate the potential for any detonation, and low energy ignition would render the compartment more vulnerable to deflagration than detonation. Therefore, it is concluded that the probability of any hydrogen detonation in the bio-shield region potentially impacting the containment integrity (from the outside) or generating missiles from the damaged bio-shield structural components that can impart on the adjacent modules is negligibly small and can be ignored.

4.4 Summary of Results (Combustion under the Bio-shield)

Table 4.2 lists the most important results from the three variants of the LCU-03T-01 scenario. Local hydrogen concentrations of up to ~13% are predicted in one case (stacked shields with suppressed deflagrations). Since this concentration is at the extreme low end of the range of detonability, and it holds only for a brief time interval (~3 minutes), detonation is deemed highly unlikely. As it is discussed above, assuming detonation, the resulting pressure could be ~32 bar.

Relevant to the idea that a damaged bio-shield might become a source of destructive missiles, the following bullets note some of the details of the bio-shield. (The source of the information is the ERR document named "ED-F012-3661 Rev3." Some dimensions rely on ruler scaling of drawings shown there.) Only the vertical part of the shield is described, and that description is only partial:

- The vertical frame weldment consists of a grid of bars made of [[ ]]$^{2\,(a),(c)}$"-wide square stainless-steel tubing, wall thickness [[ ]]$^{2\,(a),(c)}$". Each of [[ ]]$^{2\,(a),(c)}$ vertical bars is [[ ]]$^{2\,(a),(c)}$" tall and has mass ~[[ ]]$^{2\,(a),(c)}$

kg; each of [[ ]]$^{2\,(a),\,(c)}$ horizontal bars is [[ ]]$^{2\,(a),\,(c)}$ inches wide and has mass ~[[ ]]$^{2\,(a),\,(c)}$ kg. Total mass of the vertical frame weldment: ~[[ ]]$^{2\,(a),\,(c)}$ kg.

- The vertical frame weldment carries 36 polyethylene panels, each [[ ]]$^{2\,(a),\,(c)}$" wide, [[ ]]$^{2\,(a),\,(c)}$" tall, and [[ ]]$^{2\,(a),\,(c)}$" thick. There are [[ ]]$^{2\,(a),\,(c)}$, with alternate rows on the outside vs. the inside of the frame, and with the rows staggered from each other vertically such that gas flow through the shield is free but radiation through the shield is blocked.

- The distance between the vertical parts of the bio-shields of two units that directly face each other across the channel is ~[[ ]]$^{2\,(a),\,(c)}$ m (rough estimate by scaling a schematic drawing in a 2012 PowerPoint presentation given by NuScale).

Based on the actual configuration and material design of the bio-shield, one cannot rule out that the bio-shield could be severely damaged by detonation, and any bio-shield structural fragments form missiles that could damage adjacent plant modules and/or components. However, absence of strong ignition sources would most likely eliminate the potential for any detonation, and low energy ignition would render the bio-shield compartment more vulnerable to deflagration than detonation. Therefore, it is concluded that the probability of any hydrogen detonation in the bio-shield region potentially impacting the containment integrity[29] (from the outside) or generating missiles from the damaged bio-shield structural components that can impart on the adjacent modules resulting in core damage, is negligibly small and can be ignored.

[29] In this case, the integrity of the containment for the affected module is not of any importance, except for long-term post-accident stabilization standpoint.

Table 4.2 Summary of simulation results for the LCU-03T-01 scenario and several sensitivity cases

Case	Deflagrations under the bio-shield	Vent form loss	Maximum well-mixed hydrogen concentration	Maximum local hydrogen concentration	Maximum AICC Pressure (bar-abs)*	Maximum hydrogen mass (kg)	Potential for detonation	Remarks
1	Suppressed in MELCOR	[[ ]]$^{2\,(a),(c)}$	0.096	0.126	3.04	1.6	Highly unlikely	If considered detonable, maximum detonation pressure ~32 bar-abs (~473 psia).
2		[[ ]]$^{2\,(a),(c)}$	0.065	0.085	Inflammable	1.2	No	The peak well-mixed H_2 concentration is 6.5%, resulting in a peak AICC pressure of ~2.6 bar-abs.
3	Allowed in MELCOR	[[ ]]$^{2\,(a),(c)}$	0.075	0.100	Not calculated	1.6	No	Deflagration prevents local hydrogen build-up to a relatively high concentration of Case 1.

* Calculated for the well-mixed atmosphere

Intentionally left blank

5. SUMMARY AND CONCLUSIONS

5.1 Combustion inside Containment

This report reviewed Section 6.2.5 of the FSAR [1], a technical report [2], and a document available in the NuScale Electronic Reading Room [3] related to the NuScale's assessment of hydrogen combustion for conformance with 10 CFR 50.44. The main result of the NuScale analyses is a bounding estimate of the detonation pressure of [[ ]]$^{2\,(a),\,(c)}$ bar-abs ([[ ]]$^{2\,(a),\,(c)}$ psia). According to NuScale's structural analysis, given the estimated duration of the detonation pulse, subject to this estimated pressure, the containment structure will not experience impacts beyond the yield strain. For computing this bounding pressure, NuScale appears to rely little or not at all on simulations of severe accidents.

This report has been mostly concerned with the derivation of this pressure estimate, and especially with the derivation of the containment atmosphere conditions just prior to the combustion event. NuScale arrived at the pre-burn conditions by considering a supposedly bounding situation in which [[ ]]$^{2\,(a),\,(c)}$% of the cladding inventory of Zircaloy has oxidized, and the radiolytic sources of hydrogen and oxygen are as arise 3 days since the start of the accident. (100% oxidation would mean the amount equivalent to complete steam-oxidation of all the zirconium in the cladding on the active part of the fuel; this corresponds to 93.3 kg of hydrogen according to Reference [3].) According to NuScale's methods and assumptions, these and other simple considerations fix the masses of the gases present in the containment. NuScale applies the ideal gas law to calculate the pre-burn pressure and gas composition. For this calculation, NuScale assumes that the containment temperature is [[ ]]$^{2\,(a),\,(c)}$ °F ([[ ]]$^{2\,(a),\,(c)}$ °C) and that the containment gas volume is that of the entire containment vessel (with no reduction by the volume of any water that can accumulate due to condensation of steam inside the containment). The pre-transient nitrogen and oxygen inventories correspond to a pre-power-up containment pressure of 9.5 psia. The pre-burn oxygen mole fraction is [[ ]]$^{2\,(a),\,(c)}$, and indeed it appears that [[ ]]$^{2\,(a),\,(c)}$% of the cladding oxidation was assigned to arrive at this oxygen concentration. It is widely accepted that gas mixtures with oxygen concentrations below [[ ]]$^{2\,(a),\,(c)}$ are not flammable. Still, from a regulatory point of view, the permissibility of assuming less than 100% has to be assessed by NRC. Line 2 of Table 3.2 shows how ERI has applied the NuScale method and assumptions, and thereby reproduced the results documented by the Applicant. According to NuScale, the pre-burn containment pressure is [[ ]]$^{2\,(a),\,(c)}$ bar-abs, and this pressure and the associated molar composition are confirmed by the present review. The accurate AICC pressure is 20.2 bar-abs, but NuScale uses an approximate method to calculate AICC pressure, and reports [[ ]]$^{2\,(a),\,(c)}$ bar-abs = [[ ]]$^{2\,(a),\,(c)}$ psia. For the detonation pressure, NuScale applies to the AICC pressure, a multiplication factor of [[ ]]$^{2\,(a),\,(c)}$, and obtains thus the detonation pressure of [[ ]]$^{2\,(a),\,(c)}$ bar-abs ([[ ]]$^{2\,(a),\,(c)}$ psia), which is the Applicant's main combustion-related result.

The present study used the NRC-sponsored MELCOR model of the NuScale plant to simulate a variant of the scenario named LCC-05T-03 that NuScale has discussed in Chapter 19 of the FSAR [11]. The scenario is controlled to evolve to a 72-hour end state with containment oxygen molar concentration 0.05. Based on the results, the present study finds that, for use in NuScale's ideal gas method, the assumed containment gas temperature, [[ ]]$^{2\,(a),\,(c)}$ °C, is non-conservatively low. This temperature should be not less than 96.5 °C. Also non-conservative is the NuScale-assumption that the entire containment volume is available for calculating the combustion pressure (i.e., not reducing the containment gas space volume by any water that can accumulate in the containment is non-conservative). Based on the present MELCOR simulation results, the available gas volume should be reduced by at least about 28.2 m^3 due to water accumulation. Line 3 of Table 3.2 shows how NuScale's method is re-applied with, as the only changes, re-specification of the two non-conservative assumed values by the MELCOR-informed values. The pre-burn pressure is 7.1 bar-abs; the accurate AICC pressure is 24.8 bar-abs, and (using NuScale's factor [[ ]]$^{2\,(a),\,(c)}$), the estimated detonation pressure is [[ ]]$^{2\,(a),\,(c)}$ bar-abs ([[ ]]$^{2\,(a),\,(c)}$ psia). This value somewhat exceeds NuScale's "bounding" estimate, [[ ]]$^{2\,(a),\,(c)}$ psia.

The present MELCOR model uses a pre-transient containment pressure of [[ ]]$^{2\,(a),\,(c)}$ psia (i.e., not 9.5 psia). (See the discussion in Section 3.1: these pressures really apply, not just before the transient, but before the power-up to the normal-operation steady state.) The value [[ ]]$^{2\,(a),\,(c)}$ psia has been noticed in several Electronic Reading Room documents, while the NuScale NRELAP5 model specifies an even lower pressure of [[ ]]$^{2\,(a),\,(c)}$ psia. The decreased amount of oxygen initially present corresponding to [[ ]]$^{2\,(a),\,(c)}$ psia versus 9.5 psia has the result that the fraction of

core oxidation that yields 0.05 molar containment oxygen concentration at 72 hours is lowered to about 19%. The pre-burn, AICC, and detonation pressures are all correspondingly lowered; see line 1 of Table 3.1. The AICC pressure associated with the containment atmosphere that MELCOR predicts for the LCC-05T-03 variant scenario predicts is 11.12 bar-abs. Relative to NuScale's key result (given by NuScale as AICC pressure of [[ ]]$^{2\,(a),\,(c)}$ bar-abs), much milder combustion events are expected; this large difference is due to NuScale's use in Reference [3] of 9.5 psia for the pre-transient containment pressure. The basis or need for the higher pressure is not known. If the plant will actually be built and operated with pre-power-up containment pressure [[ ]]$^{2\,(a),\,(c)}$ psia, then NuScale's estimate of their bounding detonation pressure can be lowered substantially by re-doing the analysis with the lower pre-power-up containment pressure.

Besides the issue of the initial containment pressure, another difference between the present MELCOR model and the inputs used in the ideal gas computations of Reference [3] is the volume of the (dry) containment. The MELCOR model assigns the containment volume as [[ ]]$^{2\,(a),\,(c)}$ m^3 while the value used in Reference [3] is [[ ]]$^{2\,(a),\,(c)}$ m^3. Whereas the review finds that, for use in NuScale's method, the containment atmosphere temperature should be specified as at least 96.5 °C and the gas volume lost to water buildup inside containment as at least 28.2 m^3, strictly speaking these numbers apply for the containment of dry volume [[ ]]$^{2\,(a),\,(c)}$ m^3 and initial pressure [[ ]]$^{2\,(a),\,(c)}$ psia, and not for the containment of dry volume [[ ]]$^{2\,(a),\,(c)}$ m^3 and initial pressure 9.5 psia that NuScale has assumed in Reference [3] for ideal gas computations. The essential point is that NuScale should assign a higher temperature and account for the impact of water buildup. These re-assignments will raise the key result (bounding detonation pressure), but the use of [[ ]]$^{2\,(a),\,(c)}$ rather than 9.5 psia for the pre-transient containment pressure will lower the key result.

The Applicant has based his main conclusions on the assumption that the combustion event that may challenge the containment integrity should take place, at the latest, at 72 hours since the time of start of the accident. This report extends the confirmatory calculations, carried out at 72 hours, also to times as long as 60 days. (The Applicant also has considered combustion events at long times, in document ER-P020-4904 available in the electronic reading room.) As the postulated fraction of the cladding that becomes oxidized varies from ~10% to ~110%, the times at which the containment becomes flammable (and, in general, detonable) ranges from ~0.3 to ~60 days (see Figure 3.2.7). This time might indicate when operators could take actions to restore inert conditions. Inside of 60 days, the worst-case result obtained here is when 110% of the cladding oxidizes. In that case, the AICC pressure at 60 days is 58.8 bar, or 853 psia. The Applicant's combustion analysis is based on the AICC pressure of [[ ]]$^{2\,(a),\,(c)}$ psia as approximately calculated for the mixture that the Applicant predicts for the containment at 3 days (see Section 2.3, and Reference [3]).

Accidents attaining core damage will ordinarily entail oxidation of a sizable fraction of the cladding (e.g., more than 20%). The hydrogen generated thereby results in a containment atmosphere that is too rich to support combustion until the slow process of radiolysis adds enough oxygen to restore the molar concentration (of oxygen) to more than 5%. For example, if 30% of the cladding oxidizes, the present study estimates that the containment atmosphere remains not flammable for about 6 days (see Figure 3.2.7). On such long-time scales, the particular progressions of different severe accident scenarios would not be of any significance with little to distinguish them except the oxidation fraction. Therefore, Figure 3.2.7 has wide applicability, even though it is partly based in a particular scenario (very small CVCS line break with no ECCS actuation, and with imposed cessation of core oxidation at the variously considered fractions). This study finds that, with rare exceptions, the containment is detonable if it is flammable. Although the Applicant argues that the containment can withstand detonation pressures as high as ~[[ ]]$^{2\,(a),\,(c)}$ times the design pressure (i.e., [[ ]]$^{2\,(a),\,(c)}$ bar / [[ ]]$^{2\,(a),\,(c)}$), prudence probably dictates that a goal post-accident actions would be to prevent detonability. This implies keeping the oxygen concentration below 5%, for which goal Figure 3.2.7 implies the following:

- Barring the probably rather unlikely case of a severe accident that entails less than 20 % oxidation of the core, one can expect that the containment will not become flammable for at least about 2 days.
- If core oxidation stops at 10%, however, the containment could be detonable as early as ~0.3 days (~ 8 hours).
- The greater the oxidation fraction, the greater combustion-induced pressurization;
- The greater the oxidation fraction, the later will be the onset of flammability:

- for 10%, this study estimates AICC pressure as 7 bar at the time of onset of flammability (8 hours or 0.3 days);
- for 69%, this study estimates AICC pressure as 38 bar at the time of onset of flammability (24 days);
- for 110%, this study estimates AICC pressure as 59 bar at the time of onset of flammability (56 days).

Oxidation fraction 69% might be taken as a best estimate since it is the MELCOR prediction found here for the LCC-05T-03 scenario, while 110% is a case that the Applicant considered in ERR document ER-P020-4904[30]. The 10 % case leads to flammability and detonability as early as 0.3 days (~8 hours). All the AICC pressures estimated here are less than the design pressure (72.41 bar-abs), but if detonation pressures are estimated as the AICC pressure times [[ ]]$^{2\,(a),\,(c)}$ (which is the factor that the Applicant uses), then the detonation pressures corresponding to the above three sub-bullets exceed the design pressure by respective factors of [[ ]]$^{2\,(a),\,(c)}$. Probably the Applicant's TNT-equivalence and dynamic strain methods would predict that the assumed detonation occurring at 0.3 days would not result in containment failure[31]. Whether the two higher pressures can be withstood cannot be established here.

A review of NuScale's structural analysis was not within the scope of the present study. NuScale arrives at the conclusion that the containment vessel will withstand a detonation that produces a pressure of [[ ]]$^{2\,(a),\,(c)}$ bar-abs ([[ ]]$^{2\,(a),\,(c)}$ psia); this pressure is [[ ]]$^{2\,(a),\,(c)}$ times the design pressure. This conclusion depends on the very short time during which this pressure could act. According to the Applicant [2], for the considered condition whose detonation pressure is [[ ]]$^{2\,(a),\,(c)}$ bar-abs, the pulse period is [[ ]]$^{2\,(a),\,(c)}$ milliseconds. In Reference [2], the Applicant describes the method for calculating this time (the so-called pulse period) which, in addition to the pressure itself, determines the threat. However, Reference [2] is not explicit for the values of all the needed parameters. The detonation pulse period estimates that the present report provides (see Table 3.4) were made with some assumed parameters. They suggest that the pulse period does not depend very strongly on the detonation pressure. The present report makes no attempt to assess the impact on the containment integrity of these detonation pressures and pulse periods as estimated here.

5.2 Combustion under Bio-Shield

These analyses suggest that, in the considered scenario (unmitigated CVCS line break under the bio-shield), the likelihood of DDT and hydrogen detonation in the region under the bio-shield is not significant. Under the conservative assumption of suppressing deflagration of hydrogen at lower levels, the local pockets of gases approached a concentration just below the lower limits at which detonable mixtures have been reported (i.e., in this

[30] Actually, the Applicant considered 111%. The Applicant found that flammability is attained at [[ ]]$^{2\,(a),\,(c)}$ days. For 110%, the MELCOR simulation reported in the present study (Section 3.4.1) found 42 days, but this good agreement may be fortuitous. The "direct calculation" (Section 3.4.2) of the present study found 56 days. As previously discussed, the direct calculation's over-prediction, relative to MELCOR, of the time to flammability for 110% oxidation can largely be attributed to the neglect, in the direct calculation, of any dependence of the in-vessel hold-up of hydrogen on the on the oxidation fraction. A qualitative explanation for the 45-day (Applicant) vs. 56-day (this study's direct calculation) discrepancy can be suggested, although it has not been checked quantitatively. As has been discussed, the Applicant uses a higher pre-power-up containment pressure than do the analyses of the present report (9.5 vs. [[ ]]$^{2\,(a),\,(c)}$ psia). The analysis of Section 3.1 of the present report finds that core oxidation fraction 19 % is the value that yields 5 % oxygen concentration at 3 days; the Applicant found [[ ]]$^{2\,(a),\,(c)}$ % for 3 days. In other words, for given oxidation fraction, the Applicant's analysis overpredicts the time, relative to the analysis of this study. Section 3.1 discussed that the [[ ]]$^{2\,(a),\,(c)}$ % (Applicant) vs. 19% (this study) discrepancy is largely attributable to the Applicant's use of the too-high pre-power-up containment pressure. The Applicant also uses 9.5 psia for the calculation that leads to the (111%, 45 days) result. A re-calculation using [[ ]]$^{2\,(a),\,(c)}$ psia would increase the time, but by how much has not been estimated here.

[31] Those methods find that a detonation pressure of [[ ]]$^{2\,(a),\,(c)}$ bar, which is [[ ]]$^{2\,(a),\,(c)}$ times the design pressure, is not expected to fail containment. However, the ratio [[ ]]$^{2\,(a),\,(c)}$ is not known to be generally applicable. Rather, the duration of the detonation (pulse period) depends on the detonation pressure; then, the maximum amount of resulting strain depends directly on both the detonation pressure and the pulse period. In principle, the method has to be re-applied to determine whether any of these three pressures might induce containment failure. The above bullets record the AICC pressure at the time of the onset of flammability, but a postulated combustion event could occur later than the earliest possible time and would then yield a higher pressure. For example, for the case of 10% oxidation fraction, the AICC pressure at 60 days is 41 bar.

case, the well-mixed hydrogen concentration remained below 10%, while the local hydrogen concentration peaked at 12.6% according to the six nodes used for the simulation of the bio-shield gas space). Nonetheless, the application of the "$L > 7\lambda$" criterion indicated that the atmosphere with 12.6% hydrogen can support the potential for detonation under the bio-shield.

Using the CJ model for about 13% hydrogen, the detonation velocity is about 1650 m/s, the detonation to pre-burn pressure ratio (i.e., $P_{CJ}/P_{pre\text{-}burn}$) of the detonation wave of about 9, and detonation temperature of about 1900 K, were estimated. In addition, a pressure ratio associated with the reflected shock wave of about [[ ]][2] [(a), (c)], and corresponding detonation temperature of about 2250 K, were also estimated. Therefore, the estimated total pressure loading on the structure of 32 bar-abs (473 psia) resulted as the sum of the pressure due to detonation and reflected waves.

Consideration was also given to the possibility that DDT can produce pressures in excess of the CJ or reflected CJ pressure as has been reported in the literature [5]. This phenomenon of "pressure piling" was not considered to be credible for the hydrogen and oxygen concentrations calculated herein under the bio-shield (i.e., much lower than stoichiometric mixture).

The aforementioned results were obtained under the additional conservative assumption that the flow through the bio-shield vents is impeded by the stacking of another module's bio-shield on the shield of the modeled module. (Such stacking may occur when a neighboring module is being refueled.) In a calculation that assumed no such stacking, the well-mixed hydrogen concentration remained below 7% (the usually considered lower limit of flammability), while the local hydrogen concentration peaked at 8.5% (certainly not detonable). The form loss coefficient values provided by the Applicant were used to model the impedance of flows through the vents in the stacked and un-stacked configuration. The finding here is that in the considered scenario, flammable conditions never arise if there is no stacking; the constriction of the flow caused by stacking allowed flammable conditions to arise briefly (~3 minutes) but, as noted above, the possibility of detonability is small.

It was concluded that the conservatism of the conditions resulting in build-up of hydrogen beyond deflagration limit without combustion to levels as high as ~13% is highly unlikely, partly, due to uncertainties in the MELCOR-predicted concentration gradients that result in a small pocket of relatively high hydrogen concentration in the bio-shield. Furthermore, even if hydrogen concentration reaches 13%, it is not expected that detonations can be initiated through rapid flame acceleration, given the absence of any significant obstacles in the region of interest. Finally, absence of strong ignition sources would most likely eliminate the potential for any detonation, and low energy ignition would render the compartment more vulnerable to deflagration than detonation. Therefore, it is concluded that the probability of any hydrogen detonation in the biological shield region potentially impacting the containment integrity[32] (from the outside) or generating missiles from the damaged biological shield structural components that can impart on the adjacent modules resulting in core damage, is negligibly small and can be ignored.

[32] In this case, the integrity of the containment for the affected module is not of any importance, except for long-term post-accident stabilization standpoint.

6. REFERENCES

1. NuScale Final Safety Analysis Report (Revision 0, December 2016), Tier 2, Section 6.2.5 (Combustible Gas Control in Containment).

2. NuScale Technical Report, TR-0716-50424-P, Rev. 0, Combustible Gas Control, (ML17005A150).

3. EC_B020_2877_R1, ECCS Combustible Gas Analysis.

4. NUREG-0800, Section 6.2.5, Revision 2, pp. 12 and 13 (July 1981); Regulatory Guide 1.7, Table 1, Revision 2 (November 1978).

5. J. E. Shepherd, "Structural Response of Piping to Internal Gas Detonations," Journal of Pressure Vessel Technology, Volume 131, Number 3 (2009).

6. V. Schroeder and K. Holtappels, "Explosion Characteristics of Hydrogen-Air and Hydrogen-Oxygen Mixtures at Elevated Pressures," International Conference on Hydrogen Safety, Pisa, Italy (2005).

7. J. B. Zel'dovich and K. P. Staniukovich, "On the Reflection of a Plane Detonation Wave," USSR Academy of Sciences – Fluid Mechanics – Volume 55, Number 7 (1947).

8. E. Schultz and J. Shepherd, "Detailed Reaction Mechanisms for Detonation Simulations," Explosion Laboratory Report FM99-5, California Institute of Technology, Pasadena, CA (2000).

9. W. Breitung, C. Chan, S. Dorofeev, A. Eder, B. Gelfand, M. Heitsch, R. Klein, A. Malliakos, E. Shepherd, E. Studer, and P. Thibault, "Flame Acceleration and Deflagration-to-Detonation Transition in Nuclear Safety, State-of-the-Art Report by a Group of Experts," OECD Nuclear Energy Agency, NEA/CSNI/R(2000)7 (August 2007).

10. "Updated MELCOR Calculation Notebook: NuScale Integral Pressurized Water Reactor," ERI/NRC 13-205, Revision 8, March 2018.

11. NuScale Final Safety Analysis Report ("NuScale Standard Plant Design Certification Application," Revision 0), December 2016.

12. Electronic Reading Room document "NuScale MELCOR Basemodel," ER_P060_4724 (p. 125/136).

13. Electronic Reading Room document "ECCS Combustible Gas Analysis," EC_B020_2877_R1.

14. Response to RAI 9447, NuScale Power (November 2018).

15. "Updated MELCOR Calculation Notebook: NuScale Integral Pressurized Water Reactor," ERI/NRC 13-205, Revision 9 (March 2019).

16. A. L. Camp, et al., "Light Water Reactor Hydrogen Manual," Sandia National Laboratories, NUREG/CR-2726, SAND82-1137 (August 1983).

17. W. Breitung, et al., "A Mechanistic Approach to Safe Igniter Implementation for Hydrogen Mitigation," AECL-11762, NEA/CSNI/R(96) 8 (1996).

18. S. B. Dorofeev, "Turbulent Combustion and DDT Events as an Upper Bound for Hydrogen Mitigation Techniques," AECL-11762, NEA/CSNI/R(96) 8 (1996).

19. "Confirmatory Simulation of NuScale Containment Response Under Design Basis Accident Conditions," ERI/NRC 19-210, Revision 0, Proprietary, Export Control (May 2019).

20. "Updated MELCOR Calculation Notebook: NuScale Integral Pressurized Water Reactor," ERI/NRC 13-205, Revision 10 (June 2019).

APPENDIX: NODALIZATION DIAGRAMS FOR THE MELCOR MODELS

Figures A.1 through A.3 show the nodalization diagrams of the model as it existed for the simulation of the break inside containment scenario (transient LCC-05T-03, described in Section 3), used to support the analysis of combustion inside containment. Figure A.4 adds a newer version of Figure A.3; both versions show the nodalization of the reactor bay water pool. Figure A.4 comes from Revision 9 of the model, which was used for the simulation of the break outside containment scenario (transient LCU-03T-01, described in Section 4) to support the analysis of combustion under the bio-shield. Thus the simulation of the break inside containment scenario used an earlier version of the model than is now current[33]. The difference between Figures A.3 and A.4 is that the latter shows the finer nodalization and the updated connections of the gas regions under the bio-shield (i.e., bio-shield vent design as updated by NuScale in November 2018), as well as the balance of the plant. Figure A.1 is actually only slightly out of date: the important change related to that figure is only that in Revision 9 the steam generators are modeled with 12 axial levels (Figure A.1 shows four).

[33] As of January 2019, Revision 9 is current. The model version used for the break inside containment scenario can be described as a variant of Revision 7. It included the radiolytic sources, which have not been carried forward into later revisions.

[[

]][2 (a), (c)]

Figure A.1 Nodalization of the NuScale reactor pressure vessel and steam generators

[[

]]2 (a), (c)

Figure A.2 Nodalization of the NuScale containment vessel

[[

]]2 (a), (c)

Figure A.3 Nodalization of the NuScale reactor bay water pool

[[

]][2 (a), (c)]

Figure A.4 Updated (Revision 9) nodalization of the NuScale reactor bay water pool [34]

[34] The gas space under the bio-shield is bounded on three sides by vertical concrete walls, and on one side by the vertical part of the steel bio-shield. The bio-shield vents penetrate the vertical steel part, not the concrete walls (contrary to what the figure may suggest). The concrete wall does not exist on the fourth side, so at elevations below the bottom of the vertical part of the shield, there is free communication of the water below the shield with the balance of plant water via flow paths such as FL567.

Intentionally left blank